CANADIAN THESES

THÈSES CANADIENNES

Canadä

THE UNIVERSITY OF ALBERTA

DETERMINATION OF ROBOT JOINT AXIS MISALIGNMENTS

USING A VISION SYSTEM

BY

JAMES H. WARKENTIN

A THESIS

SUBMITTED TO THE FACULTY OF GRADUATE STUDIES AND RESEARCH

IN PARTIAL FULFILMENT OF THE REQUIREMENTS FOR THE DEGREE

OF MASTER OF SCIENCE

DEPARTMENT OF MECHANICAL ENGINEERING

EDMONTON, ALBERTA

SPRING, 1986

THE UNIVERSITY OF ALBERTA

RELEASE FORM

NAME OF AUTHOR: JAMES H. WARKENTIN

TITLE OF THESIS: DETERMINATION OF ROBOT JOINT AXIS

MISALIGNMENTS USING A VISION SYSTEM

DEGREE: MASTER OF SCIENCE

YEAR THIS DEGREE GRANTED: SPRING 1986

    Permission is hereby granted to THE UNIVERSITY OF
ALBERTA LIBRARY to reproduce single copies of this thesis
and to lend or sell such copies for private, scholarly or
scientific research purposes only.

    The author reserves other publication rights, and
neither the thesis nor extensive extracts from it may be
printed or otherwise reproduced without the author's
written permission.

. . . .
(Student's signature)

. . . .

. . . .

. . . .
(Student's permanent address)

Date: . . . .

THE UNIVERSITY OF ALBERTA

FACULTY OF GRADUATE STUDIES AND RESEARCH

The undersigned certify that they have read, and
recommend to the Faculty of Graduate Studies and Research
for acceptance, a thesis entitled DETERMINATION OF ROBOT
JOINT AXIS MISALIGNMENTS USING A VISION SYSTEM submitted b
JAMES H. WARKENTIN in partial fulfillment of the
requirements for the degree of MASTER OF SCIENCE.

....
(Supervisor)

....

....

Date: 6 Dec 85

ABSTRACT

Major advancements in robot programming will soon be on the factory floor because of the need for more efficient programming methods for large numbers of robots or applications which require frequent reprogramming. Advanced programming methods use high level languages to program off-line (without a robot) using the ideal robot geometry to calculate the variable joint positions (software defined targeting). However, errors in the ideal geometry of a robot arising from manufacturing tolerances, resolution of the joint position encoders, and wear, cause software defined targeting to be inaccurate. The most effective way to increase robot accuracy is to measure the true robot geometric parameters and use them in the control software.

In this investigation a linear error model reveals that orientation errors in the joint axes and errors in the joint variables cause the greatest end effector position and orientation errors. A new calibration method is developed to measure the joint axis orientations using a digital camera, mounted on the end effector and a vertical reference comprised of target lights. The calibration method determines the joint axis orientation errors, termed misalignments, by analysis of the observed movement of the target points from a vertical reference with respect to the rotation of a single link of the robot.

iv

The advantage of this new calibration method over other methods, is that it does not require a precision calibration site to conduct the procedure. The calibration procedure can easily be conducted in the work cell of the robot, only requiring the mounting of a digital camera to the end effector of the robot and the introduction of two vertical references to the work space.

The proposed calibration method has been tested on a bench top robot. Simulated misalignments were measured with accuracies ranging from -0.1 to 0.04 degrees for vertical joint axes and -0.06 to 0.03 degrees for horizontal joint axes. The calibration procedure is performed automatically using a microcomputer for both image processing and calibration sequence operations.

ACKNOWLEDGEMENT

TABLE OF CONTENTS

LIST OF TABLES

ix

LIST OF FIGURES

LIST OF SYMBOLS

A_i Homogeneous transformation representing link i using the Denavit-Hartenburg convention

a approach vector

B Base homogeneous transformation describing the origin of link 1 with respect to the base coordinate frame

C abbreviation for the cosine function

CAM digital camera transformation

c translation vector in the camera transformation, CAM

D_i homogeneous transformation representing link i using the modified Denavit-Hartenburg convention

d differential translation vector

E end effector transformation describing the end effector with respect to the end of the manipulator

I identity matrix

i subscript denoting link i

l_i link length of link i

n number of links in a manipulator

n normal vector

o orientation vector

P position transformation

p position vector

$Rot( )$ rotation transformation

r_i link distance of link i

S abbreviation for the sine function

$_iT_j$ homogeneous transformation describing link j with respect to link i

T_n homogeneous transformation describing link n with respect to the origin of link 1

Trans( )   translation transformation

(x_B , y_B , z_B) base coordinate frame

(x_i , y_i , z_i) coordinate frame of link i

(x_p , y_p) pixel coordinate frame in digital camera

α_i twist angle of link i

γ_i skew angle of link i

Δ differential transformation

δ differential rotation vector

θ_i rotation angle of link i

$[\ ]^{-1}$ inverse matrix

$[\ ]^{T}$ transpose matrix

CHAPTER 1.

INTRODUCTION

The definition of a robot adopted by the Robot

Institute of America (RIA) describes a robot as, "a

programmable multifunction manipulator designed to move and

manipulate material, parts, tools or specialized devices

through variable programmed motions for the performance of a

variety of specific tasks" (Lammineur, et al., 1984). This

definition emphasizes the characteristic flexibility of

robots which distinguishes them from fixed automation and

which has allowed for the accelerating implementation of,

robots in the manufacturing industry. A second

characteristic emphasized in this definition is that a robot

is programmable. To utilize the flexibility of a robot

effectively, it must be easily reprogrammed to carry out the

variety of tasks it may be called upon to perform.

The several existing methods for programming robots

are characterized by the type of robot they instruct. One

type of robot, called a "fixed stop" or "sequencer" robot is

a non-servo (open loop) device and has been in existence

since the early 1960's. These are used mostly for pick and

place operations. As the name of this robot implies, only

the sequence of the robot moves may be programmed. Thus, it

may be instructed to rotate or extend, but the extent of the

motion is defined by mechanical stops. Programming includes

physically adjusting the stops and determining the sequence

of moves. The sequencer robot has no provision for

trajectory control between end points.

Another classification of robots which are closed

loop devices, are the servo-controlled units. Electrical

signals from position or rotation transducers, called

encoders, in each joint provide feedback for position and

velocity control. Although servo-controlled robots are more

expensive than non-servo types, their more sophisticated

programming methods offer greater flexibility and path

control.

The point to point servo-controlled robot is the

most common robot used today. They are commonly used for

material handling or machine loading. These are completely

programmable robots where both the sequence and the extent

of motion are specified. Point to point programming is

generally performed with a hand held teach pendant. The

teach pendant is used to move the robot into desired

positions known as "knot points" which are stored in

sequence. A variation of this method is used in the

programming language, VAL I, in which knot points are

numbered when stored. A VAL I program specifies the speed,

responses to inputs, and order through which the knot points

should be traversed (Patrick, 1984).

A second type of servo-controlled robot is the

continuous path device. These robots are used for processes

requiring smooth continuous motions, such as spray painting, applying glues, or arc welding. Robots of this type are programmed using a method known as "lead through" programming. Programming is accomplished by physically moving the robot through the desired path and storing the analogue signal produced from the joint encoders. The program tape is played back to the robot which moves along the recorded signal path describing the desired motions.

The existing methods of robot programming are quite adequate for applications where small numbers of robots are being used, or where large production runs require little reprogramming. But with the advent of manufacturing firms using hundreds of robots, or flexible manufacturing systems designed to produce a whole family of components in large or small production runs, existing programming methods are tedious and error prone. Production time is valuable, so it is not desirable to take robots out of service to perform programming or waste time in long programming sessions.

Two major advancements in robot programming are presently being developed because of the need for less tedious programming of large numbers of robots using the lead through or teach pendant methods. The advancements of off-line programming and implicit programming will allow rapid instruction of robotic systems. Programming off-line (without a robot), is performed at a computer terminal using a high level language. Off-line programming permits programs to be written for new tasks or editing of existing

programs without interrupting current production.

Implicit programming will introduce a very high level of off-line programming. Instead of explicitly directing every move and response of the robot, implicit programming will allow one to imply many operations for the robot. In an assembly operation using robots with vision systems and artificial intelligence for pattern recognition, the robot would simply be instructed what part is to be picked, the location of the bin containing the part, and the assembly procedure and location where the part is to be placed. Simple English like commands would specify the operation for which the specific moves and responses to input are implied.

At present, off-line programming languages generate robot programs which often require refinement when down loaded to the actual robot. This is because the mathematical computer model of the robot assumes an exact mechanical duplicate on the work floor. Unfortunately this may not be the case. Errors in the controlled joint positions and fixed geometric parameters cause the robot to deviate from the desired trajectories and end points. The factors affecting robot performance have received increased attention with the work in advanced programming methods. (Albertson, 1983; Berlenbach, 1984; Kreamer, 1984; Stauffer, 1985).

The performance of a robot can be described by its accuracy and repeatability. Robot manufacturers usually

only quote repeatability errors when specifying the

performance of their products. The repeatability of a robot

may be +/- 0.05 mm. Although this may seem very impressive,

it is also a little misleading if one is not familiar with

the exact definitions of the robot performance terms. Robot

repeatability defines the error the robot may have in

returning to a previously taught point.

Accuracy, however, is the distance error between the

desired target point in the world reference frame and where

the robot actually positioned itself. For example, Kreamer

(1984) found that the Cincinnati Milacron T3-776 robot had a

repeatability of 0.05-0.10 mm but showed accuracy errors of

2.54 mm. Figure 1-1 illustrates the definitions of

repeatibility and accuracy. In general, the repeatability

of a robot is better than its accuracy (Toepperwein, et al.,

1983; Kreamer, 1984).

The factors which must be considered concerning

robot accuracy are quite involved. Some of the more

important factors include resolution of the joint encoders

and resolvers, number of bits of controller memory assigned

to position measurements, accuracy of robot construction,

the amount of backlash in the gears, and the link

deflections under static and dynamic conditions

(Toepperwein, et al., 1983; Stauffer, 1985). The present

work deals with one of the major factors concerning robot

accuracy in off-line programming: the accuracy of the actual

robot geometry with respect to the ideal geometry.

Repeatability

Tool Tip
Positions

Target Point
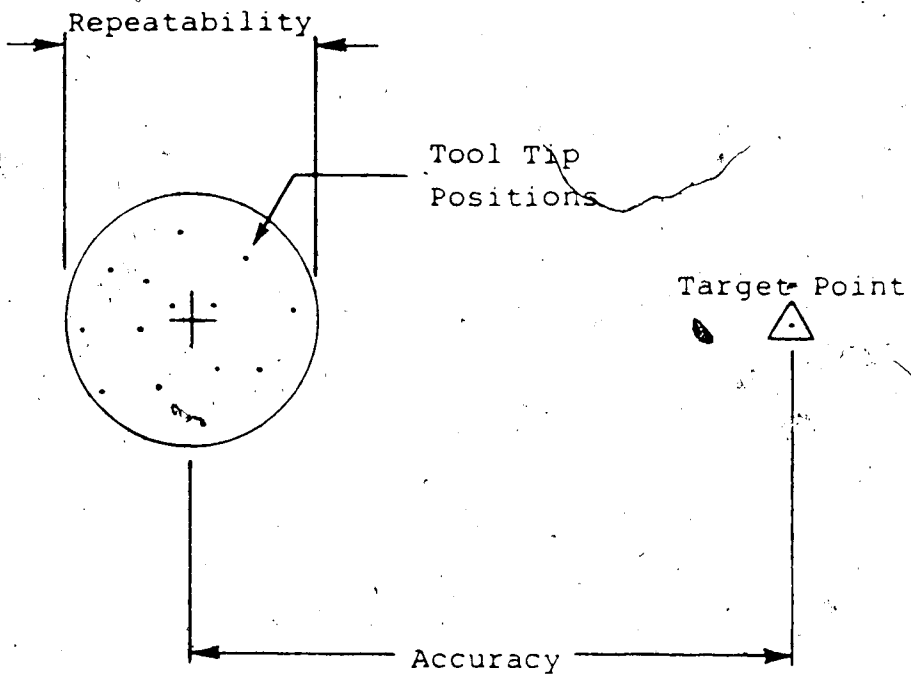
Accuracy

Figure 1-1   Two Dimensional Depiction of Tool Tip Positions
Comparing Repeatability to Accuracy

Accuracy of the robot geometry with respect to the ideal geometry has only become a problem with the introduction of off-line programming. With teach pendant and lead through programming, errors in the ideal geometry are automatically corrected by placing the robot in the desired position and recording the joint variables (physically defined targeting). For physically defined targeting, repeatability is the important robot performance characteristic.

In off-line programming, the joint variables are calculated (software defined targeting) to place the end effector in a specific position using the ideal robot geometry. Figure 1-2 illustrates a robot with an error in its shoulder joint orientation termed a misalignment. The shoulder misalignment results in a position and orientation error of the end tool when positioned by software defined targeting. Both accuracy and repeatability are important performance characteristics for software defined targeting. It is essential that the correct geometric parameters describing the robot are known so that the software can accurately position the robot.

As an introduction to robot geometry a single link is illustrated in figure 1-3. A serial link manipulator consists of a sequence of links connected together by actuated joints. Each link is described by two embedded coordinate frames. Link i is described by the relationship between joint i and joint i+1. Six parameters are required

Shoulder Joint Axis
Misaligned From Perfect
Orientation

Orientation Error

Position Error
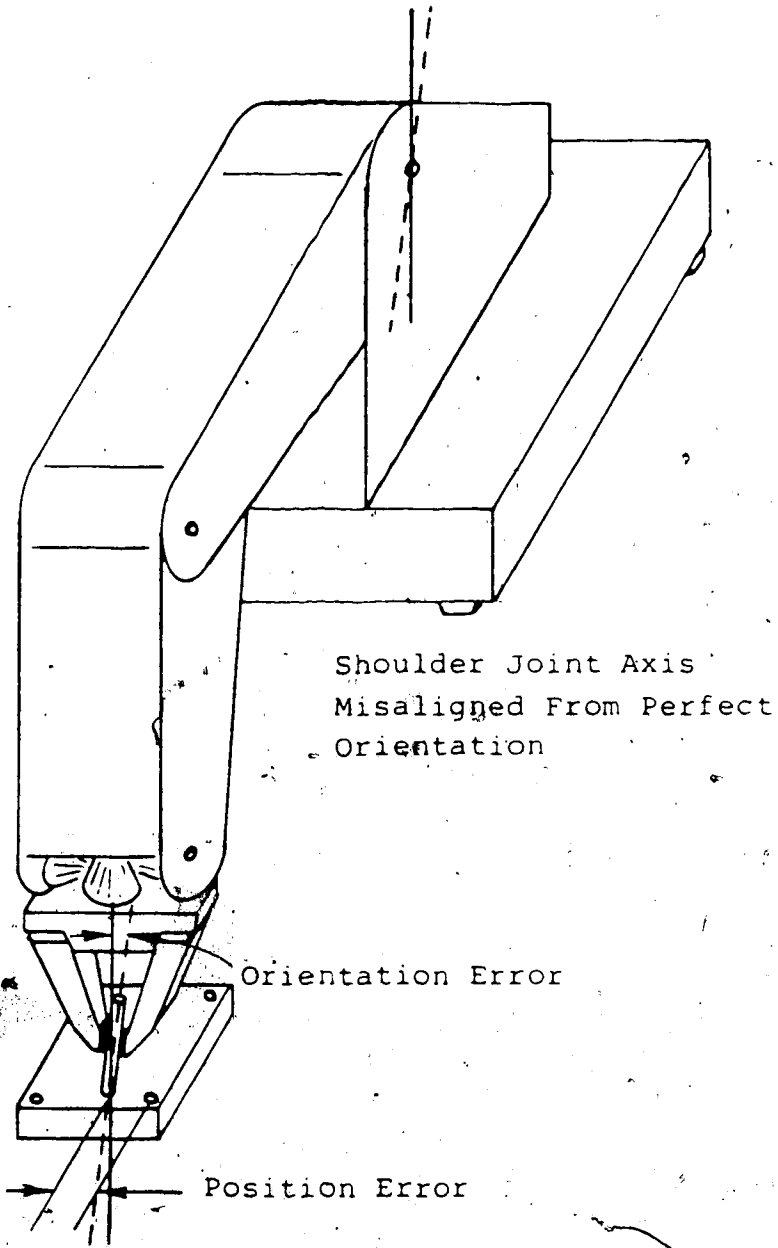
Figure 1-2 End Effector Errors Caused by an Error in the
Ideal Robot Geometry
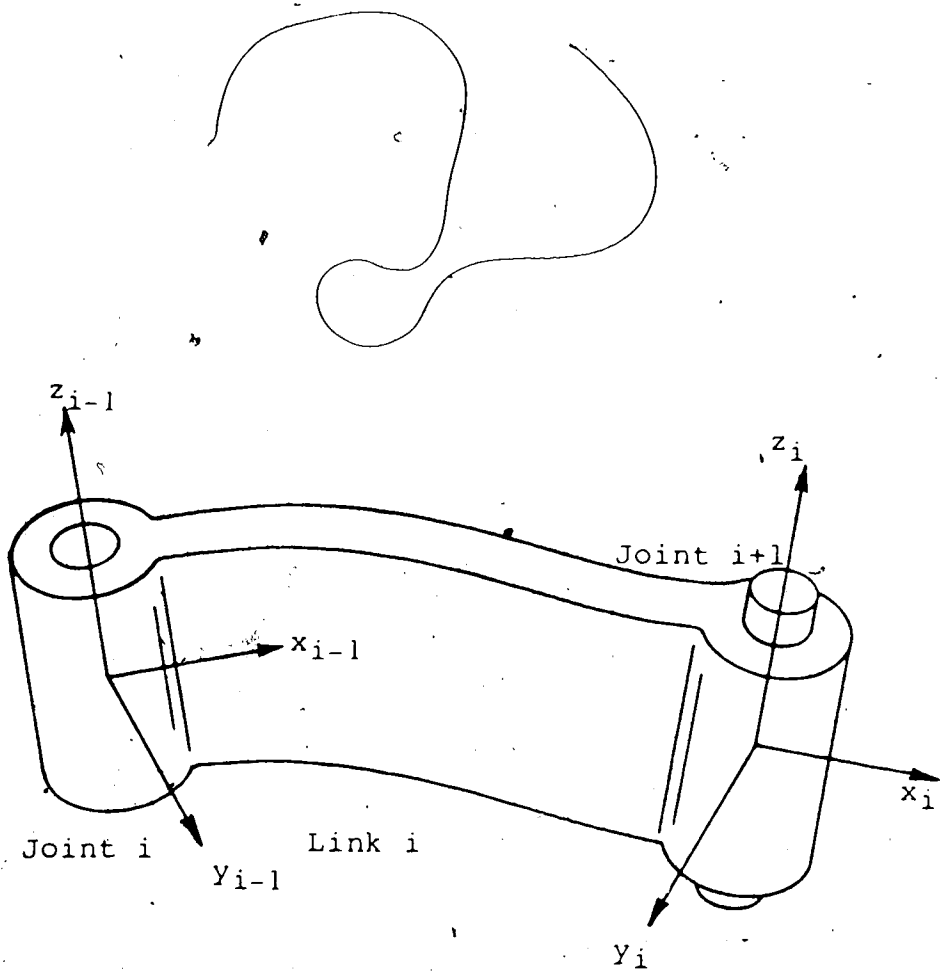
Figure 1-3 Coordinate Frames in a Single Link

to describe the location and orientation of joint i+1 with respect to joint i. Three of the parameters describe the location of joint i+1; one of which generally describes the link length. The other three parameters describe the orientation of joint i+1.

The dependent or controlled parameter of a link, varied to achieve desired positions is called the joint variable. The dependent variable for a prismatic joint (see figure 1-4) is contained in the position terms for link i and describes a translation. The dependent variable for a revolute joint (see figure 1-5) describes a rotation of the coordinate frame describing joint i.

This investigation deals with the accuracy of the geometric parameters of the actual robot for accurate software defined targeting in off-line programming. Decreasing manufacturing tolerances to remove geometric errors and increase robot accuracy would be cost prohibitive. The most logical way to accomodate geometric errors is to include them in the mathematical model of the robot. This investigation uses homogeneous transformations to describe robot geometry in a modified convention similar to the one described by Denavit and Hartenburg (1955). A description of homogeneous transformations and the Denavit-Hartenburg convention are contained in appendices A and B respectively.

Work investigating the effects of errors in the ideal link geometry began as early as 1975 in which Dubowsky

y_{i-1}

x_{i-1}

Joint Variable

z_i

y_i

Joint i

z_{i-1}

x_i

Joint i+1

Link i
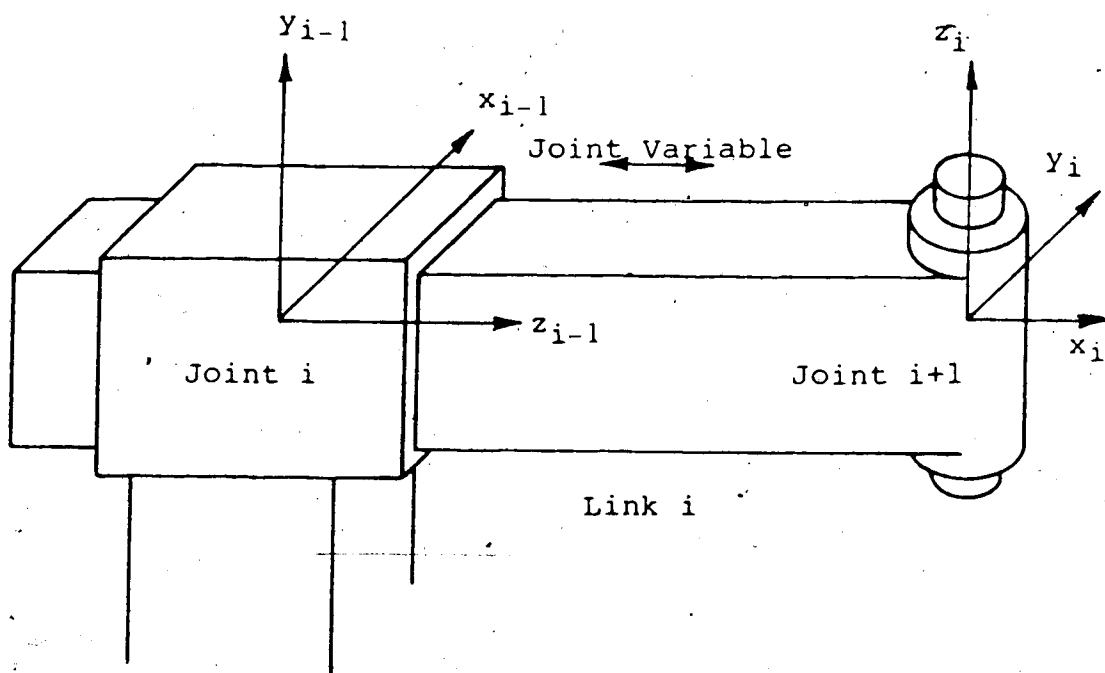
Figure 1-4 Prismatic Joint
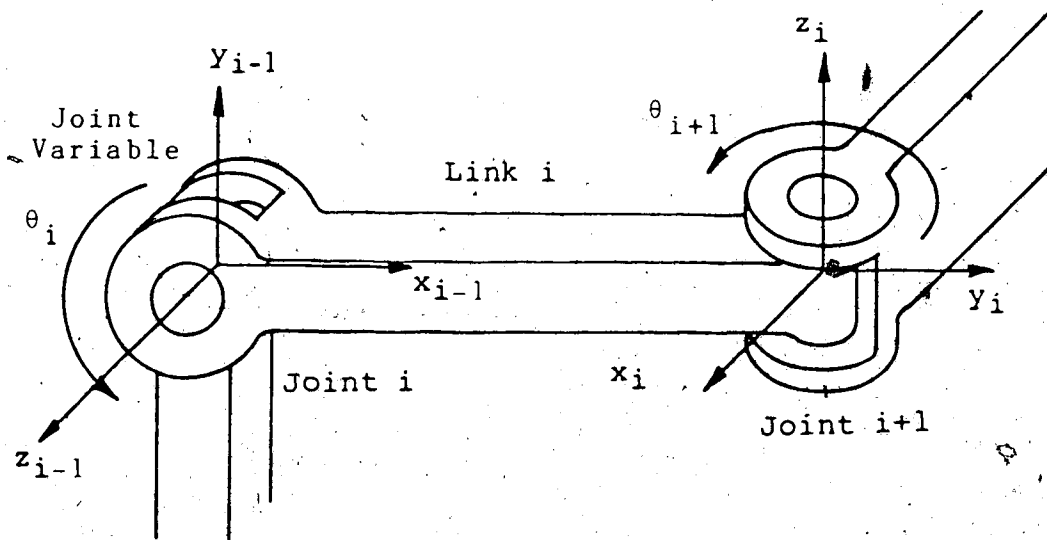
Figure 1-5   Revolute Joint

developed a computer technique for identifying link length errors and clearances in machine connections. Scheffer (1982) developed a calibration method for industrial robots. His method payed special attention to the joint variables determining initial encoder values and effective gear ratios. His work introduced a new branch to traditional metrology he termed "robot metrology" and developed several instruments that met the requirements for calibrating robots.

Yu and Zhang (1983) outlined a method to generate a single 4 by 4 correction matrix from repetitive position measurements of the end effector in a defined work volume. Mooring (1983) investigated the effects of joint axis misalignments on robot positioning accuracy. Mooring showed that the Denavit-Hartenburg convention of homogeneous transformations for describing individual links became ill-conditioned for some small joint axis misalignments. Using an alternate formulation described by Suh and Radcliffe (1978), Mooring showed that a 1 degree misalignment in the shoulder joint of a typical industrial robot, the Unimation Puma 600, resulted in a maximum position error of 32.6 mm. The Puma 600 robot has an arm length of 1295 mm with a quoted repeatability error of 0.1 mm. He further outlined a parameter identification algorithm in which the robot is mounted in an instrumented workspace. Locations of points on the robot gripper are determined before and after the rotation of a single joint.

The joint axis misalignments are determined from the position data.

Wu (1984) used the Denavit-Hartenburg homogeneous transformation convention to develop an explicit linear mathematical error model which not only generates robot error envelopes but can be used to aid in robot design. Wu further outlined a calibration method in which the robot end effector is moved to precise Cartesian positions from which the kinematic parameters may be estimated.

Foulloy and Kelley (1984) employed a least square error method to robot position data to improve robot accuracy. In this method, a cube with holes on two faces for which the positions are known very accurately is used as a reference frame. The calibration procedure consists of determining the robot positions required to place a special calibration tool in the holes of the cube. This informaiton is used to determine a 6 by 6 correction matrix to adjust the joint variables over the working volume in the region around the cube.

The calibration procedures described above have several drawbacks which make them difficult to implement in industrial settings or inadequate for developing an accurate geometric description of the robot for use in off-line programming. The earlier works by Dubowsky and Scheffer do not consider joint axis orientation errors. In chapter 2 these are shown to cause the most significant manipulator errors. The methods described by the teams of Yu-Zhang and

Foulloy-Kelley incorporated single correction matrices which may provide adequate adjustment in a small work space but do not accurately describe the robot or its end effector over the entire work volume.

The other calibration methods developed by Mooring and Wu required either precision measurements of the robot position and orientation or precision locations in the robot work space to determine the correction terms. It would not be desirable to turn the robot work environment into a precision measurement site due to the cost of instrumenting each work space or the down time it would take for the conversion. Removal of the robot to a calibration site is also undesirable since errors in the orientation of the base of the robot can only be measured in the work location and would also require considerable down time.

Ideally a calibration procedure should be conducted in the work environment without requiring costly or major changes. The procedure should also determine the correct kinematic parameters which accurately describe the robot in its entire work volume.

In the present investigation a new calibration procedure for revolute joints is developed which overcomes several of the short comings of the previously mentioned methods. The requirements for the new calibration method were that it could be conducted in the work environment without requiring extensive or time consuming changes. It was also desired that the calibration procedure be automated

to increase the speed and ease of conducting the calibration.

The development of the new calibration method begins in chapter 2 where a linear error model is used to describe the individual link geometry and the entire manipulator. The linear error model parallels Wu's model with the exception of the use of a modified Denavit-Hartenburg transformation convention. The modified transformation was used to avoid the ill-conditioning problems associated with the conventional model. The linear error model reveals that for the four fixed geometric parameters for each link, errors in the orientation of the joint axis cause the most significant manipulator errors. Errors in the joint axis orientation are described as twist and skew misalignments (see figure 1-6).

Chapter 3 describes the development of the calibration method using a digital camera and two vertical references. A camera mounted on the end effector of a robot should be able to observe the position errors caused by the joint misalignments relative to a vertical reference. The equations from the linear error model of chapter 2 are used to determine the robot configurations and motions which reveal the joint axes misalignments in the camera pictures.

The calibration method is then implemented on a typical revolute robot configuration in chapter 4. The calibration method is developed for both vertical and horizontal joint axes. The transformation equations which

actual axis
orientation

α

theoretical
axis
orientation

a)   Twist Misalignment, α

actual axis
orientation

γ

theoretical
axis
orientation
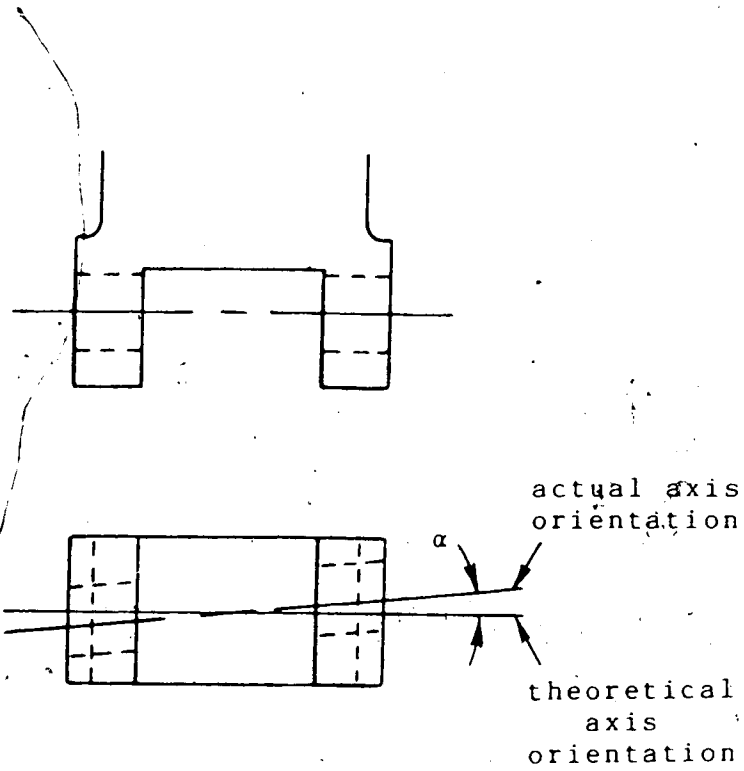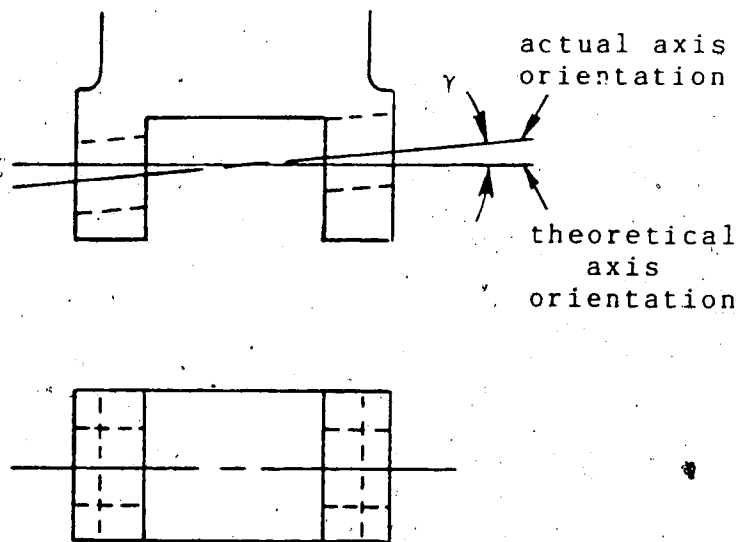
b)   Skew Misalignment, γ

Figure 1-6   Twist and Skew Joint Axis Misalignments

describe the robot-camera system are used to develop the equations which determine the misalignments.

The calibration method was tested on a Mitsubishi RM-101 robot using a Micromint Micro D-cam digital camera with a resolution of 256 by 256 pixels. The results of the tests are given in chapter 5. Chapter 6 discusses the accuracy of the link joint variable with respect to end effector accuracy.

CHAPTER 2

Identification of Dominant Contributers to

Position Errors

This investigation develops a calibration method for manipulators with revolute links. Errors in each of the kinematic parameters for each link will cause position and/or orientation errors in the end effector of the manipulator. If errors in specific parameters dominate end effector errors then determination of those parameters is of prime importance. This chapter determines which errors in the kinematic parameters cause the largest manipulator errors.

To model a general manipulator a modified Denavit-Hartenburg transformation convention is used which adequately describes potential errors in the link geometry. A linear error model is developed which parallels Wu's (1984) work with the conventional Denavit-Hartenburg model. The resulting equations of the linear error model reveal which errors in the kinematic parameters are most important.

An n degree-of-freedom manipulator consists of n links and n joints. The use of homogeneous transformations to describe the relationship between connected links was first implemented by Denavit and Hartenburg (1955). Unfamiliar readers are refered to appendices A, B, and

references by Paul (1981) and Snyder (1985). The kinematic
parameters which define a homogeneous transformation
determine the relationship between the coordinate frames
embedded in consecutive links. By placing specific
restrictions on the orientations of the coordinate frames on
each link, Denavit and Hartenburg were able to describe
manipulator links using only four parameters rather than the
usual six required to describe any general position and
orientation transformation.

An illustration of the link parameters used in the
Denavit-Hartenburg convention for a revolute link is given
in figure 2-1 and the associated A matrix is given by

$$A_i = \begin{bmatrix} C\theta_i & -S\theta_i Ca_i & S\theta_i Sa_i & l_i C\theta_i \\ S\theta_i & C\theta_i Ca_i & -C\theta_i Sa_i & l_i S\theta_i \\ 0 & Sa_i & Ca_i & r_i \\ 0 & 0 & 0 & 1 \end{bmatrix} \qquad (2-1)$$

Abbreviations for cosine and sine are given by C and S
respectively throughout this work. The joint variable for a
revolute link is given by θ_i. The position of the joint
axis of the connected link is described by the link length,
l_i, and the distance between the normals, r_i. The
orientation of the joint axis is described by the twist
angle, α_i, and the geometric combination of the link length
and distance.

Small errors in the joint axis orientation can cause
difficulties for the Denavit-Hartenburg convention. Small
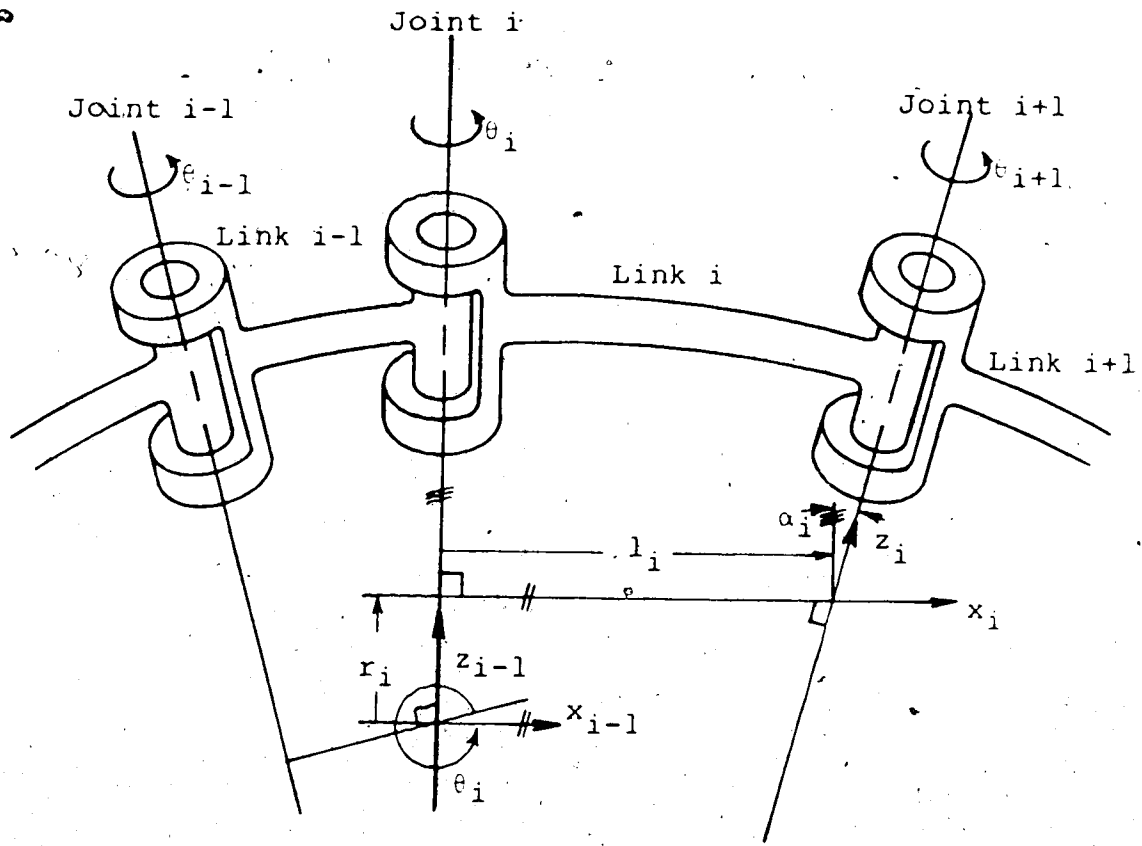
Figure 2-1   Link Parameters for a Revolute Joint Using the
Denavit-Hartenburg Convention

skew errors in the joint axis orientation cause the link

transformation to become ill-conditioned as shown by Mooring

(1983). Figure 2-2 illustrates two joint axes which are

"almost" parallel with a small skew misalignment. The link

coordinate system is located at the point where the two

joint axes intersect, which will be some large distance from

the physical link. By definition, the link length then

becomes zero because the two joint axes intersect. The link

distance, which is defined as zero for parallel joint axes,

becomes very large describing the location of the link

coordinate system. These effects result in an

ill-conditioned transformation matrix. To avoid this

ill-conditioned state for describing small skew errors

Kermack (1986) modified the Denavit-Hartenburg

transformation by including a rotation, γ, about the link y

axis. Details of the modified Denavit-Hartenburg convention

are given in appendix B.

The Denavit-Hartenburg A matrix is replaced by the

following D transformation matrix.

$$D_i = A_i \, Rot(y,\gamma_i) \qquad\qquad (2-2)$$

$$= \begin{bmatrix}
C\theta_i C\gamma_i - S\theta_i S\alpha_i S\gamma_i & -S\theta_i C\alpha_i & C\theta_i S\gamma_i + S\theta_i S\alpha_i C\gamma_i & l_i C\theta_i \\
S\theta_i C\gamma_i + C\theta_i S\alpha_i S\gamma_i & C\theta_i C\alpha_i & S\theta_i S\gamma_i - C\theta_i S\alpha_i C\gamma_i & l_i S\theta_i \\
-C\alpha_i S\gamma_i & S\alpha_i & C\alpha_i C\gamma_i & r_i \\
0 & 0 & 0 & 1
\end{bmatrix}$$

θ is the joint variable for the revolute link. The position
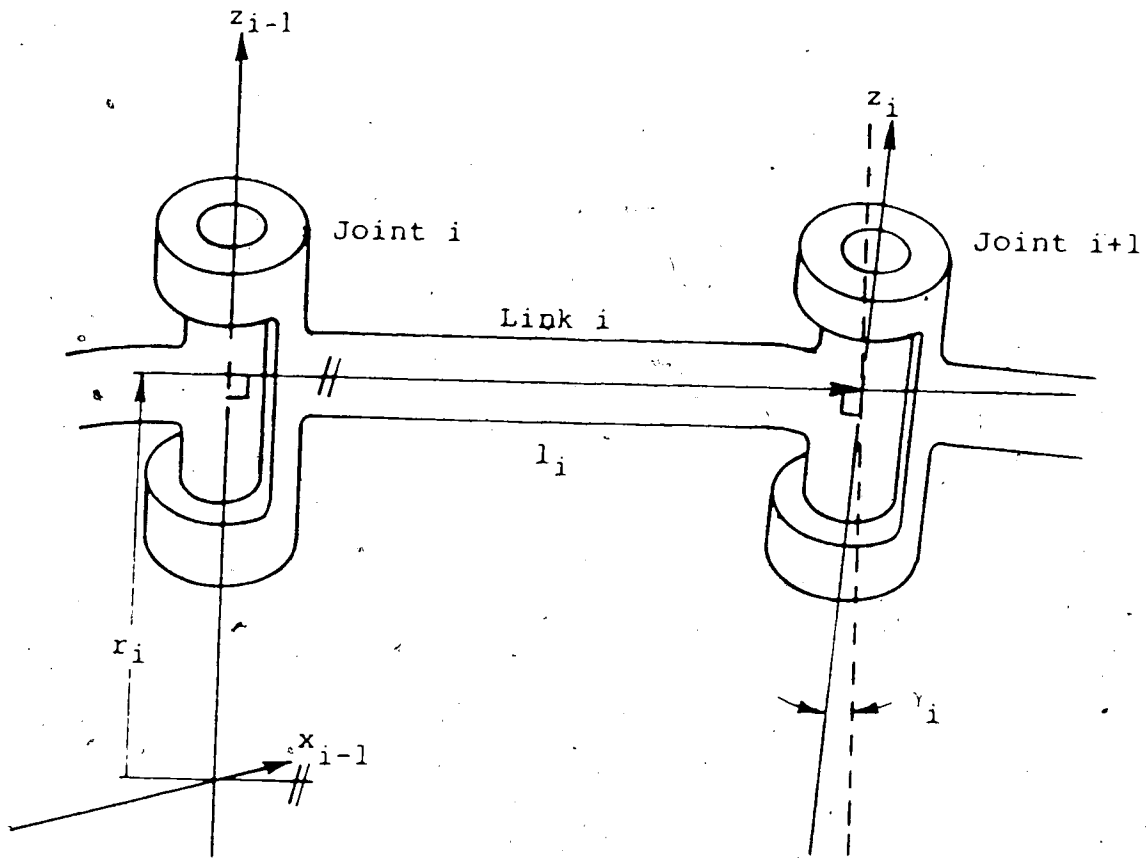
z_{i-1} and z_i will intersect at
some large distance from link i

For small skew misalignments (γ_i)

$$l_i \rightarrow 0$$

$$r_i \rightarrow \infty$$

Figure 2-2   Sensitivity of the Denavit-Hartenburg Convention
to Small Skew Misalignments

of the joint axis of the connected link is described by the
link length, l_i, and the distance between the normals, r_i.
The orientation of the joint axis is now described by the
twist angle, α_i, and the new term, the yaw angle, γ_i. With
this modified convention the link coordinate system will
always be located at the physical joint and not at some
far-removed location in space. This geometric model will
therefore not exhibit an ill-conditioned state when
describing skew misalignments. Errors in the five kinematic
parameters (l_i, r_i, θ_i, α_i, γ_i) will cause position and/or
orientation errors in the end effector of the manipulator.

The method which follows parallels the work outlined
by Wu (1984). Wu developed an error model using the
Denavit-Hartenburg convention as a tool for designing robot
manipulators. Due to the weakness of the Denavit-Hartenburg
convention for describing skew misalignments, Wu's error
model did not reveal their significance in causing errors in
the end effector.

In the pages following in this chapter a linear
error model is developed using the modified
Denavit-Hartenburg convention. The differential change in
an individual link transformation due to kinematic parameter
errors is described by both a differential translation and
rotation matrix and a linear relationship for the kinematic
error terms. The differential relationships for an
individual link may then be applied to determine the
differential changes for the entire manipulator. The error

model using the modified convention reveals that position errors are dominated by errors in both the twist and skew joint axis parameters.

2.1 Differential Changes of Transformation Matrices

For convenience the modified Denavit-Hartenburg transformation for a single link may be represented as

$$D_i = \begin{bmatrix} n_i & o_i & a_i & p_i \\ 0 & 0 & 0 & 1 \end{bmatrix} \qquad (2\text{-}3)$$

where n_i, o_i, a_i, and p_i are the 3 by 1 normal, orientation, approach, and position vectors respectively. For an n degree-of-freedom manipulator the nth link will be described with respect the origin of link 1 by the product of the link transformations (Paul, 1981).

$$T_n = D_1 D_2 D_3 \dots D_n \qquad (2\text{-}4)$$

Small changes in a manipulator transformation can be expressed as a differential transformation with respect to the base coordinate frame and the manipulator transformation, T. For a small translation and rotation a manipulator transformation can be expressed as

$$T + dT = Trans(dx,dy,dz) \ Rot(k,d\phi) \ T \qquad (2\text{-}5)$$

where $Trans(dx,dy,dz)$ is a differential translation transformation of dx, dy, dz in base coordinates and

Rot(k,$d\phi$) represents a differential rotation of $d\phi$ about the vector k also with respect to base coordinates.

An alternate expression for the differential translation and rotation may be given by

$$T + dT = T\ Trans(dx,dy,dz)\ Rot(k,d\phi) \qquad (2-6)$$

where the differential translations and rotation are made with respect to the coordinate frame T. For the small change in the transformation, dT, the differential translation and rotation transformations of equations (2-5) and (2-6) will differ because they are defined with respect to different coordinate frames.

Equation (2-5) may be rewritten as

$$dT = \Delta\ T \qquad (2-7)$$

where the differential translation and rotation matrix, is given by the expression

$$\Delta = Trans(dx,dy,dz)\ Rot(k,d\phi) - I \qquad (2-8)$$

and I denotes the identity matrix. Equation (2-6) may also be expressed in a similar form where dT is given by

$$dT = T\ {}^{T}\!\Delta \qquad (2-9)$$

where ${}^{T}\!\Delta$ represents a differential translation and rotation matrix with respect to the coordinate frame T indicated by the leading superscript. The relationship between differential transformations with respect to the base

coordinate frame and the coordinate frame T may be obtained by equating the expressions of equations (2-7) and (2-9) to give the following result

$$\Delta T = T^T\Delta \qquad (2\text{-}10)$$

and

$$^T\Delta = T^{-1} \Delta\ T \qquad (2\text{-}11)$$

Equation (2-11) relates the differential transformations described with respect to the base coordinate frame and the coordinate frame T.

Paul (1981) showed that the differential translation and rotation matrix, Δ, may be represented in the following form

$$\Delta = \begin{bmatrix} 0 & -\delta_z & \delta_y & d_x \\ \delta_z & 0 & -\delta_x & d_y \\ -\delta_y & \delta_x & 0 & d_z \\ 0 & 0 & 0 & 0 \end{bmatrix} \qquad (2\text{-}12)$$

where the vectors d and δ

$$d = [d_x \quad d_y \quad d_z]^T \qquad (2\text{-}13)$$

$$\delta = [\delta_x \quad \delta_y \quad \delta_z]^T \qquad (2\text{-}14)$$

represent differential translation and rotation vectors respectively. The trailing superscript T, in equations (2-13) and (2-14) indicate the vector transpose.

Using equations (2-11) and (2-12) Paul (1981)

determined that the differential translation and rotation

vectors, ^Td and $^T\delta$, described with respect to the coordinate

frame T are given as

$$^Td_x = \delta \cdot (p \times n) + d \cdot n \qquad\qquad (2\text{-}15)$$

$$^Td_y = \delta \cdot (p \times o) + d \cdot o \qquad\qquad (2\text{-}16)$$

$$^Td_z = \delta \cdot (p \times a) + d \cdot a \qquad\qquad (2\text{-}17)$$

$$^T\delta_x = \delta \cdot n \qquad\qquad (2\text{-}18)$$

$$^T\delta_y = \delta \cdot o \qquad\qquad (2\text{-}19)$$

$$^T\delta_z = \delta \cdot a \qquad\qquad (2\text{-}20)$$

where n, o, a, and p are the 3 by 1 vectors of T. Equations

(2-15) through (2-20) describe the differential translation

and rotation transformation with respect to the coordinate

frame T.

To determine the effect of kinematic parameter

errors on positioning accuracy of a manipulator, the

differential error transformations for individual links must

first be determined. When the transformations describing

each link are determined they may be combined using the form

of equation (2-4) to determine the complete manipulator

relationship.

2.2   Error Model for a Single Link

The transformation for an individual link describing

the relationship between the i-1 and i coordinate frames

with kinematic parameter errors present is given by

$$D_i + dD_i \qquad (2\text{-}21)$$

where dD_i is given by the linear relationship

$$dD_i = \frac{\partial D_i}{\partial \theta_i} \Delta\theta_i + \frac{\partial D_i}{\partial r_i} \Delta r_i + \frac{\partial D_i}{\partial l_i} \Delta l_i + \frac{\partial D_i}{\partial \alpha_i} \Delta\alpha_i + \frac{\partial D_i}{\partial \gamma_i} \Delta\gamma_i \qquad (2\text{-}22)$$

Small errors in the link parameters are represented by $\Delta\theta_i$, Δr_i, Δl_i, $\Delta\alpha_i$, and $\Delta\gamma_i$.

.To obtain the differential error transformation for each link, dD_i is written in the form of equation (2-9).

$$dD_i = D_i \, {}^{D_i}\Delta \qquad (2\text{-}23)$$

${}^{D_i}\Delta$ represents the differential error transformation of the ith link due to the errors in the link kinematic parameters.

To determine an expression for the link differential transformation, ${}^{D_i}\Delta$, equation (2-22) is manipulated into the form of equation (2-23) where the link transformation, D_i, premultiplies the link differential error transformation. To achieve this, the partial derivative terms of equation (2-22) are expressed in a form where the link transformation, D_i, premultiplies a Q transformation. The link transformation, D_i, may then be factored out leaving a relationship of Q transformations and the link error terms.

The partial derivative term for θ in equation (2-22) is expressed as

$$\frac{\partial D_i}{\partial \theta_i} = D_i \, Q_\theta \qquad (2\text{-}24)$$

where Q_θ is determined by

$$Q_\theta = D_i^{-1} \frac{\partial D_i}{\partial \theta_i} \qquad (2-25)$$

Determining Q_θ from equation (2-25) gives

$$Q_\theta = \begin{bmatrix} 0 & -C\alpha_i C\gamma_i & S\alpha_i & l_i S\alpha_i S\gamma_i \\ C\alpha_i C\gamma_i & 0 & C\alpha_i S\gamma_i & l_i C\alpha_i \\ -S\alpha_i & -C\alpha_i S\gamma_i & 0 & -l_i S\alpha_i C\gamma_i \\ 0 & 0 & 0 & 0 \end{bmatrix} \qquad (2-26)$$

Similarly

$$\frac{\partial D_i}{\partial l_i} = D_i Q_l \qquad (2-27)$$

$$Q_l = \begin{bmatrix} 0 & 0 & 0 & C\gamma_i \\ 0 & 0 & 0 & 0 \\ 0 & 0 & 0 & S\gamma_i \\ 0 & 0 & 0 & 0 \end{bmatrix} \qquad (2-28)$$

$$\frac{\partial D_i}{\partial r_i} = D_i Q_r \qquad (2-29)$$

$$Q_r = \begin{bmatrix} 0 & 0 & 0 & -C\alpha_i S\gamma_i \\ 0 & 0 & 0 & S\alpha_i \\ 0 & 0 & 0 & C\alpha_i S\gamma_i \\ 0 & 0 & 0 & 0 \end{bmatrix} \qquad (2-30)$$

$$\frac{\partial D_i}{\partial \alpha_i} = D_i Q_\alpha \qquad (2-31)$$

$$Q_\alpha = \begin{bmatrix} 0 & -S\gamma_i & 0 & 0 \\ S\gamma_i & 0 & -C\gamma_i & 0 \\ 0 & C\gamma_i & 0 & 0 \\ 0 & 0 & 0 & 0 \end{bmatrix} \qquad (2\text{-}32)$$

$$\frac{\partial D_i}{\partial \gamma_i} = D_i \, Q_\gamma \qquad (2\text{-}33)$$

$$Q_\gamma = \begin{bmatrix} 0 & 0 & 1 & 0 \\ 0 & 0 & 0 & 0 \\ -1 & 0 & 0 & 0 \\ 0 & 0 & 0 & 0 \end{bmatrix} \qquad (2\text{-}34)$$

Using the expressions from equations (2-24), (2-27), (2-29), (2-31), and (2-33) for the partial derivatives of the link transformation, equation (2-22) may be rewritten as

$$dD_i = D_i \, (Q_\theta \, \Delta\theta_i + Q_r \cdot \Delta r_i + Q_l \, \Delta l_i + Q_\alpha \, \Delta\alpha_i + Q_\gamma \, \Delta\gamma_i) \qquad (2\text{-}35)$$

The change in the link transformation, dD_i, may now be compared in equations (2-23) and (2-35). The comparison of these equations reveals that the link differential error transformation, $^{D_i}\Delta$, is given by

$$^{D_i}\Delta = Q_\theta \, \Delta\theta_i + Q_r \, \Delta r_i + Q_l \, \Delta l_i + Q_\alpha \, \Delta\alpha_i + Q_\gamma \, \Delta\gamma_i \qquad (2\text{-}36)$$

Combining the results of the transformations in equations (2-26), (2-28), (2-30), (2-32), and (2-34), and noting the locations of the elements in equation (2-12) gives the following results for the differential translation and rotation vectors

$$^{D_i}d = \begin{bmatrix} 1_i Sa_i Sy_i \\ 1_i Ca_i \\ -1_i Sa_i Cy_i \end{bmatrix} \Delta\theta_i + \begin{bmatrix} -Ca_i Sy_i \\ Sa_i \\ Ca_i Cy_i \end{bmatrix} \Delta r_i + \begin{bmatrix} Cy_i \\ 0 \\ Sy_i \end{bmatrix} \Delta l_i \qquad (2\text{-}37)$$

$$^{D_i}\delta = \begin{bmatrix} -Ca_i Sy_i \\ Sa_i \\ Ca_i Cy_i \end{bmatrix} \Delta\theta_i + \begin{bmatrix} Cy_i \\ 0 \\ Sy_i \end{bmatrix} \Delta\alpha_i + \begin{bmatrix} 0 \\ 1 \\ 0 \end{bmatrix} \Delta y_i \qquad (2\text{-}38)$$

The leading superscript indicates the vectors are determined with respect to the link transformation D_i. These vectors describe the translation and rotation errors in the ith link due to the errors in the kinematic parameters.

To shorten the expressions for equations (2-37) and (2-38) the following vectors are defined

$$k_i^1 = [1_i Sa_i Sy_i \quad 1_i Ca_i \quad -1_i Sa_i Cy_i]^T \qquad (2\text{-}39)$$

$$k_i^2 = [-Ca_i Sy_i \quad Sa_i \quad Ca_i Cy_i]^T \qquad (2\text{-}40)$$

$$k_i^3 = [Cy_i \quad 0 \quad Sy_i]^T \qquad (2\text{-}41)$$

$$k_i^4 = [0 \quad 1 \quad 0]^T \qquad (2\text{-}42)$$

Rewriting equations (2-37) and (2-38) gives

$$^{D_i}d = k_i^1 \Delta\theta_i + k_i^2 \Delta r_i + k_i^3 \Delta l_i \qquad (2\text{-}43)$$

$$^{D_i}\delta = k_i^2 \Delta\theta_i + k_i^3 \Delta\alpha_i + k_i^4 \Delta y_i \qquad (2\text{-}44)$$

The differential error transformation for each link is defined by the translation and rotation vectors in

equations (2-43) and (2-44). The relationship between two connected links can be expressed in terms of the differential error transformation as

$$D_i + dD_i = D_{i}(I + {}^{D_i}\Delta) \qquad (2\text{-}45)$$

This expression for the link transformation describes each link with kinematic errors present. The relationships for each link are now used to determine the complete manipulator transformation.

2.3   Error Model for a Manipulator

For an n degree-of-freedom manipulator the total manipulator transformation is the product of the link transformations, equation (2-4), i.e.

$$T_n + dT_n = (D_1 + dD_1)(D_2 + dD_2) \ldots (D_n + dD)$$

$$= \prod_{i=1}^{n} (D_i + dD_i) \qquad (2\text{-}46)$$

where dT_n represents the total differential change of the end of the manipulator due to the 5n kinematic parameter errors. To determine the position accuracy of the manipulator an expression for dT_n is extracted from equation (2-46).

Expanding equation (2-46) and ignoring higher order terms results in the following expression (Wu, 1984).

$$T_n + dT_n = T_n + \sum_{i=1}^{n} (D_1 \ldots D_{i-1}\, dD_i\, D_{i+1} \ldots D_n) \qquad (2\text{-}47)$$

Substituting equation (2-23) into equation (2-47) gives the result

$$T_n + dT_n = T_n + \sum_{i=1}^{n} (D_1 \ldots D_i\, {}^{D_i}\Delta\, D_{i+1} \ldots D_n) \qquad (2\text{-}48)$$

Then the expression for dT_n is given by

$$dT_n = \sum_{i=1}^{n} (D_1 \ldots D_i\, {}^{D_i}\Delta\, D_{i+1} \ldots D_n) \qquad (2\text{-}49)$$

which may also be rewritten as

$$dT_n = \sum_{i=1}^{n} (T_n (D_{i+1} \ldots D_n)^{-1}\, {}^{D_i}\Delta\, (D_{i+1} \ldots D_n)) \qquad (2\text{-}50)$$

By defining U_i as

$$U_i = D_i\, D_{i+1} \ldots D_n \qquad (2\text{-}51)$$

equation (2-50) may be rewritten as

$$dT_n = \sum_{i=1}^{n} (T_n\, U_{i+1}^{-1}\, {}^{D_i}\Delta\, U_{i+1}) \qquad (2\text{-}52)$$

The total manipulator error transformation, dT_n, describes the error of the end of the manipulator due to the kinematic errors in all of the links. Equation (2-52) is used to determine the form of the manipulator differential error transformation, ${}^{T_n}\Delta$, by the relationship

$$dT_n = T_n\, {}^{T_n}\Delta \qquad (2\text{-}53)$$

Then from equation (2-52) the expression for the manipulator differential error transformation is given by

$$^T_n\Delta = \sum_{i=1}^{n} (U_{i+1}^{-1} \; {}^{D_i}\Delta \; U_{i+1}) \tag{2-54}$$

where $^T_n\Delta$ will have the form of the differential transform matrix described in equation (2-12). Using the results of : equations (2-15) through (2-20) the following set of translation and rotation vectors are obtained for the error terms of the manipulator differential transformation

$$^T_{n}d_x = \sum_{i=1}^{n} (n^{U_{i+1}} \cdot {}^{D_i}d + (p^{U_{i+1}} \times n^{U_{i+1}}) \cdot {}^{D_i}\delta) \tag{2-55}$$

$$^T_{n}d_y = \sum_{i=1}^{n} (o^{U_{i+1}} \cdot {}^{D_i}d + (p^{U_{i+1}} \times o^{U_{i+1}}) \cdot {}^{D_i}\delta) \tag{2-56}$$

$$^T_{n}d_z = \sum_{i=1}^{n} (a^{U_{i+1}} \cdot {}^{D_i}d + (p^{U_{i+1}} \times a^{U_{i+1}}) \cdot {}^{D_i}\delta) \tag{2-57}$$

$$^T_{n}\delta_x = \sum_{i=1}^{n} (n^{U_{i+1}} \cdot {}^{D_i}\delta) \tag{2-58}$$

$$^T_{n}\delta_y = \sum_{i=1}^{n} (o^{U_{i+1}} \cdot {}^{D_i}\delta) \tag{2-59}$$

$$^T_{n}\delta_z = \sum_{i=1}^{n} (a^{U_{i+1}} \cdot {}^{D_i}\delta) \tag{2-60}$$

where $n^{U_{i+1}}$, $o^{U_{i+1}}$, $a^{U_{i+1}}$, and $p^{U_{i+1}}$ are the 3 by 1 vectors of U_{i+1} and, ${}^{D_i}d$ and ${}^{D_i}\delta$ are the error vectors of ${}^{D_i}\Delta$ when expressed in the form of equations (2-13) and (2-14). Substituting for ${}^{D_i}d$ and ${}^{D_i}\delta$ from equations (2-43) and (2-44) respectively, gives the following expressions for the differential error terms

$$^Tn_{d_x} = \sum_{i=1}^{n} ([n^{U_{i+1}} \cdot k_i^1 + (p^{U_{i+1}} \times n^{U_{i+1}}) \cdot k_i^2]\Delta\theta_i$$

$$+ [n^{U_{i+1}} \cdot k_i^2]\Delta r_i + [n^{U_{i+1}} \cdot k_i^3]\Delta l_i + [(p^{U_{i+1}} \times n^{U_{i+1}}) \cdot k_i^3]\Delta\alpha_i$$

$$+ [(p^{U_{i+1}} \times n^{U_{i+1}}) \cdot k_i^4]\Delta\gamma_i) \tag{2-61}$$

$$^Tn_{d_y} = \sum_{i=1}^{n} ([o^{U_{i+1}} \cdot k_i^1 + (p^{U_{i+1}} \times o^{U_{i+1}}) \cdot k_i^2]\Delta\theta_i$$

$$+ [o^{U_{i+1}} \cdot k_i^2]\Delta r_i + [o^{U_{i+1}} \cdot k_i^3]\Delta l_i + [(p^{U_{i+1}} \times o^{U_{i+1}}) \cdot k_i^3]\Delta\alpha_i$$

$$+ [(p^{U_{i+1}} \times o^{U_{i+1}}) \cdot k_i^4]\Delta\gamma_i) \tag{2-62}$$

$$^Tn_{d_z} = \sum_{i=1}^{n} ([a^{U_{i+1}} \cdot k_i^1 + (p^{U_{i+1}} \times a^{U_{i+1}}) \cdot k_i^2]\Delta\theta_i$$

$$+ [a^{U_{i+1}} \cdot k_i^2]\Delta r_i + [a^{U_{i+1}} \cdot k_i^3]\Delta l_i + [(p^{U_{i+1}} \times a^{U_{i+1}}) \cdot k_i^3]\Delta\alpha_i$$

$$+ [(p^{U_{i+1}} \times a^{U_{i+1}}) \cdot k_i^4]\Delta\gamma_i) \tag{2-63}$$

$$^Tn_{\delta_x} = \sum_{i=1}^{n} ([n^{U_{i+1}} \cdot k_i^2]\Delta\theta_i + [n^{U_{i+1}} \cdot k_i^3]\Delta\alpha_i$$

$$+ [n^{U_{i+1}} \cdot k_i^4]\Delta\gamma_i) \tag{2-64}$$

$$^{T_n}\delta_y = \sum_{i=1}^{n} ([o^{U_{i+1}} \cdot k_i^2]\Delta\theta_i + [o^{U_{i+1}} \cdot k_i^3]\Delta\alpha_i$$

$$+ [o^{U_{i+1}} \cdot k_i^4]\Delta\gamma_i) \qquad (2-65)$$

$$^{T_n}\delta_z = \sum_{i=1}^{n} ([a^{U_{i+1}} \cdot k_i^2]\Delta\theta_i + [a^{U_{i+1}} \cdot k_i^3]\Delta\alpha_i$$

$$+ [a^{U_{i+1}} \cdot k_i^4]\Delta\gamma_i) \qquad (2-66)$$

The expressions for the differential translation and rotation errors for the manipulator may be expressed by the following equations

$$^{T_n}d = M^1 \Delta\theta + M^2 \Delta r + M^3 \Delta l + M^4 \Delta\alpha + M^5 \Delta\gamma \qquad (2-67)$$

$$^{T_n}\delta = M^2 \Delta\theta + M^3 \Delta\alpha + M^4 \Delta\gamma \qquad (2-68)$$

where ^{T_n}d is the translation error vector [$^{T_n}d_x$, $^{T_n}d_y$, $^{T_n}d_z$]^T and $^{T_n}\delta$ is the rotation error vector [$^{T_n}\delta_x$, $^{T_n}\delta_y$, $^{T_n}\delta_z$]^T. The link parameter errors are represented by the vectors

$$\Delta\theta = [\Delta\theta_1 \quad \Delta\theta_2 \cdots \Delta\theta_n]^T \qquad (2-69)$$

$$\Delta r = [\Delta r_1 \quad \Delta r_2 \cdots \Delta r_n]^T \qquad (2-70)$$

$$\Delta l = [\Delta l_1 \quad \Delta l_2 \cdots \Delta l_n]^T \qquad (2-71)$$

$$\Delta\alpha = [\Delta\alpha_1 \quad \Delta\alpha_2 \cdots \Delta\alpha_n]^T \qquad (2-72)$$

$$\Delta\gamma = [\Delta\gamma_1 \quad \Delta\gamma_2 \cdots \Delta\gamma_n]^T \qquad (2-73)$$

The M^j matrices of equations (2-67) and (2-68) are 3 by n matrices where the ith column is given by

$$M_i^1 = \begin{bmatrix} {}^U n_{i+1} \cdot k_i^1 + ({}^U p_{i+1} \times {}^U n_{i+1}) \cdot k_i^2 \\[2ex] {}^U o_{i+1} \cdot k_i^1 + ({}^U p_{i+1} \times {}^U o_{i+1}) \cdot k_i^2 \\[2ex] {}^U a_{i+1} \cdot k_i^1 + ({}^U p_{i+1} \times {}^U a_{i+1}) \cdot k_i^2 \end{bmatrix} \qquad (2\text{-}74)$$

$$M_i^2 = \begin{bmatrix} {}^U n_{i+1} \cdot k_i^2 \\[2ex] {}^U o_{i+1} \cdot k_i^2 \\[2ex] {}^U a_{i+1} \cdot k_i^2 \end{bmatrix} \qquad (2\text{-}75)$$

$$M_i^3 = \begin{bmatrix} {}^U n_{i+1} \cdot k_i^3 \\[2ex] {}^U o_{i+1} \cdot k_i^3 \\[2ex] {}^U a_{i+1} \cdot k_i^3 \end{bmatrix} \qquad (2\text{-}76)$$

$$M_i^4 = \begin{bmatrix} ({}^U p_{i+1} \times {}^U n_{i+1}) \cdot k_i^3 \\[2ex] ({}^U p_{i+1} \times {}^U o_{i+1}) \cdot k_i^3 \\[2ex] ({}^U p_{i+1} \times {}^U a_{i+1}) \cdot k_i^3 \end{bmatrix} \qquad (2\text{-}77)$$

$$M_i^5 = \begin{bmatrix} ({}^U p_{i+1} \times {}^U n_{i+1}) \cdot k_i^4 \\[2ex] ({}^U p_{i+1} \times {}^U o_{i+1}) \cdot k_i^4 \\[2ex] ({}^U p_{i+1} \times {}^U a_{i+1}) \cdot k_i^4 \end{bmatrix} \qquad (2\text{-}78)$$

$$M_i^6 = \begin{bmatrix} {}_n^{U_{i+1}} \cdot k_i^4 \\ {}_o^{U_{i+1}} \cdot k_i^4 \\ {}_a^{U_{i+1}} \cdot k_i^4 \end{bmatrix}$$ (2-79)

Equations (2-67) and (2-68) define the vectors which comprise the differential error transformation, ${}^{T_n}\Delta$, for the complete manipulator. Having determined the components of ${}^{T_n}\Delta$ the error transformation, dT_n, may be determined by equation (2-53)

$$dT_n = T_n \, {}^{T_n}\Delta$$

$$= \begin{bmatrix} dn & do & da & dp \\ 0 & 0 & 0 & 0 \end{bmatrix}$$ (2-80)

where

$$dn = o^{T_n} \, {}^{T_n}\delta_z - a^{T_n} \, {}^{T_n}\delta_y$$ (2-81)

$$do = - n^{T_n} \, {}^{T_n}\delta_z + a^{T_n} \, {}^{T_n}\delta_x$$ (2-82)

$$da = n^{T_n} \, {}^{T_n}\delta_y - o^{T_n} \, {}^{T_n}\delta_x$$ (2-83)

$$dp = n^{T_n} \, {}^{T_n}\delta_x + o^{T_n} \, {}^{T_n}\delta_y + a^{T_n} \, {}^{T_n}\delta_z$$ (2-84)

and n, o, a, and p are the 3 by 1 vectors of manipulator transformation, T_n. Equations (2-81) through (2-84) define the vectors for the total manipulator error transformation. Equation (2-84) represents the position error of the

manipulator and equations (2-81), (2-82), and (2-83), the errors in the normal, orientation, and approach vectors, respectively.

Having obtained the total manipulator error transformation, dT_n, the equations may be examined to determine which errors in the kinematic parameters will cause the most significant manipulator errors. To determine the dominant error terms one must examine equations (2-81) through (2-84). The normal, orientation, approach, and position vectors of the manipulator transformation, T_n, will vary depending on the position of the manipulator. Thus, the errors in the manipulator will vary with its position, as expected.

The dominant error terms will be identified in the differential translation and rotation vectors which define the manipulator geometry with respect to the kinematic parameter errors. The dominant components of these vectors, defined in equations (2-67) and (2-68) will be determined by the M^j matrices and the magnitude of the errors in the kinematic parameters.

The M^j matrices defined in equations (2-74) through (2-79) consist of the normal, orientation, approach, and position vectors of U_{i+1}, and the k vectors of D_i (equations (2-39) through (2-42)). The vectors, $n^{U_{i+1}}$, $o^{U_{i+1}}$, and $a^{U_{i+1}}$ are by definition of unit magnitude. The vectors k_i^2, k_i^3, and k_i^4 are also of unit magnitude while k_i^1 has a magnitude of l_i, the link length. The position vector $p^{U_{i+1}}$

of the U_{i+1} matrix describes the position of the end of the manipulator with respect to link i+1. The $p^{U_{i+1}}$ vector is therefore dependent upon the kinematic parameters which describe the i+1 through n links of the manipulator. The position vector of the U_{i+1} matrix is the dominant vector of those which determine the M^j matrices.

The dominant M^j matrices will therefore contain the $p^{U_{i+1}}$ or k_i^1 vectors which corresponds with the M^1, M^4, and M^5 matrices. Equation (2-67) reveals that θ, α, and γ are multiplied by these matrices. This separates the kinematic parameters into two groups: the angular parameters, θ, α, and γ multiplied by M^1, M^4, and M^5 respectively, and the length parameters, l and r, multiplied by M^2 and M^3 respectively.

To determine which of these groups of parameters dominate manipulator errors the magnitude of the error terms are examined. Consider an average sized manipulator with an arm length of 1000 mm with approximately equivalent errors with respect to manufacturing tolerences in the length and angular parameters of 0.1 mm and 0.1 degrees (0.002 radians) respectively. Wu (1984) comments that the manufactured accuracy of the length parameters, r and l are in fact much higher than the angular parameters, though he does not specifically define "higher". The maximum value of a component in the M^2 or M^3 matrices is 1. Therefore, the maximum error term resulting from the product of the M matrice with the length error of 0.1 mm is 0.1 mm.

Considering the angular terms, the maximum value of a component in the M^1, M^4, or, M^5 matrices is the manipulator arm length, 1000 mm. The product of the arm length with the angular error of 0.002 radians results in a position error of 2 mm, 20 times greater than the position error caused by a length parameter error.

By comparing the error terms it is apparent that a manipulator is sensitive to errors in θ, α, and γ. These terms will be the dominant parameters which cause manipulator position errors. These are also the only parameters which cause orientation errors; equation (2-68).

For a revolute joint, θ is the joint variable and its accuracy will depend on the resolution of the encoders and resolvers, the accuracy of the robot construction, as well as the number of bits of controller memory assigned for storage. The fixed link parameters of major concern for describing the robot geometry are the twist (α) and skew (γ) angles.

The results of the linear error model correspond with what one would expect to be the dominant error terms. Errors in the joint axis orientation described by the twist and skew angles and the joint variable, θ, are magnified over the length of the successive links due to the dominance of the link length terms in the position vector. Thus, angular parameter errors near the base, in the body or shoulder, are more significant than equal errors in the elbow or wrist (see figure 2-3). If the angular parameter
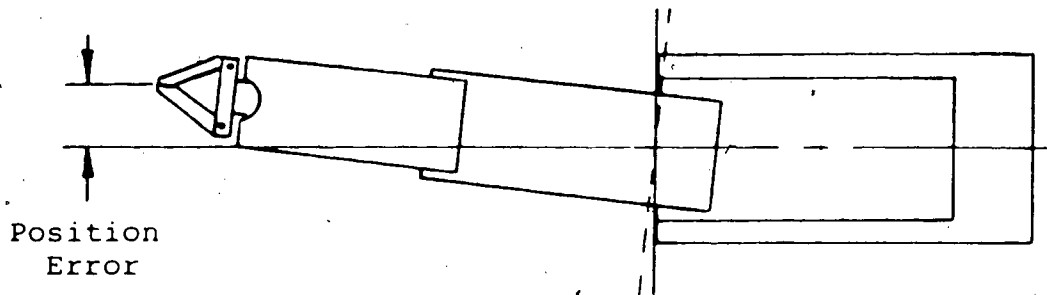
a) Shoulder Joint Axis Misalignment
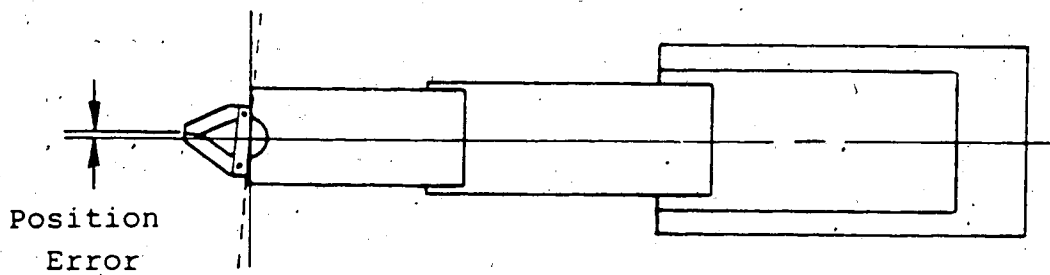
b) Wrist Joint Axis Misalignment

Figure 2-3   Comparison of Position Errors Caused by Joint
            Axis Misalignments in the Shoulder and Wrist

errors of a robot manipulator are known its position accuracy could be greatly increased by using the correct parameters in the control software.

A new calibration method using a digital camera and two vertical sets of target points is developed to measure the twist and skew misalignments which describe the joint axes orientations. This investigation does not deal with the calibration of the joint variable, θ. However, in chapter 6 the calibration of the joint variable will be discussed with respect to the new calibration method. The following chapter uses the equations from the linear error model to determine which motions of the robot will reveal the joint axes misalignments in the camera pictures. This information is then used to develop the general method of the new calibration procedure.

CHAPTER 3

Development of the Calibration Method

In chapter 2 it was shown that errors in the fixed joint axis twist and skew parameters cause the greatest manipulator errors for software defined targeting. This chapter develops a new calibration method for measuring joint axis misalignments using the equations from chapter 2. The general method is then applied to the two general cases of horizontal and vertical joint axes.

In the introduction, the shortcomings and disadvantages of several existing calibration methods are mentioned. The major drawback exhibited by the previous methods was the need for a precision measurement environment to conduct the procedures. The methods which estimated the correct kinematic parameters for a manipulator either required precision measurements of the end effector location for a prescribed set of joint variables, or measurement of the joint variables for the end effector in a precision location. This required either moving the robot to a precision environment to conduct the calibration and neglect measurement of the base orientation errors, or, the conversion of the robot work space into a precision calibration site. Both of these methods would be time consuming and therefore undesirable.

45

The decision to develop a new calibration method was made because it was intuitively visualized that a digital camera mounted on the end effector of a robot would be able to observe joint axis misalignments relative to a vertical reference. A vertical reference could easily be obtained at any location. Thus, the new calibration method could be conducted without the need for a precision calibration site. Further, the calibration method could be conducted in the work environment where measurement of the working base misalignments would be possible without requiring extensive and time consuming changes to the work space. By using a digital camera to acquire the calibration information it would also be possible to automate the calibration method to increase the speed and ease of conducting the procedure.

The new calibration method consists of three components: a digital camera, a vertical set of reference target points, and the procedure to use the camera, reference points, and robot to determine the joint axis misalignments. Each of these components is dealt with individually in this chapter pointing out the role each plays in the new method and the advantages of the new calibration method compared to the previous methods.

3.1   Digital Camera

A digital camera was chosen for the new calibration procedure because it was visualized that a camera mounted on

the end effector of a robot would be able to observe joint

axis misalignments with respect to a vertical reference.

This section in fact shows that a digital camera observes

position errors much larger than those which must be

measured by previous methods. This is shown by comparing

the kinematic description of the previous robot calibration

methods with the present robot-camera method.

The previous calibration methods measured the robot

errors at the end effector. The equations for a robot in a

base coordinate frame without a camera on the end effector

are described by transformation equation (3-1) (see figure

3-1).

$$B \; T_n \; E = P \qquad\qquad (3-1)$$

The base transformation, B, describes link 1 of the

manipulator with respect to the base coordinate frame. The

manipulator transformation, T_n, describes link n of the

manipulator with respect to the first link, and E is the end

effector or gripper transformation describing the end of the

working tool of the robot with respect to link n.

The product of the transformations on the left side

of equation (3-1), B T_n E, describes the end of the working

tool with respect to the base coordinate frame using

transformations describing the robot. The right side of

equation (3-1) is the translation-orientation

transformation, P, which describes the position and

orientation of the end effector with respect to the base
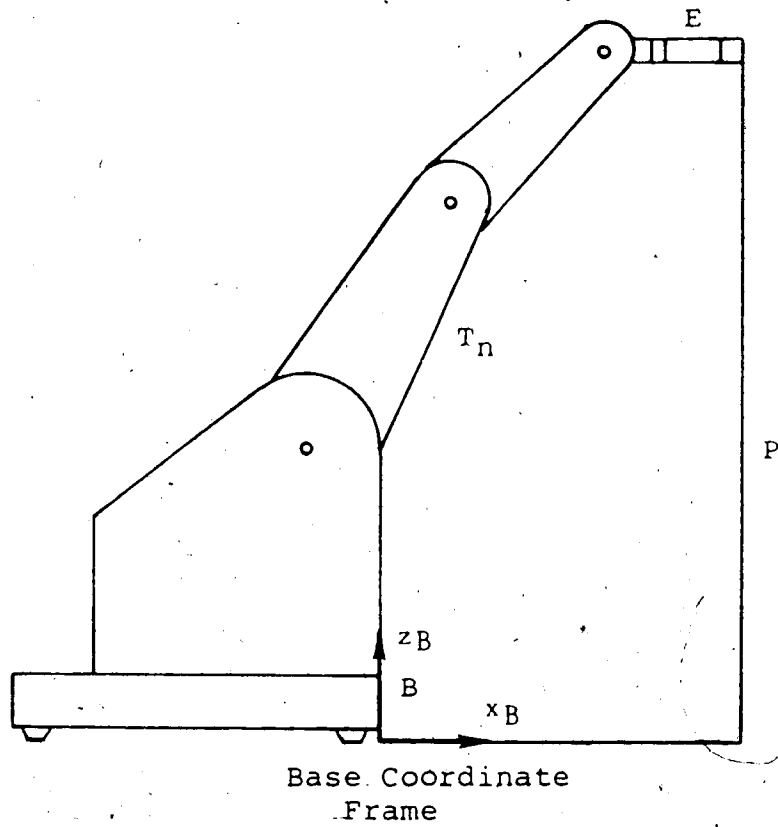
$$B \ T_n \ E \ = \ P$$

Figure 3-1 Transformations for a Robot in a Base Coordinate
Frame

coordinate frame. If the end effector of the manipulator is placed in a position and orientation described by P then 12 non-trivial equations are obtained which may be solved for the joint variables.

The present calibration method places a camera on the end effector which magnifies the misalignment producing even larger position errors in the camera coordinate frame. The robot-camera configuration is described by the following transformation equation (see figure 3-2).

$$B \ T_n \ E \ CAM = P \qquad (3-2)$$

As in equation (3-1), B is the base transformation, T_n is the manipulator transformation and E is the end effector transformation. The camera transformation, CAM, describes objects in the camera coordinate frame with respect to the end effector. The transformation, P, now describes objects in the camera coordinate frame with respect to the base coordinate frame.

The left side of equation (3-2), $B \ T_n \ E \ CAM$, describes objects in the camera frame with respect to the base coordinate frame using transformations describing the robot and camera. The right side of equation (3-2), P, describes objects in the camera frame with respect to the base coordinate frame by a single translation-orientation transformation.

The camera transformation may be represented in the general form
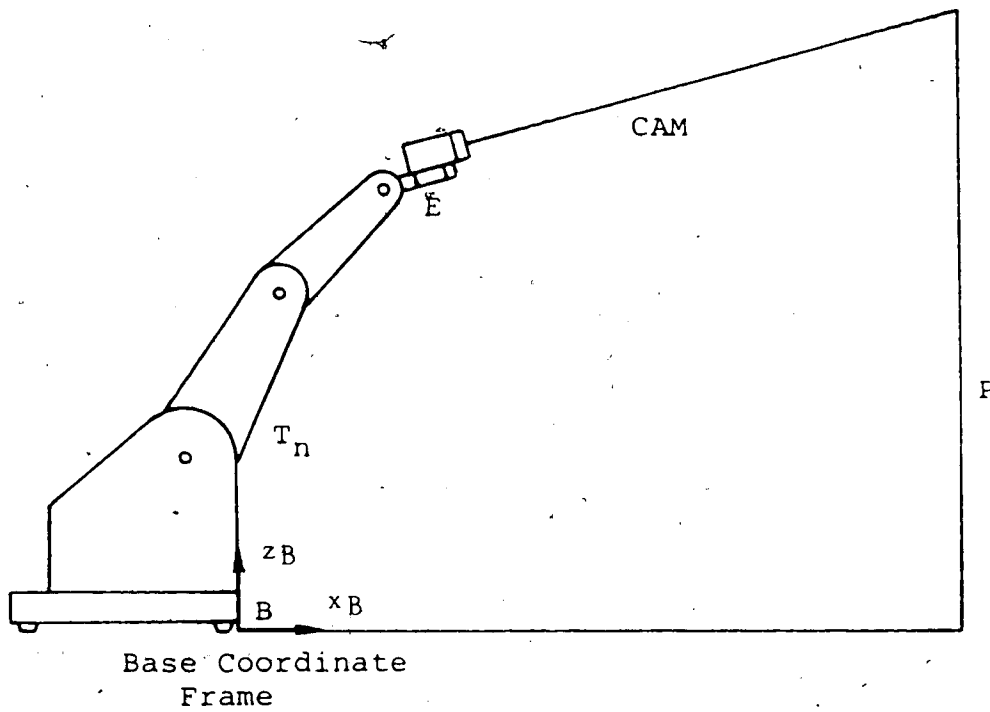
$$B \; T_n \; E \; CAM \; = \; P$$

Figure 3-2   Transformations for a Robot in a Base Coordinate
Frame with a Digital Camera on the End Effector

$$
CAM = \begin{bmatrix} n_x & o_x & a_x & c_x \\ n_y & o_y & a_y & c_y \\ n_z & o_z & a_z & c_z \\ 0 & 0 & 0 & 1 \end{bmatrix} \qquad (3-3)
$$

The vectors, **n**, **o**, and **a** describe the orientation of an object in the camera frame with respect to the camera. The orientation of any single point in the camera frame is essentially arbitrary. The orientation of a reference target point is defined as the orientation of the line passing through the position of the point in the camera frame and the location of the point on the camera lens (figure 3-3).

The camera position vector, **c**, describes the location of a point in the camera coordinate frame. Figure 3-3 illustrates the position vector in which c_z is the perpendicular distance from the camera to the point being considered. The components c_x and c_y of the position vector give the coordinates of the object in a plane perpendicular to the c_z vector.

The camera transformation is obtained by the product of the following translation and rotation transformations

$$
CAM = Trans(c_x, c_y, c_z) \; Rot(x, \lambda) \; Rot(y, \mu) \qquad (3-4)
$$

where λ and μ are the orientation angles shown in figure 3-3. The camera transformation may be expressed in terms of
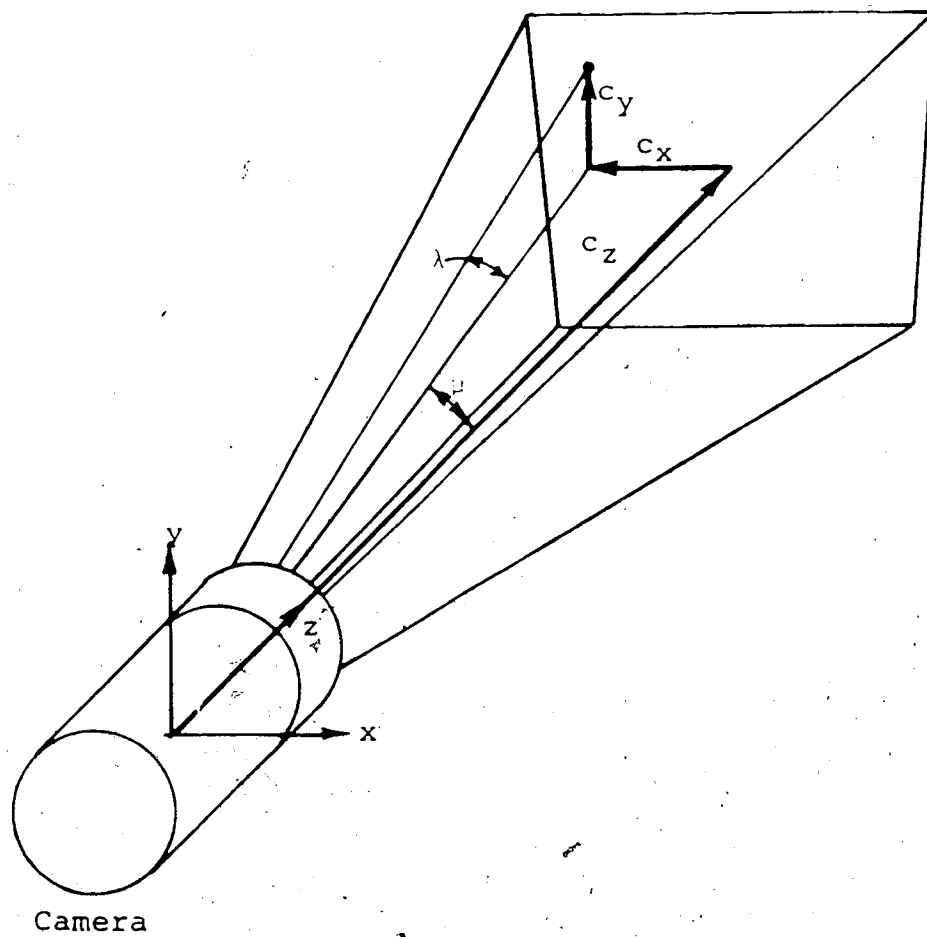
Figure 3-3   Coordinate Frame for the Digital Camera

the camera position vector as

$$
CAM = \begin{bmatrix} f/g & 0 & c_x/g & c_x \\ c_x c_y/fg & c_z/f & -c_y/g & c_y \\ -c_x c_z/fg & c_y/f & c_z/g & c_z \\ 0 & 0 & 0 & 1 \end{bmatrix} \tag{3-5}
$$

where

$$
f = (c_y{}^2 + c_z{}^2)^{1/2} \tag{3-6}
$$

and

$$
g = (c_x{}^2 + c_y{}^2 + c_z{}^2)^{1/2} \tag{3-7}
$$

To compare the two calibration configurations of a robot with and without the digital camera on the end effector, it must be remembered why joint axis misalignments cause the most significant position errors. Errors in the joint axis parameters are magnified over the lengths of the successive links from the misalignment to cause a position error at the end effector. The previous calibration methods measured the position errors at the end effector or the errors in the joint variables for precisely known positions. to determine kinematic parameter errors.

The present calibration method places a camera on the end effector and gathers information from target points several meters from the manipulator. Figures 3-2 and 3-3 illustrate the position vector introduced into the robot-camera equations by placing a camera on the end effector. The camera effectively acts as another link at

the end of the manipulator. Position errors for the robot-camera calibration are measured at the end of the camera transformation where the misalignment has been further magnified by the length of the camera position vector (see figure 3-4). The position error for the present calibration method will be larger than the position error at the end effector measured for the previous methods.

The main advantage of using a digital camera mounted on the end effector in the new calibration method is that the manipulator position errors are magnified in the camera pictures. The digital camera can also be easily mounted to the robot in the work environment and is ideally suited for an automated calibration procedure.

The digital camera generates the CAM transformation on the left side of equation (3-2). The right side of equation (3-2), the position transformation, P, is determined by a vertical reference in the global coordinate frame.

3.2   Vertical Set of Reference Target Points

The second component of the calibration method is a vertical set of reference target points. For any calibration procedure a reference is always needed. To determine the relationships between the robot, camera and global coordinate frames, a reference in the global coordinate frame is needed. In general, the joint axis

Position error observed in camera coordinate frame

Position error at end effector

Elbow joint axis misalignment
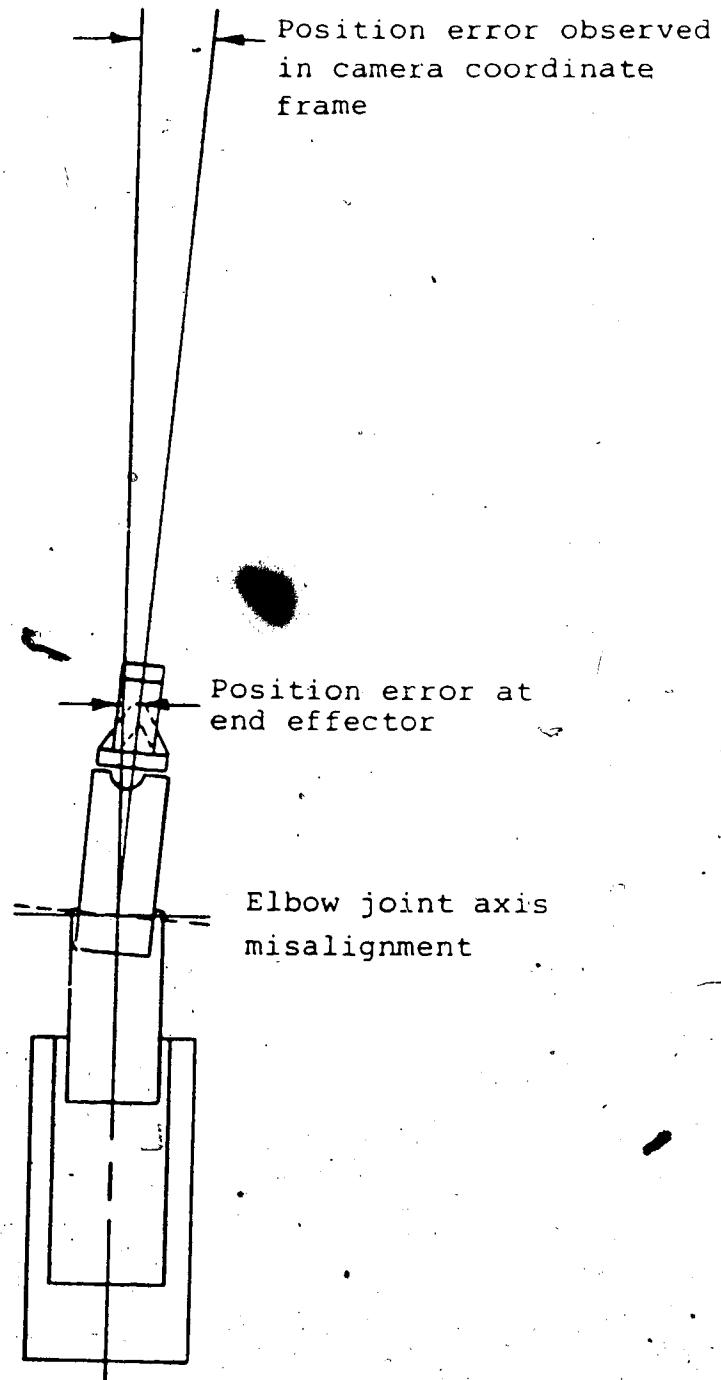
Figure 3-4 Comparison of Position Errors at the Robot End Effector and in the Camera Coordinate Frame

being calibrated will either be horizontal or vertical. A vertical set of target points is chosen for the global reference because of the ease with which it can be obtained at any location.

The ease with which this reference can be determined allows the new calibration method to be conducted in the robot working environment without requiring extensive and time consuming changes.

3.3   Calibration Procedure

The physical components of the robot calibration method have been defined: the digital camera and the vertical reference in the global coordinate frame. The specific procedure defining how the camera and reference can be used to determine the joint axis errors is determined from the linear error model of chapter 2. The equations from the linear error model verify the motions and configurations of the robot which would be intuitively expected to reveal the joint axis misalignments.

The general method for determining the joint misalignments for a manipulator begins at the base of the manipulator. The transformation equations which describe a manipulator start at the base and proceed toward the end effector. Therefore, the misalignments of the base of the robot are determined first. Then the shoulder misalignments are determined using the transformation equations with ,

respect to the base misalignments. The calibration method proceeds to the end effector determining each set of misalignments with respect to the misalignments of the previous joints.

The general procedure for determining the misalignments of each joint consists of taking two pictures of the reference target points separated by the rotation of that joint. The locations of the target points in the camera pictures with respect to their locations on the vertical reference and the single joint rotation will describe the joint axis orientation. By only rotating one joint the relative motion of the target points in the camera pictures will only describe the misalignments of the rotated link. This effectively decouples the effect which all of the misalignments have on the end effector errors and allows the measurement of a single misalignment at a time.

Comparing the locations of the target points from the same vertical reference in two pictures relaxes several requirements for the calibration procedure. The positions of the target points in the global coordinate frame do not have to be very precise because it is the change in location of the target points in the camera frame which determines the misalignment and not the precise locations of the target points. Of course the integrity of the vertical reference is still important. The orientation of the camera on the end effector also does not have to be extremely accurate since two pictures are compared and the errors caused by

camera orientation errors will appear in both pictures.

In summary, the relationship between two pictures of
the target points from the vertical reference will determine
the joint axis misalignments with respect to the vertical
reference and not the precise locations of the points or the
orientation of the camera. This avoids the drawback of
several of the previous calibration methods which required
precision points located throughout the global coordinate
frame.

The optimum manipulator motions and configurations
for the calibration procedure are determined by applying the
linear error model of chapter 2 to a three link manipulator.
A three link manipulator with parallel joints, typical of a
shoulder, elbow, wrist configuration, is illustrated in
figure 3-5a showing the individual link coordinate frames
defined by the Denavit-Hartenburg convention. The three
links have twist and skew parameters of 0 degrees. The
error model is used to determine the appropriate link
rotations for revealing the twist and skew misalignments of
link 1.

For the Denavit-Hartenburg convention link i rotates
about the z_{i-1} axis. Therefore, the joint variable of link
2 is varied, causing rotations about the z_1 axis described
by the twist and skew parameters of link 1. The twist and
skew misalignments for link 1 are defined by rotations about
the x_1 and y_1 axis respectively. For a camera directed
along the x_3 axis the largest manipulator error that is
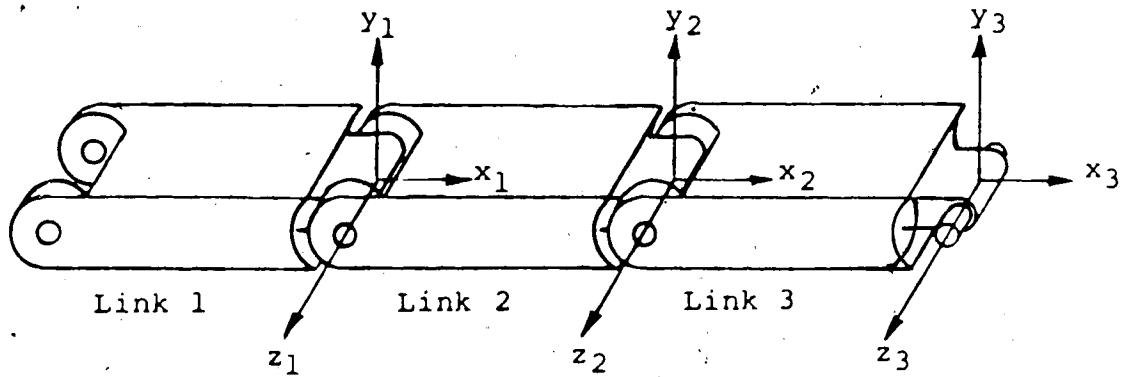
a) Coordinate Frames of a Three Link Manipulator
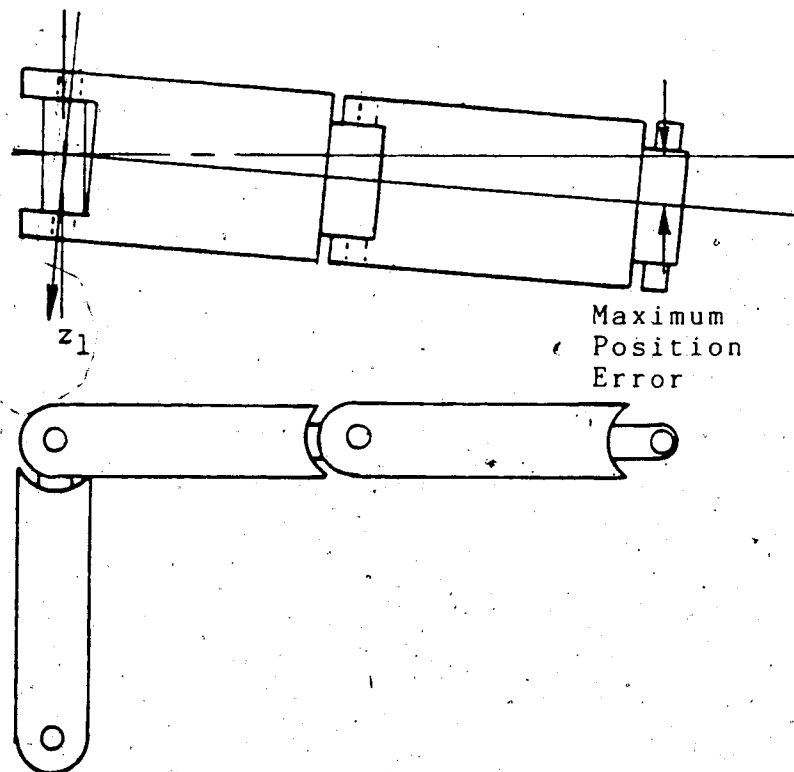
b) Twist Misalignment of Link 1

Figure 3-5 Three Link Manipulator

observed in the camera frame is a position error in the z_1, direction as illustrated in figure 3-5b for a twist misalignment.

The position error described with respect to the manipulator z_1 direction is given by $^T_n d_z$ in equation (2-63). For a twist misalignment of link 1, $^T_n d_z$ reduces to

$$^T_n d_z = [(p^{U_2} \times a^{U_2}) \cdot k_1^3]\Delta\alpha_1$$

$$= q \, \Delta\alpha_1 \qquad\qquad (3-8)$$

where q is defined as the sensitivity of the manipulator to an error in the twist angle of link 1. The position vector, p^{U_2}, and approach vector, a^{U_2}, for links with twist and skew parameters of 0 degrees are given by

$$p^{U_2} = \begin{bmatrix} l_3 C(\theta_2 + \theta_3) + l_2 C\theta_2 \\ l_3 S(\theta_2 + \theta_3) + l_2 S\theta_2 \\ 0 \end{bmatrix} \qquad\qquad (3-9)$$

and

$$a^{U_2} = [0 \quad 0 \quad 1]^T \qquad\qquad (3-10)$$

The k vector, k_1^3, is given by

$$k_1^3 = [C\gamma_1 \quad 0 \quad S\gamma_1]^T$$

$$= [1 \quad 0 \quad 0]^T \qquad\qquad (3-11)$$

The sensitivity is therefore given by

$$q = l_3 S(\theta_2 + \theta_3) + l_2 S\theta_2 \qquad\qquad (3-12)$$

The joint angles at which the sensitivity, q,

becomes a maximum is determined by examining the first derivatives of q with respect to θ_2 and θ_3. The derivatives of q are given by

$$\frac{\partial q}{\partial \theta_2} = l_3 C(\theta_2 + \theta_3) + l_2 C\theta_2 \qquad (3-13)$$

and

$$\frac{\partial q}{\partial \theta_3} = l_3 C(\theta_2 + \theta_3) \qquad (3-14)$$

The location of the maximum sensitivity is determined by the pair of solutions which cause the first derivatives to equal zero. The pair of solutions which statisfy this requirement are

$$\theta_2 = m\pi/2; \qquad m=1,2,3.....$$

and $\qquad \theta_3 = m\pi; \qquad m=0,1,2.....$

The solutions which are of practical significance are

$$\theta_2 = +/- 90 \text{ degrees}$$

and $\qquad \theta_3 = 0 \text{ degrees.}$

The maximum effect of a twist misalignment will therefore be observed when θ_3 is 0 degrees and θ_2 is +/- 90 degrees. This result was expected as can be visualized in figure 3-6.

A rotation of link 2 from -90 to 90 degrees would give the maximum amount of information about a twist misalignment but a rotation this large is generally impractical for the calibration procedure. It would be difficult to accurately place target points in the appropriate positions vertically above and below a horizontal joint axis or in the case of a vertical axis, at
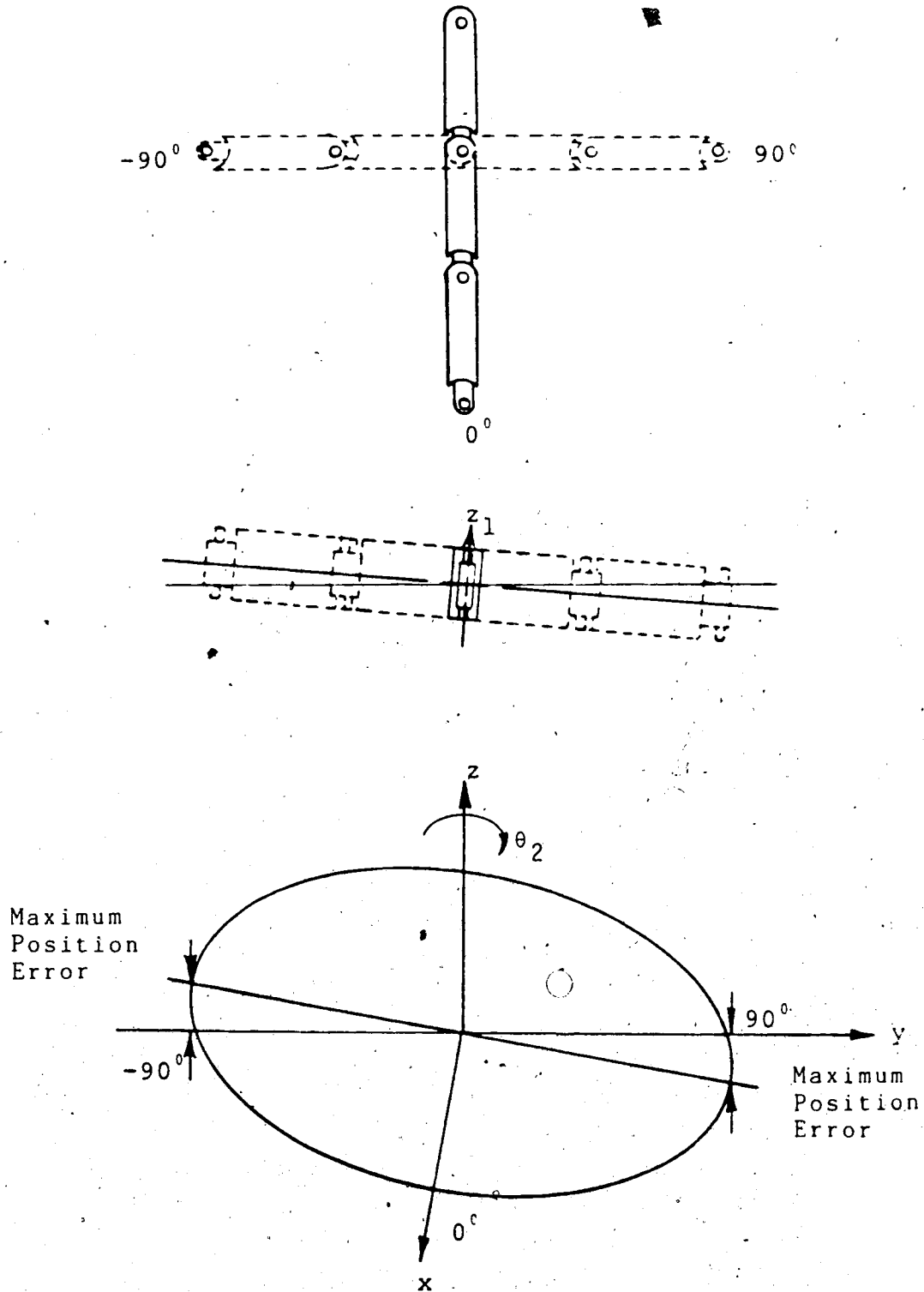
Figure 3-6   Joint Variable Locations of the Maximum Position
              Errors due to a Twist Misalignment

precisely known vertical positions. This would require precision points in the robot work space which are undesirable.

The region where the maximum effect of a twist misalignment is observed for smaller rotations of θ_2 is determined where the rate of change of the sensitivity with respect to θ_2 is a maximum. This region is determined by the second derivative of the sensitivity with respect to θ_2, with θ_3 equal to 0 degrees. The second derivative is given by

$$\frac{\partial^2 q}{\partial \theta_2^2} = -l_3 S(\theta_2 + \theta_3) - l_2 S\theta_2 \qquad (3\text{-}15)$$

which is equal to zero when θ_2 is 0 degrees. Therefore, rotations of θ_2 in the vicinity of 0 degrees will produce the maximum amount of information for determining a twist misalignment, as expected.

Examination of the equations for skew misalignments also produces expected results. For a skew misalignment, $^T_n d_z$ reduces to

$$^T_n d_z = [(p^{U_2} \times a^{U_2}) \cdot k_1^4]\Delta\gamma_1$$
$$= q\,\Delta\gamma_1 \qquad (3\text{-}16)$$

where q is now the sensitivity of the manipulator to errors in the skew parameter. p^{U_2} and a^{U_2} are defined in equations (3-9) and (3-10). The vector k_1^4 is defined in equation (2-42) as

$$k_1^4 = [0 \quad 1 \quad 0]^\top \qquad (3\text{-}17)$$

The expression for q will therefore be given as

$$q = l_3 C(\theta_2 + \theta_3) + l_2 C\theta_2 \qquad (3\text{-}18)$$

The first derivatives of q with respect to θ_2 and θ_3 reveal where the sensitivity is a maximum. The first derivatives are given by

$$\frac{\partial q}{\partial \theta_2} = -l_3 S(\theta_2 + \theta_3) - l_2 S\theta_2 \qquad (3\text{-}19)$$

and

$$\frac{\partial q}{\partial \theta_3} = -l_3 S(\theta_2 + \theta_3) \qquad (3\text{-}20)$$

Equating these derivatives to 0 and observing the manipulator geometry reveals that the maximum effect of a skew misalignment is observed when

$$\theta_2 = 0 \text{ or } 180 \text{ degrees}$$

$$\text{and} \quad \theta_3 = 0 \text{ degrees}.$$

The second derivative of q with respect to θ_2 again reveals the region in which the maximum effect of a misalignment is observed for small rotations of θ_2. The second derivative with respect to θ_2 is given by

$$\frac{\partial^2 q}{\partial \theta_2^2} = -l_3 C(\theta_2 + \theta_3) \qquad (3\text{-}21)$$

Equating the second derivative to 0 with θ_3 equal to 0

degrees reveals that rotations of θ_2 in the vicinity of +/-
90 degrees will produce the maximum position errors for a
skew misalignment.

The examination of three link manipulator revealed
the regions in which the joint variable should be varied to
reveal twist and skew misalignments. For both twist and
skew misalignments with twist and skew parameters ideally 0
degrees, successive joints from the link being rotated
should be positioned at 0 degrees. By examining the link
geometry it can be seen that this corresponds with
positioning the forward links to produce the largest
position vector for the robot. To determine twist
misalignments, pictures of the target points should be taken
separated by rotations of the joint variable in the vicinity
of 0 degrees. Skew misalignments are revealed in pictures
of the target points separated by rotations of the joint
variable in the vicinity of +/- 90 degrees.

In general, the calibration procedure will be used
to determine misalignments for joint axis which should be
either horizontal or vertical. The procedures for dealing
with these two cases are considered separately.

3.3.1   Horizontal Joint Axes

The vertical reference used in the calibration
procedure is ideally suited for measuring misalignments of
horizontal axes. The rotation of the camera about a

perfectly horizontal axis will result in target points which appear in the same horizontal position in the camera frame.

Figure 3-7 illustrates the target point locations observed in the camera for a misaligned horizontal axis. The robot-camera equations are used to determine the joint axis parameters which describe the positions of the target points in the camera pictures. The global vertical reference is taken into account by the fact that two points from the same vertical reference are observed separated by the rotation of the appropriate link. Therefore, the camera information describes the misalignment with respect to the global vertical reference.

3.3.2   Vertical Joint Axes

Vertical joint axes would best be calibrated by a horizontal reference. However, a horizontal reference is not as easy to obtain as a vertical one. Therefore, a calibration procedure was developed using the vertical reference. Determination of the joint axis parameters for a vertical axis using a vertical reference is accomplished by determining the vertical orientation of the reference points in the camera frame and observing the movement of a single point in the camera frame.

Since information about the movement of a single target point is used in the robot-camera equations, the misalignment is not determined with respect to the global
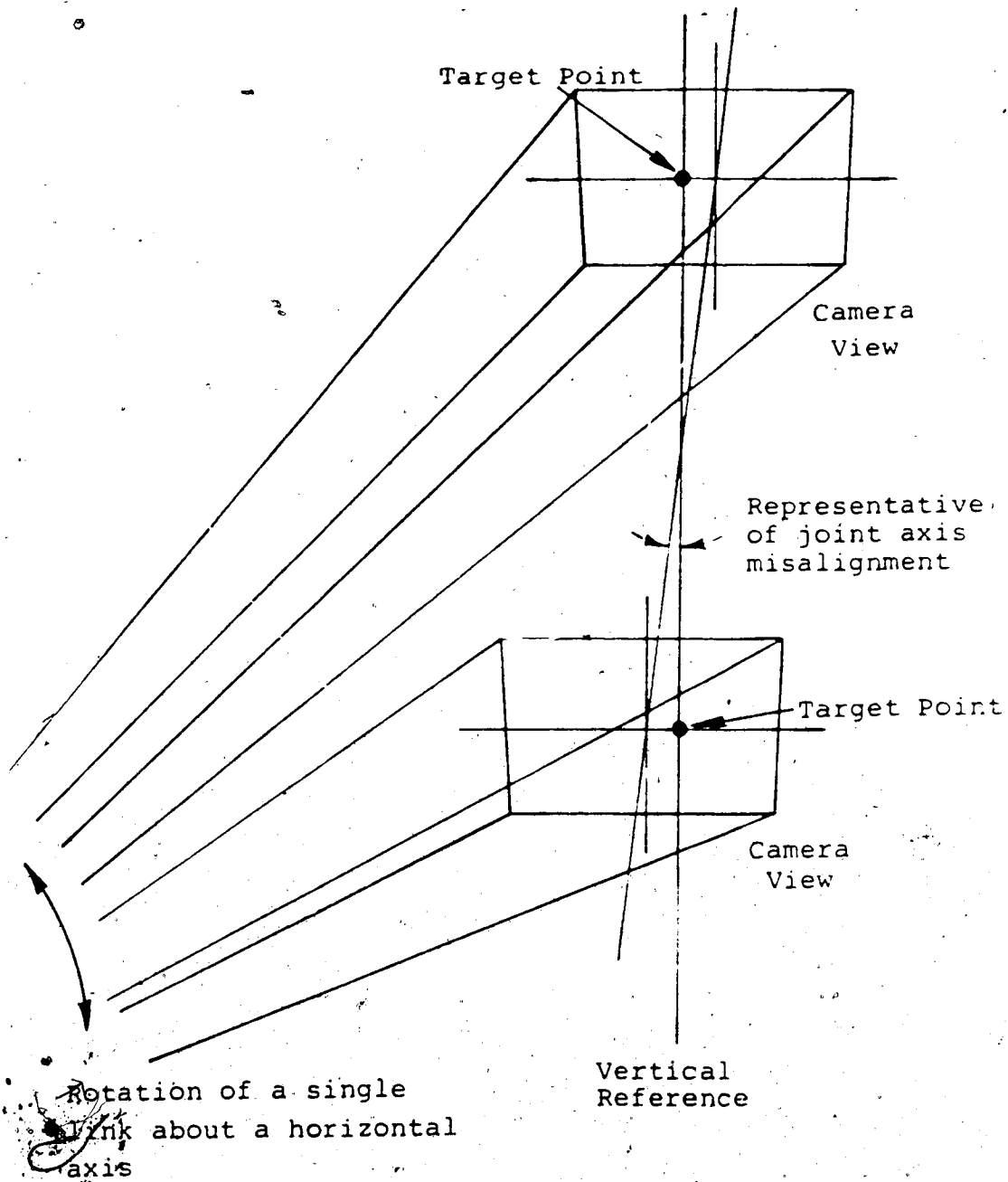
Figure 3-7   Observation of a Misalignment in the Camera for
a Horizontal Joint Axis

vertical reference, but with respect to the camera

coordinate frame. The orientation of the camera coordinate

frame is determined by observing several target points from

a vertical reference in a single camera picture. These

points will define the global vertical reference in the

camera coordinate frame. By comparing the misalignment and

the global vertical reference, both determined with respect

to the camera coordinate frame, the joint misalignment can

be obtained.

Essentially, if a selected target point does not

move in a line perpendicular to the global vertical

reference observed in the camera frame, the target point

motions define a misalignment with respect to the vertical

reference. Figure 3-8 illustrates the vertical reference

and motions of a target point for a misaligned vertical

axis.

In summary, the new calibration method determines

the misalignments of joint axes beginning at the base of the

robot and progresses to the end effector. The calibration

procedure uses a digital camera mounted on the end effector

to determine the joint axes misalignments with respect to a

vertical set of reference target points. Two pictures of

the target points, separated by the rotation of a single

link are compared to determine each joint axis error.

This new calibration method can be conducted without

a precision environment and therefore can be carried out in

the robot work space. The sets of vertical reference points

Link Rotation to
the Right

Central View

Link Rotation to
the Left

Four Target Points
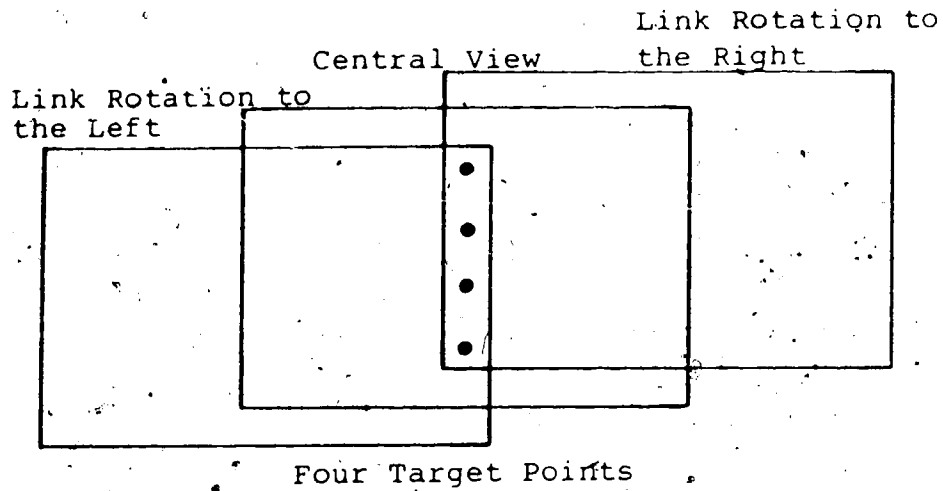
Effective Camera Information

Representative
of the
Misalignment
in the Camera
Coordinate Frame

Orientation of the Vertical
Reference in the Camera
Coordinate Frame
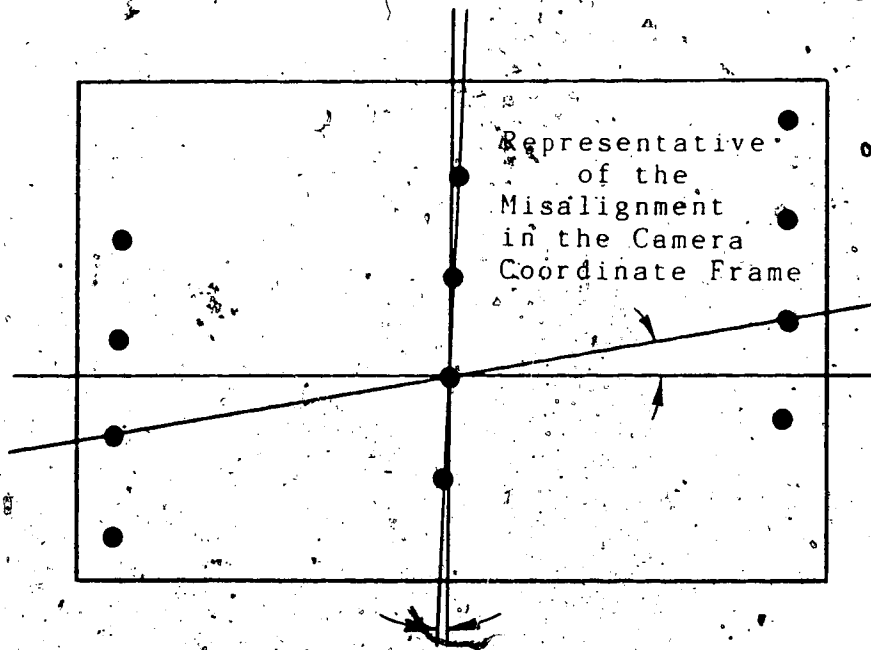
Figure 3-8   Observation of a Misalignment in the Camera for
a Vertical Joint Axis

can easily and quickly be moved in and out of a work space without requiring extensive changes. The digital camera and calibration method also readily afford themselves to an automated procedure.

To present, only the outline of the calibration procedure has been given. The following chapter applies the calibration procedure to a common robot configuration. The robot-camera transformation equation is examined more closely showing the equations generated which must be solved to determine the joint axes misalignments.

CHAPTER 4

Implementation of the Calibration Method

The general calibration method consists of determining the joint axis misalignments by observing target points in a digital camera mounted on the end effector with respect to rotations of a single link. The camera target point locations are used in the robot-camera transformation equations to determine the correct joint axis orientation. This chapter applies the calibration method to a typical robot configuration. The robot-camera transformation equations are examined to reveal the specific equations which describe the joint axis misalignments.

The implementation of the new calibration procedure is examined for a typical industrial robot configuration common to Unimation, Hitachi, Prab, GMF, ASEA, and many other manufacturers. The robot has revolute joints with a vertical body axis, and horizontal shoulder, elbow, and wrist axes.

Figure 4-1 shows a Mitsubishi RM-101 educational robot with this common robot configuration. The figure also shows a camera mounted on the end effector of the robot. The Mitsubishi RM-101 robot has five degrees of freedom, only accomodating pitch and roll at the wrist. Yaw motions of the wrist are not available. The system base coordinate

Target •
Points

Body Rotation

z_0

z_{Base}

Body Twist Axis
x_0
x_{Base}

Body Skew
Axis
y_0
y_{Base}
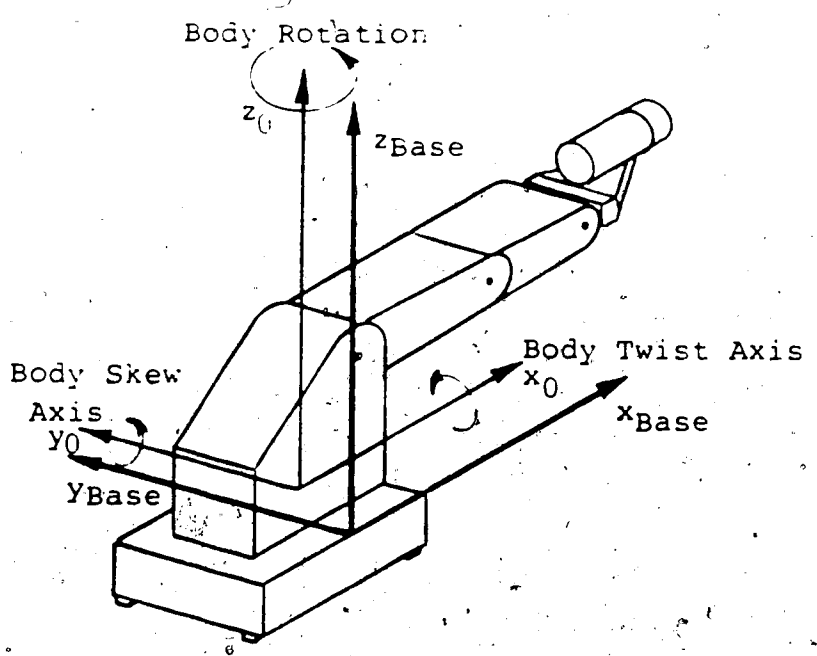
Figure 4-1/ Robot Configuration for the Body Twist Calibration

frame is shown with the x axis directed from the front of the robot and the z axis coincident with the vertical direction.

It was shown in chapter 2 that joint axis errors dominate manipulator errors because their effect is magnified over the length of the successive links from the misaligned joint axis. Therefore, it is most important to calibrate joints closer to the base of the robot. For this reason, the calibration procedure is only developed for the body, shoulder and elbow links. The wrist misalignments can also be calibrated using the same method applied to the other joints, but the errors caused by wrist misalignments will be small compared to the other joints. The body axis is analyzed first since it is the first axis to be calibrated in the procedure.

4.1   Body Misalignments   (Vertical Axis)

The body rotates about a vertical joint axis described by the base transformation, B, as described in equation (3-2). In the Denavit-Hartenburg convention the ith joint rotates about the z_{i-1} axis. Therefore, body misalignments are described in the base transformation which describes the position and orientation of the z_0 axis. Similarly, the shoulder misalignments are described in the body transformation, D_1, and the elbow misalignments described in the shoulder transformation, D_2.

The robot-camera system describing the calibration method is given by transformation equation (3-2). To accomodate a twist and skew misalignment of the body axis the base transformation is modified from its original form. Originally, the base transformation is a simple transform describing the position and orientation of the body axis where it intersects the horizontal shoulder axis. The base transformation is modified to take the form:

$$B = Trans(u_x,u_y,u_z) \; Rot(x,\alpha_B) \; Rot(y,\gamma_B) \; Trans(v_x,v_y,v_z) \qquad (4\text{-}1)$$

The first transformation, $Trans(u_x,u_y,u_z)$, is a translation from the base coordinate frame to the position of the physical body joint. At the body joint the coordinate frame undergoes a rotation about the x axis of the twist angle, α_B, followed by a rotation about the y axis of the skew misalignment, γ_B. The base transformation is then completed by a translation, $Trans(v_x,v_y,v_z)$, to the original location where the body axis intersects the shoulder.

It was shown in the third chapter that twist misalignments are best revealed by rotations in the vicinity of 0 degrees and skew misalignments in the vicinity of +/- 90 degrees. For the vertical body axis, the calibration procedure therefore requires two vertical references. Figure 4-1 illustrates the robot in a position with the body link at 0 degrees for calibrating the body twist misalignment.

The calibration procedure for the body twist misalignment was outlined for vertical axes in the third chapter. The robot is oriented in a position with the body, shoulder and elbow joints near zero degrees with the camera oriented to observe a set of three or four target points from a vertical reference. The first step in the calibration of a vertical axis is to determine the orientation of the global vertical reference in the camera coordinate frame. The orientation of a least squares fit line through the observed target points with respect to the orientation of the camera, determines the global vertical reference in the camera coordinate frame.

The movement of the target points in the camera frame is then used to determine the body misalignments. The body joint is rotated about its vertical axis so that the reference points appear to one side of the camera view. The camera x-y coordinates of one target point is recorded for determining the misalignment. The body joint is then rotated so that the target points appear on the opposite side of the camera view. The location of the same target point is again recorded in the camera coordinate frame. The pictures generated by this procedure were illustrated for a vertical axis in figure 3-8.

The locations of the target point separated by the rotation of the body link describe the body misalignment with respect to the camera coordinate frame. The equation which determines the misalignment is obtained from the

transformation equation (4-2) which is similar to equation (3-2) with the exception of a pitch yaw transformation, PY.

$$B \ T_5 \ E \ PY \ CAM \ = \ P \tag{4-2}$$

A new pitch yaw transformation is placed between the end effector and camera to accomodate the orientation of the camera in its mount and the end effector position error caused by the joint axis misalignments in each joint. The "roll" orientation of the camera is accomodated in the orientation of the global vertical reference in the camera coordinate frame. The pitch yaw terms are calculated before determining the body misalignment terms from the picture of the target points used to determine the global vertical reference orientation.

Equation (4-2) defines twelve equations describing the position and orientation of the camera coordinate frame with respect to the base coordinate frame. Fortunately, nine of these equations are trivial since the camera is observing points in space. The target points have locations, but no specific orientation. The orientation of a target point observed in the camera frame is defined as the orientation of the line passing through the point itself, and the point where it appears on the camera lens. Therefore, the nine orientation equations are trivial since the orientation of a target point is determined by the orientation of camera observing the point.

Of the remaining three position equations only one
is used to determine the body twist misalignment. Recalling
that the dominant position error due to a twist or skew
misalignment will appear in the joint z axis direction (see
figure 3-6), it can be seen in figure 4-1 that the body
twist misalignment will appear as a z position error in the
global base coordinate frame. The z position equation from
equation (4-2) may be represented in the form

$$b^1 c_z + b^2 c_x + b^3 c_y + b^4 = p_z \qquad (4-3)$$

where

$$b^j = BT_5EPY(3,j)$$

$$[c_x, c_y, c_z]^T = \text{camera position vector}$$

$$p_z = \text{z position of target point in the base coordinate frame}$$

In the representation above $BT_5EPY(i,j)$ are the components
of the matrix product $B\ T_5\ E\ PY$.

The first picture with the target points on one side
of the camera view are represented by equation (4-3). The
second picture with the target points on the opposite side
of the camera view is described by a similar equation
denoted by primed coefficients.

$$b^{1'} c_z' + b^{2'} c_x' + b^{3'} c_y' + b^{4'} = p_z \qquad (4-4)$$

Figure 4-2 contains a simplied geometric description
of equations (4-3) and (4-4) for the vertical axis
calibration with the camera in a horizontal orientation.
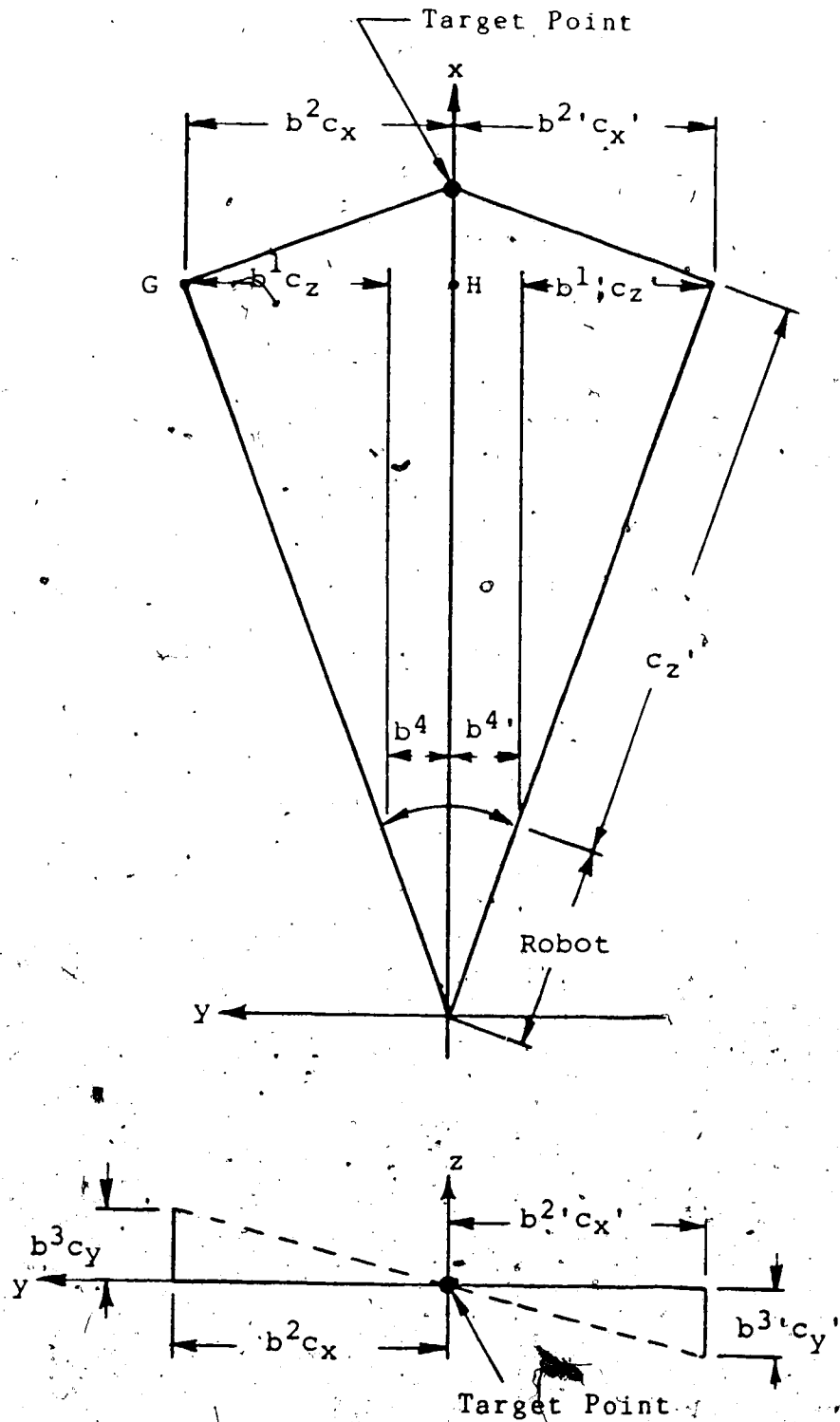
Figure 4-2 Illustration of the Body Misalignment Equation Terms

The terms b^4 and $b^4{}'$ describe the position of the robot end effector. The horizontal distance GH is described twice in equation (4-3) by $b^2 c_x$, and the sum of $b^1 c_z$ and the horizontal component of b^4. These two groups of terms are equal in magnitude but opposite in sign. The vertical z components of equation (4-3) are described by $b^3 c_y$ and the vertical component of b^4.

To compare the locations of the target point in equations (4-3) and (4-4) for determining the misalignment, the terms, $b^1 c_z$, $b^1{}' c_z{}'$, and the horizontal components of b^4 and $b^4{}'$ are cancelled. These terms are removed from the equations because they cancel out the description of the horizontal movement of the target point in the camera pictures, $b^2 c_x$ and $b^2{}' c_x{}'$. The remaining components of the left sides of equations (4-3) and (4-4) are equated since p_z is the coordinate of the same target point in both equations. The vertical components of b^4 and $b^4{}'$ are also equal and cancel, since only the body link is rotated.

The lower view in figure 4-2 illustrates the components of equations (4-3) and (4-4) which are used to describe the misalignment. Only the camera terms are required to describe the movement of the single target point between the two pictures. The resulting equation which describes the body twist misalignment is given by

$$b^2 c_x + b^3 c_y = b^2{}' c_x{}' + b^3{}' c_y{}' \qquad (4-5)$$

Following the pictures taken near the 0 degree body

angle for the twist misalignment, the body is rotated to +/- 90 degrees to observe a second set of target points for determining the skew misalignment. The skew misalignment is determined using the same procedure used for the twist misalignment giving a second equation in the form of equation (4-5).

The two equations in the form of equation (4-5) describing the twist and skew misalignments are solved simultaneously for the correct body axis orientation. These nonlinear equations are solved using an under relaxed Gauss-Seidel iterative method. The proper arrangement of the equations is critical for the Gauss Seidel method. The appropriate arrangement of the equations was determined by analyzing the magnitude of the terms in the equations with respect to the link geometry and robot configuration.

The arrangement of equation (4-5) for the body twist misalignment is given by

$$S\alpha_B \ (T_5EPY(2,2)' \ c_x' - T_5EPY(2,2) \ c_x) =$$
$$(b^3 \ c_y - b^{3'} \ c_y')$$
$$+ \ ((B(3,1) \ T_5EPY(1,2) + B(3,3) \ T_5EPY(3,2)) \ c_x$$
$$- (B(3,1) \ T_5EPY(1,2)' + B(3,3) \ T_5EPY(3,2)') \ c_x')$$

$$(4-6)$$

where

α_B = the twist parameter in the Base (B) transformation

$B(i,j)$ = the components of B

$T_5EPY(i,j)$ = the components of the matrix product

$$T_5 \; E \; PY$$

The primed expressions differentiate between terms from the two pictures.

The arrangement of equation (4-5) for the body skew misalignment is given by

$$-S\gamma_B C\alpha_B \; (T_5 EPY(1,2)' \; c_x' - T_5 EPY(1,2) \; c_x) \; =$$
$$(b^3 \; c_y - b^{3'} \; c_y') \;$$
$$+ \; ((B(3,2) \; T_5 EPY(2,2) + B(3,3) \; T_5 EPY(3,2)) \; \dot{c}_x$$
$$- \; (B(3,2) \; T_5 EPY(2,2)' + B(3,3) \; T_5 EPY(3,2)') \dot{c}_x')$$
$$(4-7)$$

where

γ_B = the skew parameter in the Base (B) transformation

and the other expressions are the same as described for equation (4-6).

These two arrangements of equation (4-5) converged rapidly on the misalignment parameters in 4 to 7 iterations. The misalignment terms obtained from these equations are defined with respect to the camera coordinate frame. By comparing the misalignment terms with the orientation of the global vertical reference in the camera coordinate frame the true misalignments are obtained. An improper arrangement of equations (4-6) and (4-7) resulted in attempting to obtain the inverse sine of a value greater than 1, clearly warning that the equation arrangement was not suitable.

When the body misalignments are determined the base transformation describes the correct orientation of the body

joint axis. With the body axis calibrated, the orientation of the shoulder joint axis is determined next.

4.2   Shoulder Misalignments   (Horizontal Axis)

The orientation of the shoulder axis is described in the modified body transformation D_1 given by

$$D_1 = \begin{bmatrix} C\theta_1 C\gamma_1 - S\theta_1 S\alpha_1 S\gamma_1 & -S\theta_1 C\alpha_1 & C\theta_1 S\gamma_1 + S\theta_1 S\alpha_1 C\gamma_1 & 0 \\ S\theta_1 C\gamma_1 - C\theta_1 S\alpha_1 S\gamma_1 & C\theta_1 C\alpha_1 & S\theta_1 S\gamma_1 - C\theta_1 S\alpha_1 C\gamma_1 & 0 \\ -C\alpha_1 S\gamma_1 & S\alpha_1 & C\alpha_1 C\gamma_1 & 0 \\ 0 & 0 & 0 & 1 \end{bmatrix}$$

$$(4-8)$$

The twist angle, α_1, is ideally 90 degrees and the skew angle, γ_1, 0 degrees. θ_1 is the joint variable and both the link length, l_1, and distance, r_1, are zero.

The transformation equation which describes the robot-camera system contains the modified transform for the shoulder misalignments given by

$$B \ D_1 \ {}_1T_5 \ E \ PY \ CAM \ = \ P \qquad (4-9)$$

The transformation, ${}_1T_5$, describes the manipulator from link 2 through link 5. The base transformation, B, has been corrected in the body calibration.

The vertical reference most effectively measures misalignments of horizontal joint axes because observing two target points allows larger rotations of the link being calibrated. This results in larger position errors observed

in the camera. The procedure for measuring the twist misalignment of the shoulder axis begins with orienting the shoulder and elbow joints near 0 degrees and observing a target point to determine the pitch yaw parameters for the shoulder calibration.

The procedure then continues as outlined for horizontal joint axes in chapter 3. The shoulder joint is rotated to view a lower and upper target point from the same vertical reference. From figure 4-1 it can be noted that the dominant position error for a twist misalignment in the shoulder z axis (by definition, the axis about which the shoulder rotates) will appear as a position error in the base y coordinate direction. The y position equation is therefore used to generate the misalignment equation. The location of the lower target point will give the following y position equation:

$$s^1 c_z + s^2 c_x + s^3 c_y + s^4 = p_y \qquad (4\text{-}10)$$

where

$$s^j = BD_{11}T_5EPY(2,j)$$

$$[c_x, c_y, c_z]^T = \text{the camera position vector}$$

$$p_y = \text{the y position of the target point in the base coordinate frame}$$

In this representation the terms $BD_{11}T_5EPY(i,j)$ are the terms from the matrix product $B\ D_{1\ 1}T_5\ E\ PY$. The observation of the upper target point will give a similar equation denoted by the primed coefficients.

$$s^{1\prime} c_z{}' + s^{2\prime} c_x{}' + s^{3\prime} c_z{}' + s^{4\prime} = p_y \qquad (4-11)$$

Figure 4-3 gives a simplified geometric description of equations (4-10) and (4-11) for θ_1 equal to 0 degrees and a vertical reference intersecting the base coordinate x axis. The terms s^4, and $s^{4\prime}$ describe the position of the robot end effector. The terms $s^1 c_z$, $s^3 c_y$, s^4, $s^{1\prime} c_z{}'$, $s^{3\prime} c_y{}'$, and $s^{4\prime}$ describe the vertical position of the target points with respect to the robot and camera in the base coordinate frame. The position error caused by the misalignment appears as a change in the target point x coordinate location in the camera frame contained in the terms $s_2 c_x$, and $s_2{}' c_x{}'$.

In figure 4-3 it can be seen that all the terms of equations (4-10) and (4-11) are required to describe the twist misalignment of the shoulder axis with respect to the robot camera transformations. The y target point position, p_y, in both equations are the same since both target points are from the same vertical reference. The twist misalignment equation is generated by equating the left sides of equations (4-10) and (4-11) to give the equation

$$s^1 c_z + s^2 c_x + s^3 c_y + s^4 = s^{1\prime} c_z{}' +$$
$$s^{2\prime} c_x{}' + s^{3\prime} c_y{}' + s^{4\prime} \qquad (4-13)$$

The skew misalignment of the shoulder axis presents a difficulty for the vertical reference. The skew misalignment of the shoulder cannot be determined using a
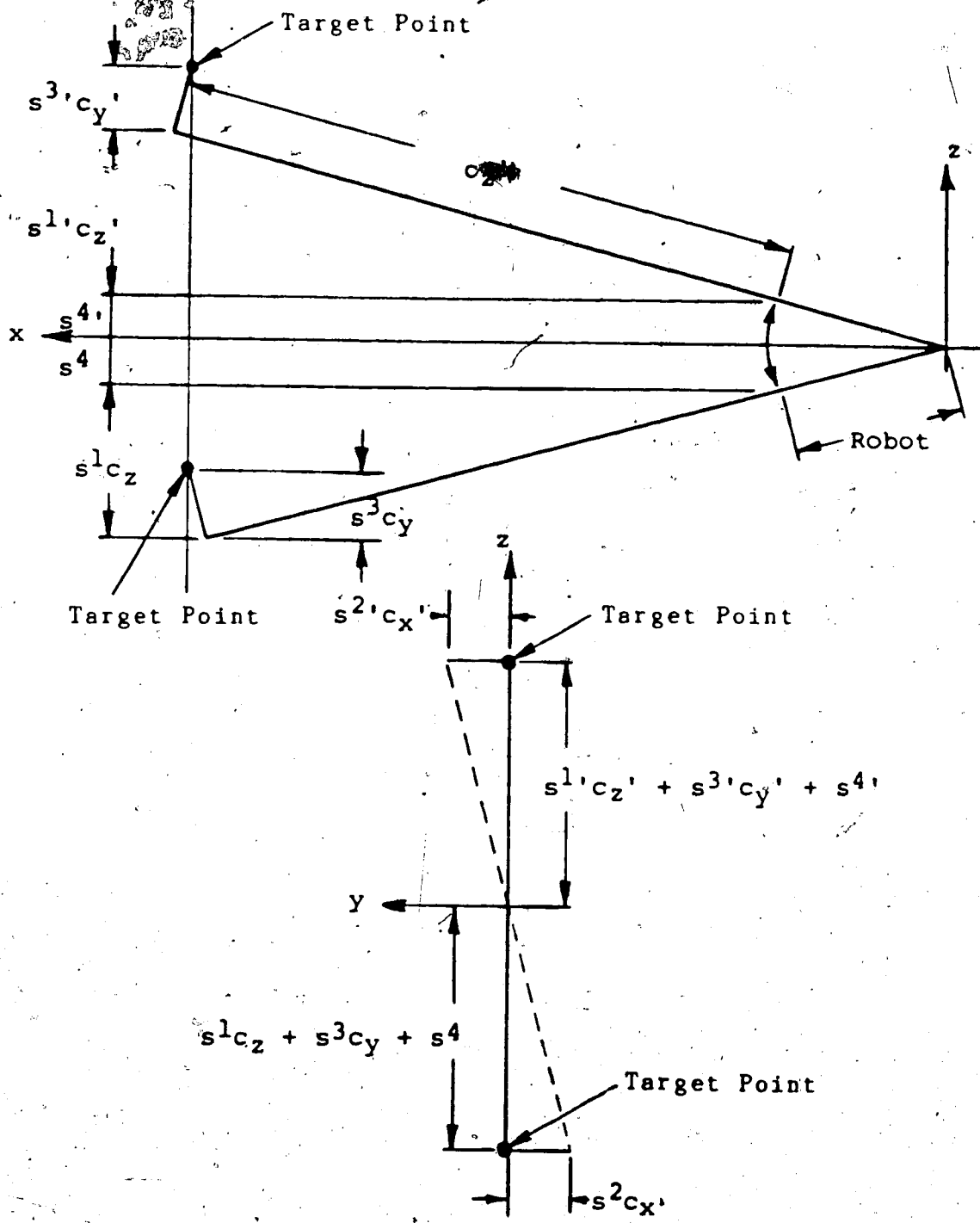
Figure 4-3   Illustration of the Shoulder Misalignment
             Equation Terms

vertical set of reference points. The y axis about which

the skew misalignment is described for the shoulder joint is

parallel to the vertical reference and therefore cannot be

measured by this reference. The shoulder skew misalignment

is in fact indistinguishable from an error in the body joint

variable because the shoulder y axis (skew misalignment

axis) is coincident with the body z joint axis.

To measure the shoulder skew misalignment a set of

target points would have to be positioned above the shoulder

joint axis such that the points could be observed with the

shoulder rotating in the vicinity of 90 degrees. This

however, would require that the locations of the target

points be known very precisely which is not desirable. Even

if this were accomplished, the measured skew misalignment

would be the combination of the true skew misalignment and

an error in the body joint variable.

The calibration of the shoulder skew misalignment is

neglected because of this difficulty. It should be noted

however, that errors caused by skew misalignments in the

shoulder can be corrected by adjusting the body joint

variable.

Therefore, for the shoulder joint, only the twist

misalignment is determined. Equation (4-13) is solved for

the twist misalignment using the Gauss-Seidel method. The

appropriate arrangement of equation (4-13) to determine the

twist misalignment is given by

$$C\alpha_1 C\theta_1 C\alpha_B ({}_1T_5 EPY(2,1)\ c_z - {}_1T_5 EPY(2,1)'\ c_z') =$$

$$(s^{2'}\ c_x' - s^2\ c_x) + (s^{3'}\ c_y' - s^3\ c_y) + (s^{4'} - s^4)$$

$$- ((BD_1(2,1)\ {}_1T_5 EPY(1,1) + BD_1(2,3)\ {}_1T_5 EPY(3,1))\ c_z$$

$$- (BD_1(2,1)\ {}_1T_5 EPY(1,1)' + BD_1(2,3)\ {}_1T_5 EPY(3,1)')\ c_z')$$

$$- ((B(2,1)\ D_1(1,2) + B(2,3)\ D_1(3,2))\ ({}_1T_5 EPY(2,1)\ c_z$$

$$- {}_1T_5 EPY(2,1)'\ c_z')) \qquad\qquad (4\text{-}14)$$

where

$$\alpha_1 = \text{the shoulder twist parameter}$$

$${}_1T_5 EPY(i,j) = \text{the components of the matrix product } {}_1T_5\ E\ PY$$

$$BD_1(i,j) = \text{the components of the matrix product } B\ D_1$$

The correct twist parameter will be in the vicinity of 90 degrees, therefore, as can be seen in equation (4-14), the correct arrangement of the twist misalignment equation determines the cosine of the twist angle.

Upon completing the shoulder calibration, both the base and body transformations have been adjusted to accurately describe the body and shoulder joint axes. The calibration procedure moves to the next transformation which describes the elbow joint axis.

4.3   Elbow Misalignments   (Horizontal Axis)

The orientation of the elbow axis is described by a modified shoulder transformation, D_2, given by

$$D_2 = \begin{bmatrix} C\theta_2 C\gamma_2 - S\theta_2 S\alpha_2 S\gamma_2 & -S\theta_2 C\gamma_2 & C\theta_2 S\gamma_2 + S\theta_2 S\alpha_2 C\gamma_2 & l_2 C\theta_2 \\ S\theta_2 C\gamma_2 + C\theta_2 S\alpha_2 S\gamma_2 & C\theta_2 C\alpha_2 & S\theta_2 S\gamma_2 - C\theta_2 S\alpha_2 C\gamma_2 & l_2 S\theta_2 \\ -C\alpha_2 S\gamma_2 & S\alpha_2 & C\alpha_2 C\gamma_2 & 0 \\ 0 & 0 & 0 & 1 \end{bmatrix}$$

$$(4-15)$$

Ideally, the twist and skew angles for the elbow are both 0 degrees. The joint variable is θ_2; the link length is l_2, and the link distance is 0.

The robot-camera transformation equation may now be represented with the modified shoulder transform given by

$$B\ D_1\ D_2\ {_2}T_5\ E\ PY\ CAM\ =\ P \qquad (4-16)$$

where ${_2}T_5$ represents a transformation from link 3 to link 5. The base, B, and link 1, D_1, transformations have been calibrated and the twist and skew parameters in D_2 are determined next.

The calibration procedure for the elbow misalignments is similar to the shoulder procedure since both are horizontal axes. However, both the twist and skew parameters can be determined for the elbow joint axis.

The twist misalignment is determined with both the body and shoulder joint variables near 0 degrees. The x twist axis of the elbow joint axis will therefore be perpendicular to the vertical reference. The wrist is rotated to observe a single target point and determine the pitch yaw parameters for the PY transformation. Two target points from the same vertical string are then observed by

rotating the forearm about the elbow axis as shown in figure 4-4a.

The position errors observed by the two pictures will appear in the y position equation, similar to the shoulder procedure since the elbow z joint axis is horizontal. The first picture of a target point will give the following equation

$$e^1 c_z + e^2 c_x + e^3 c_y + e^4 = p_y \qquad (4\text{-}17)$$

where

$$e^j = BD_1D_{22}T_5EPY(2,j)$$

$$p_y = \text{y position of target light in the base coordinate frame}$$

The transformation terms $BD_1D_{22}T_5EPY(i,j)$ represent terms from the matrix product $B\ D_1\ D_2\ _2T_5\ E\ PY$.

The second picture of a target point gives a similar equation denoted by the primed coefficients.

$$e^{1\prime} c_z{}' + e^{2\prime} c_x{}' + e^{3\prime} c_y{}' + e^{4\prime} = p_y \qquad (4\text{-}18)$$

The equation describing the twist misalignment is obtained by equating the left sides of equations (4-17) and (4-18) since the y locations of the observed target points are the same. This gives the following equation for the elbow twist misalignment:

$$e^1 c_z + e^2 c_x + e^3 c_y + e^4 = e_1{}' c_z{}' +$$
$$e^{2\prime} c_x{}' + e^{3\prime} c_y{}' + e^{4\prime} \qquad (4\text{-}19)$$

Horizontal
Upper Arm

Rotate Forearm

Target
Points
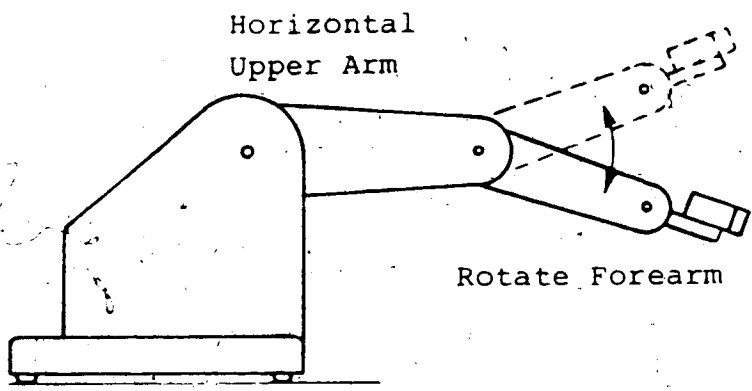
a) Elbow Twist Calibration

Vertical
Upper Arm

Rotate Forearm

Target
Points
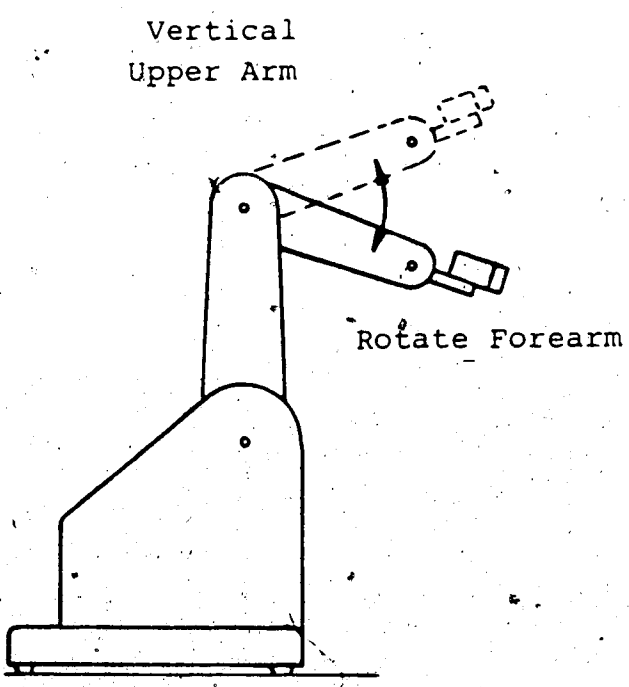
b) Elbow Skew Calibration

Figure 4-4 Robot Configuration for the Elbow Twist and Skew
Calibration

similar in form to the shoulder misalignment equation (4-13).

To determine the skew misalignment, the y skew axis is oriented perpendicular to the vertical reference. This is accomplished by rotating the upper arm about the shoulder to +90 degrees. The forearm is then rotated about the elbow to the vicinity of -90 degrees to observe the target points. Figure 4-4b illustrates the motions and configuration of the robot to calibrate the elbow skew parameter.

The pitch yaw terms are first determined from the location of a single target point. The forearm is then rotated to observe the positions of two target points from the same vertical reference. This generates a second equation in the form of equation (4-19) for the elbow skew misalignment.

The equations for the elbow twist and skew misalignments are solved simultaneously using the Gauss-Seidel method. The appropriate arrangement of equation (4-19) for determining the twist misalignment is given by

$$S\alpha_2 \; BD_1(2,3) \; (_2T_5EPY(2,1) \; c_z - _2T_5EPY(2,1)' \; c_z') \; =$$
$$(e^{2'} \; c_x' - e^2 \; c_x) + (e^{3'} \; c_y' - e^3 \; c_y) + (e^{4'} - e^4)$$
$$- ((BD_1D_2(2,1) \; _2T_5EPY(1,1) + BD_1D_2(2,2) \; _2T_5EPY(3,1)) \; c_z$$
$$- (BD_1D_2(2,2) \; _2T_5EPY(1,1)' + BD_1D_2(2,2) \; _2T_5EPY(3,1)') \; c_z')$$
$$-((BD_1(2,1) \; D_2(1,2) + BD_1(2,2) \; D_2(2,2)) \; (_2T_5EPY(2,1) \; c_z$$
$$-_2T_5EPY(2,1)' \; c_z')) \qquad\qquad (4-20)$$

where

$BD_1(i,j)$ = the components of the matrix product $B \, D_1$

$BD_1D_2(i,j)$ = the components of the matrix product $B \, D_1 \, D_2$

$_2T_5EPY(i,j)$ = the components of the matrix product
$_2T_5 \; E \; PY$

The primed coefficients distinguish between the components from the two pictures of the different target points. The appropriate arrangement of equation (4-19) for determining the elbow skew misalignment is given by

$$-S\gamma_2 C\alpha_2 \; BD_1(2,3) \; (_2T_5EPY(1,1) \; c_z - \; _2T_5EPY(1,1)' \; c_z') =$$
$$(e^2{}' \; c_x' - e^2 \; c_x) + (e^3{}' \; c_y' - e^3 \; c_y) + (e^4{}' - e^4)$$
$$-((BD_1D_2(2,2) \; _2T_5EPY(2,1) + BD_1D_2(2,3) \; _2T_5EPY(3,1)) \; c_z$$
$$-(BD_1D_2(2,2) \; _2T_5EPY(2,1)' + BD_1D_2(2,3) \; _2T_5EPY(3,1)') \; c_z')$$
$$-((BD_1(2,1) \; D_2(1,1) + BD_1(2,2) \; D_2(2,1)) \; (_2T_5EPY(1,1) \; c_z$$
$$- \; _2T_5EPY(1,1)' \; \bar{c}_z')) \hspace{2cm} (4\text{-}21)$$

where the expressions in the equation have been defined for equation (4-20). The solution of the twist and skew misalignments for the elbow joint axis completes the calibration procedure for this robot. The joint axes of the robot are now calibrated from the body through to the elbow. The wrist joint axis could also be calibrated using the same procedures, but since the length of the wrist and end effector is usually small compared to the length of the preceeding links, wrist misalignments would introduce very small manipulator errors.

The calibration method was implemented on the common

revolute configuration of the Mitsubishi RM-101 robot. The
procedure for determining the joint axis misalignments of
the body, shoulder, and elbow where outlined. The equations
describing the robot-camera system were then used to
determine the equations which describe the joint
misalignments.

The following chapter describes the testing of the
new calibration method. The calibration method was tested
by introducing known misalignments into the base of a
Mitsubishi RM-101 robot. The test results and discussion of
the sources of error in the calibration method are also
analyzed.

CHAPTER 5

Test and Results of the Calibration Method

The calibration method was implemented on the common
robot configuration found on the Mitsubishi RM-101 robot.
The robot configurations and rotations were described in
chapter 4 with the resulting equations which are used to
determine the misalignments. This chapter describes the
algorithm which conducts and tests the calibration method on
the Mitsubishi RM-101 robot using a Micromint, Micro D-cam
digital camera.

The description of the test of the calibration
method begins with a description of the equipment used: the
RM-101 robot and the Micro D-cam camera. The calibration
algorithm is then outlined describing the robot motions and
configurations which must be determined to conduct the
calibration. The test results and discussion are contained
in the final section of this chapter describing the method's
accuracy and sources of error.

5.1   Mitsubishi RM-101 Robot

The implementation and testing of the calibration
method was conducted on a Mitsubishi RM-101 robot. The
RM-101 is an educational micro-robot. The dimensions of the

robot are given in figure 5-1. Table 1 contains the ideal kinematic parameters used to describe the robot geometry in the modified Denavit-Hartenburg transformation convention.

The RM-101 has 5 degrees of freedom plus gripper movement, lacking yaw motions in the wrist joint. Six stepper motors actuate the RM-101 joint positions. An IBM PC was interfaced with the RM-101 which controls the stepper motors through the printer port.

5.2   Micromint, Micro D-cam Digital Camera

The vision system used to test the calibration method was an inexpensive Micro D-cam digital camera retailing for $300 US. This digital camera developed by Micromint Inc. uses an IS32, 64K bit dynamic RAM chip from Micron Technology. The IS32 optic RAM contains two image arrays separated by a small gap, both with 256 by 128 pixels. The camera was also linked to the IBM PC through an interface card and controlled through assembler language subroutines called from BASICA.

The heart of the Micro D-cam digital camera is the IS32 optic RAM. The IS32 is a dynamic RAM chip with a quartz cover over its 65,536 memory cells arranged in two convenient rectangular arrays. Light from viewed objects is focused on these arrays through a lens. When the memory cells in the arrays are struck by photons of light a capacitor in each cell begins to discharge from a prefixed
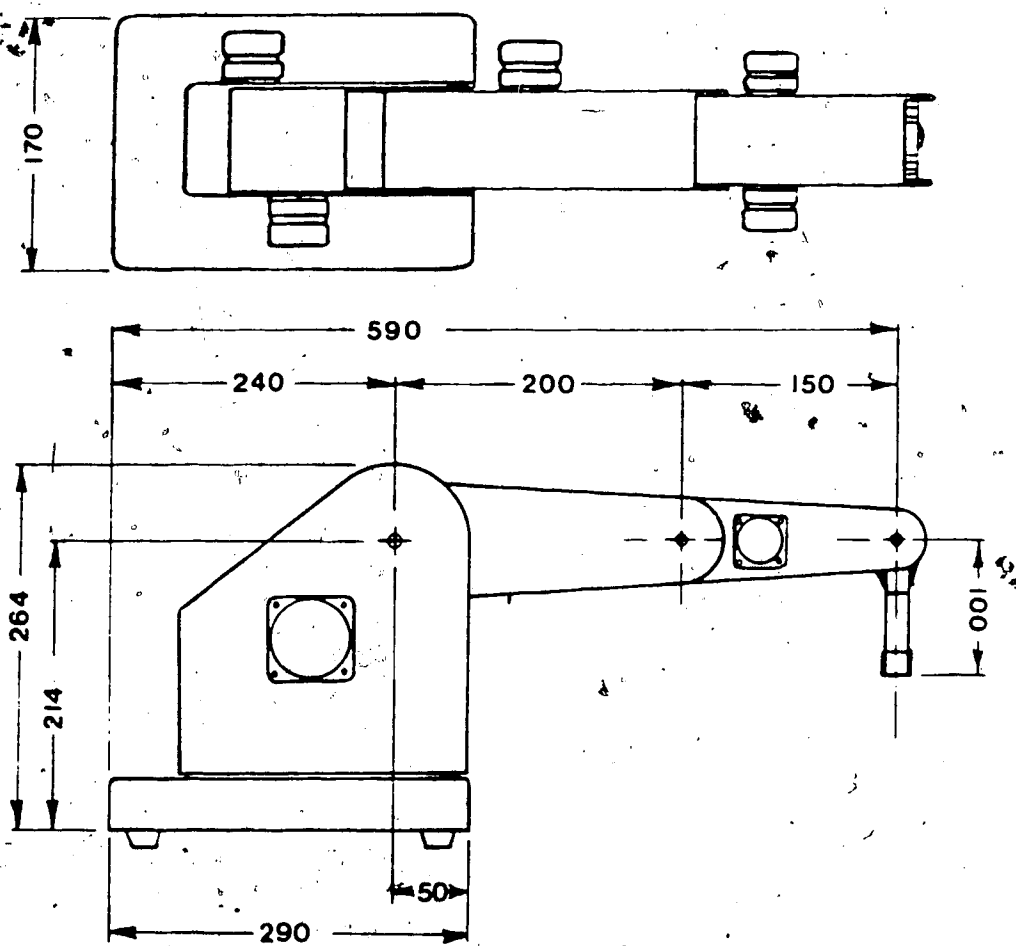
all dimensions in mm

Figure 5-1   Dimensions of the Mitsubishi RM-101 Robot

TABLE 1

LINK PARAMETERS FOR THE MITSUBISHI RM-101 ROBOT

LINK	JOINT VARIABLE	LENGTH l (mm)	DISTANCE r (mm)	TWIST α (°)	SKEW γ (°)
1	BODY θ_1	0	0	0	0
2	SHOULDER θ_2	200	0	90	0
3	ELBOW θ_3	150	0	0	0
4	WRIST PITCH θ_4	0	0	90	0
5	WRIST ROLL θ_5	0	0	0	0

voltage. The capacitor discharges at a rate proportional to the light intensity striking the element during its exposure.

Following an exposure interval the capacitor voltages of the memory cells are compared to a threshold voltage to determine the intensity of the light striking each cell. If the cell voltage has decayed below the threshold voltage it is declared white, or high. If the cell voltage is still above the threshold voltage it is considered black, or low. The camera circuitry reads each element by addressing each location as a memory cell and transmits the information to the IBM PC.

The camera is controlled by a command byte which is serviced through assembler language subroutines. Each bit in the command byte controls one of the several operating modes of the camera. One bit controls whether one or both of the 256 by 128 arrays are transmitted to the computer. Another bit controls whether the camera is in a "soak" mode allowing the incoming light to discharge the memory cells or in a "refresh" mode restoring the cells back to their nominal voltage. A "send" bit is used to request transmission of the images from the arrays.

The exposure time for a picture is determined by the amount of time the camera is left in the soak mode before transmission of the image to the computer. The images sent from the camera require some processing due to the nature of the arrangement of the memory cells in the two arrays and

the digital camera circuitry. The memory cells in the
arrays are in a honeycomb pattern shown in figure 5-2.
Picture processing includes forming the honeycomb pattern in
the IBM PC memory from the data received and filling in the
holes of the pattern. A hole is determined to be high, or
white, if two or more of the three surrounding pixels are
also high. This picture processing results in two image
arrays with 512 by 128 pixels.

The images in the camera pictures are further
processed by assigning coordinate locations to each pixel.
The target points observed by the camera can then be located
in the camera coordinate frame by determining the centroid
of the high pixels which represent the target point, A
complete picture processing operation including the
transmission time of the image to the IBM PC takes
approximately 1 second for each array.

The reference target points used in the calibration
test were small incandescant light bulbs because the camera
was very sensitive to infra-red light, which is common with
most silicon based image sensors. Under normal room light
conditions the target lights were clearly visible at 3
meters using exposures of 1 millisecond.

The camera was calibrated to determine the
relationship between the camera coordinate frame and the
pixel locations in the camera. Figure 5-3 illustrates the
two pixel arrays, the pixel coordinate frame, and the camera
position vector used in the camera transformation for the

Honeycomb Pixel Pattern

Holes   Bright Object
             Pixel Bit Values are High (1)

0 0   0 0   0 1   1 1   Pixel Bit Values (High = 1)
                                             (Low = 0)
6 7   4 5   2 3   0 1   Camera Pixel Numbering
                               Pattern
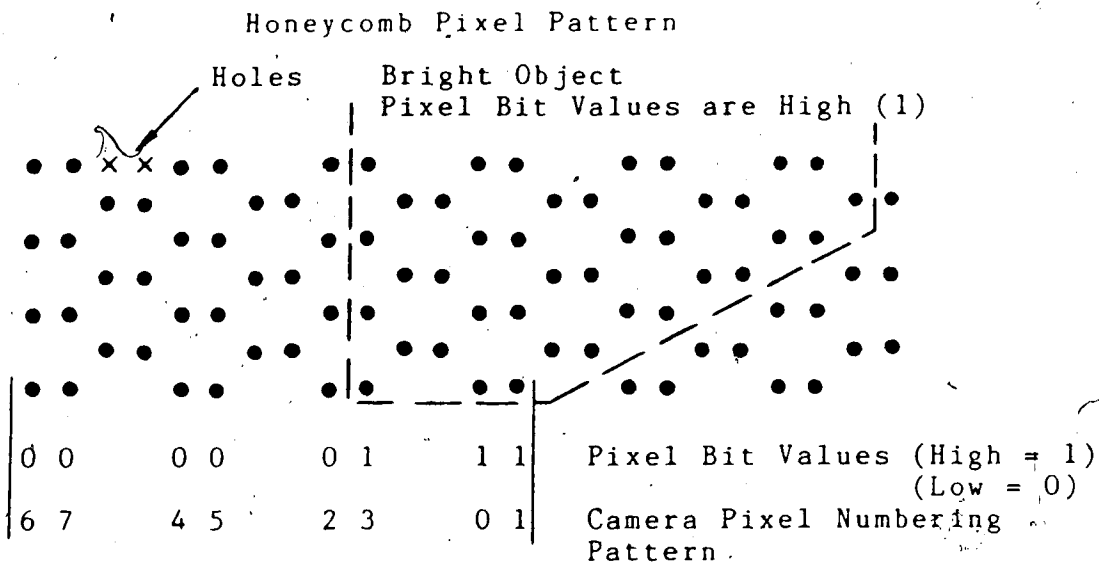
Pixel Bit Pattern of Each Byte
Received from Camera

76543210

The Byte is Rearranged to Form the Honeycomb
Pixel Pattern with the Camera Pixel Numbering
Pattern

67xx45xx23xx01

Holes

Figure 5-2 Digital Camera Picture Processing
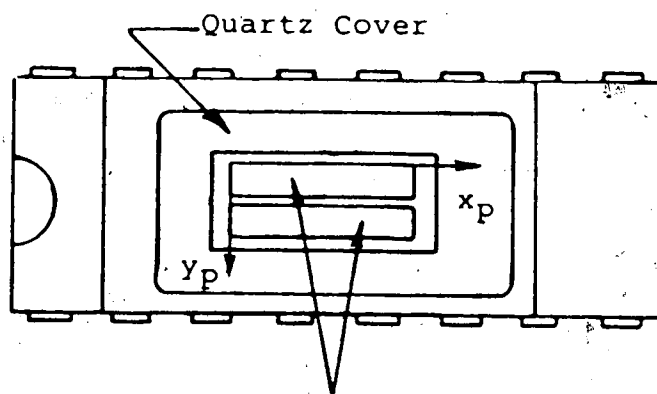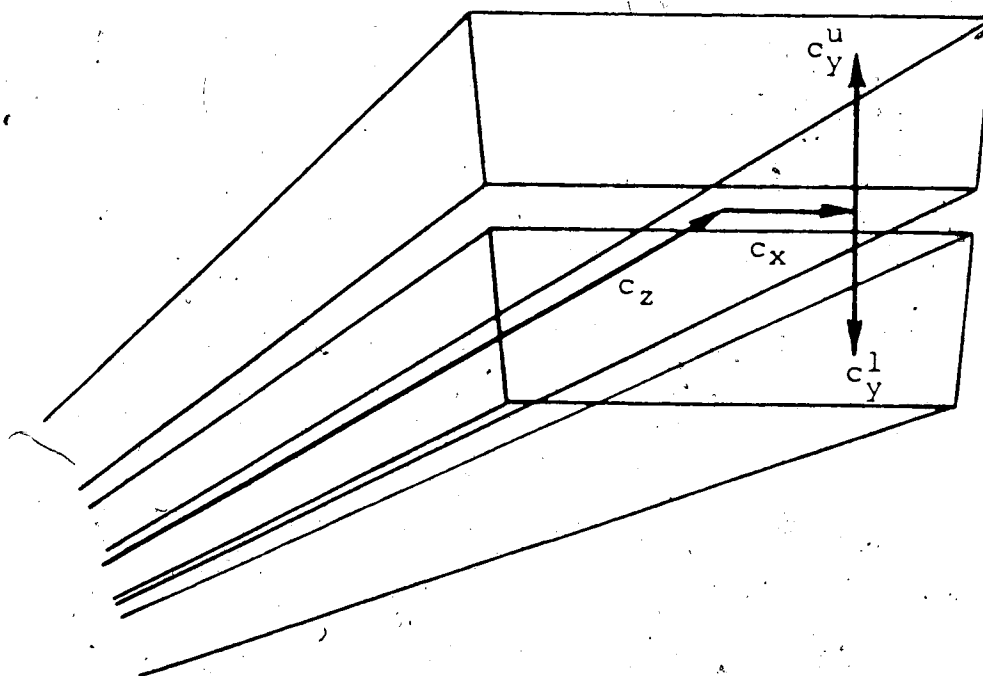
IS32 Optic RAM

$$c_x = (256 - x_p)(0.000531\ c_z + 0.0036)$$

$$c_y^u = (136.823 - y_p)(0.000418\ c_z + 0.0058)$$

$$c_y^l = (y_p - 118.177)(0.000418\ c_z + 0.0058)$$

Figure 5-3 Digital Camera IS32 Optic RAM and Camera
Position Vectors

calibration procedure.

5.3   Calibration Algorithm

The calibration algorithm was written in BASICA for the IBM PC which operated both the robot and digital camera. The digital camera was controlled through assembler language subroutines, while the robot was operated using "lprint" statements defining the number and direction of steps the robot stepper motors should perform.

Figure 5-4 contains a 6 page flowchart of the calibration algorithm. The flowchart outlines the steps required to follow the calibration procedure with illustrations of the robot at the various stages. Below each illustration of the robot is the corresponding camera view of the vertical reference target points.

5.4   Test of the Calibration Method

The calibration method was tested by placing known misalignments in the robot and measuring them using the calibration algorithm. Misalignments were produced in the robot by tipping it to one side using shims of known thickness as illustrated in figure 5-5. This places a misalignment in the body joint axis which is described by the base transformation.

When the body misalignments are measured the

CALIBRATION ALGORITHM

Robot

θ_1 = body joint
θ_2 = shoulder joint
θ_3 = elbow joint
θ_4 = wrist joint, pitch
θ_5 = wrist joint, roll

-start

-input coordinate locations
 of target points

-calculate θ_1, θ_2, θ_3 to
 observe central target
 points in front of robot

-move robot
-take pictures

-input adjustments to robot
 to observe all 4 central
 target points

-take pictures
-determine camera target
 point coordinates
-calculate camera orientation
 wrt vertical reference

Camera View

-determine pitch yaw, PY,
 transformation
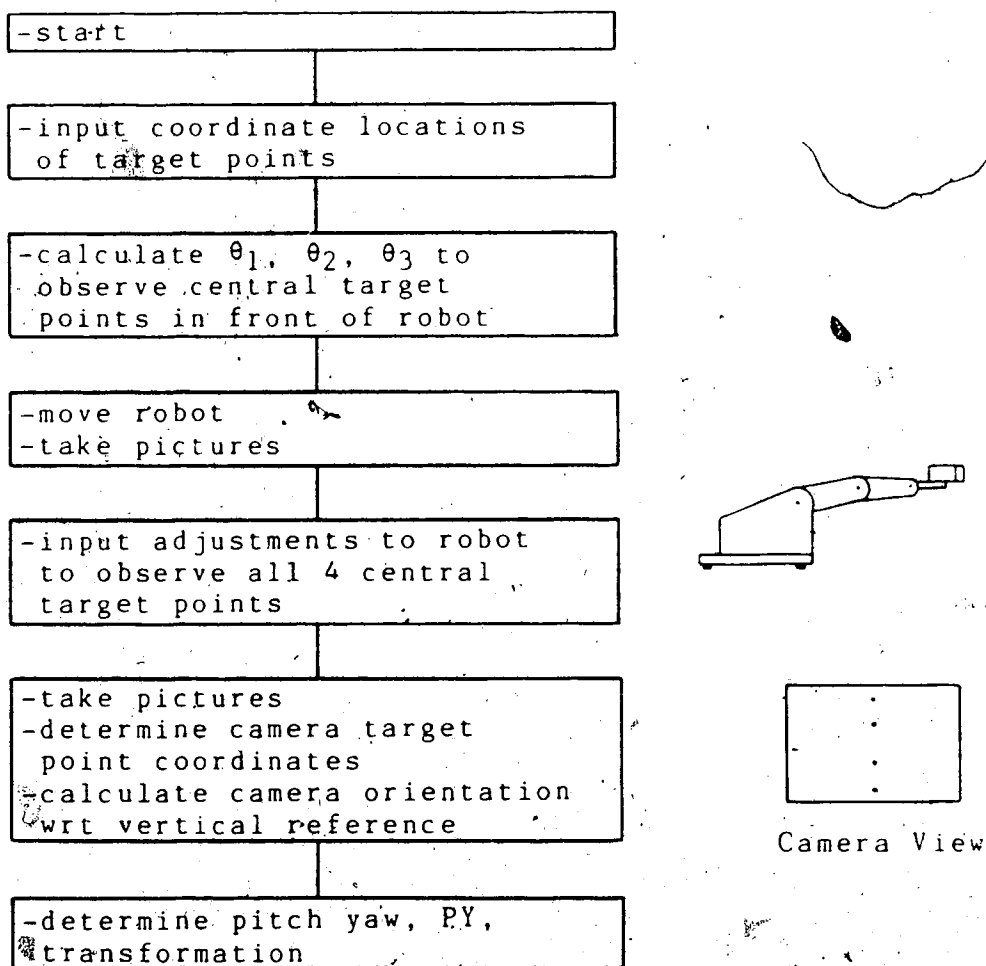
Figure 5-4 Calibration Algorithm

```
┌─────────────────────────────┐
│ -calculate θ₁ to observe    │
│  target points in left side │
│  of camera view             │
└─────────────────────────────┘
              │
┌─────────────────────────────┐
│ -rotate body right          │
│ -take pictures              │
│ -determine camera target    │
│  point coordinates          │
└─────────────────────────────┘
              │
┌─────────────────────────────┐
│ -calculate θ₁ to observe    │
│  target points in right     │
│  side of camera view        │
└─────────────────────────────┘
              │
┌─────────────────────────────┐
│ -rotate body left           │
│ -take pictures              │
│ -determine camera target    │
│  point coordinates          │
└─────────────────────────────┘
              │
┌─────────────────────────────┐
│ -calculate θ₁, θ₂, θ₃ to    │
│  observe central target     │
│  points at side of robot    │
└─────────────────────────────┘
              │
┌─────────────────────────────┐
│ -move robot                 │
│ -take pictures              │
└─────────────────────────────┘
              │
┌─────────────────────────────┐
│ -input adjustments to robot │
│  to observe all 4 central   │
│  target points              │
└─────────────────────────────┘
              │
┌─────────────────────────────┐
│ -take pictures              │
│ -determine camera target    │
│  point coordinates          │
│ -calculate camera orientation│
│  wrt vertical reference     │
└─────────────────────────────┘
              │
┌─────────────────────────────┐
│ -determine pitch yaw, PY,   │
│  transformation             │
└─────────────────────────────┘
```

$$\text{-calculate } \theta_1 \text{ to observe target points in left side of camera view}$$

-calculate θ_1 to observe
 target points in left side
 of camera view

-rotate body right
-take pictures
-determine camera target
 point coordinates

Camera View

-calculate θ_1 to observe
 target points in right
 side of camera view

-rotate body left
-take pictures
-determine camera target
 point coordinates

-calculate θ_1, θ_2, θ_3 to
 observe central target
 points at side of robot

-move robot
-take pictures

Camera View

-input adjustments to robot
 to observe all 4 central
 target points

-take pictures
-determine camera target
 point coordinates
-calculate camera orientation
 wrt vertical reference

-determine pitch yaw, PY,
 transformation

Camera View

Continued on next page

Figure 5-4 (continued) Calibration Algorithm

-calculate θ_1 to observe
 target points in left side
 of camera view

-rotate body right
-take pictures
-detemine camera target
 point coordinates

-calculate θ_1 to observe
 target points in right
 side of camera view

Camera View

-rotate body left
-take pictures
-determine camera target
 point coordinates

-calculate body twist and
 skew parameters
-update base, B, transform

-move robot to observe
 central target points in
 front of robot

Camera View

-take pictures
-determine camera target
 point coordinates

-determine pitch yaw, PY,
 transformation

-calculate θ_2 to observe
 lower target point

Continued on next page

Camera View

Figure 5-4 (continued) Calibration Algorithm

```
┌──────────────────────────────┐
│ -rotate shoulder down        │
│ -take pictures               │
│ -determine camera target     │
│  point coordinates           │
└──────────────────────────────┘
               │
┌──────────────────────────────┐
│ -calculate θ₂ to observe     │
│  upper target point          │
└──────────────────────────────┘
               │
┌──────────────────────────────┐
│ -rotate shoulder up          │
│ -take pictures               │
│ -determine camera target     │
│  point coordinates           │
└──────────────────────────────┘
               │
┌──────────────────────────────┐
│ -calculate shoulder twist    │
│  misalignment                │
│ -update body, D₁, transform  │
└──────────────────────────────┘
               │
┌──────────────────────────────┐
│ -calculate θ₁, θ₃, θ₄ with   │
│  θ₂=0 to observe upper       │
│  point with elbow rotation   │
│  limited to θ₃ ≤ 0           │
└──────────────────────────────┘
               │
┌──────────────────────────────┐
│ -calculate θ₃ to observe     │
│  central target points       │
└──────────────────────────────┘
               │
┌──────────────────────────────┐
│ -move robot                  │
│ -take pictures               │
└──────────────────────────────┘
               │
┌──────────────────────────────┐
│ -input adjustments to robot  │
│  to observe all 4 central    │
│  target points               │
└──────────────────────────────┘
               │
┌──────────────────────────────┐
│ -take pictures               │
│ -determine camera target     │
│  point coordinates           │
└──────────────────────────────┘
               │
┌──────────────────────────────┐
│ -determine pitch yaw, PY,    │
│  transformation              │
└──────────────────────────────┘
```
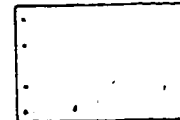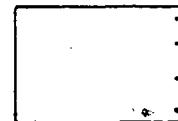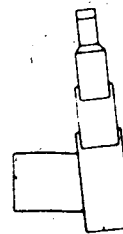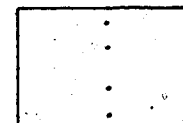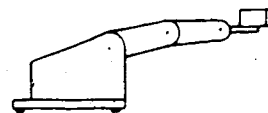
- rotate shoulder down
- take pictures
- determine camera target point coordinates

- calculate θ_2 to observe upper target point

- rotate shoulder up
- take pictures
- determine camera target point coordinates

- calculate shoulder twist misalignment
- update body, D_1, transform

- calculate θ_1, θ_3, θ_4 with $\theta_2=0$ to observe upper point with elbow rotation limited to $\theta_3 \leq 0$

- calculate θ_3 to observe central target points

- move robot
- take pictures

- input adjustments to robot to observe all 4 central target points

- take pictures
- determine camera target point coordinates

- determine pitch yaw, PY, transformation

Camera View

Camera View

Camera View

Continued on next page

Figure 5-4 (continued) Calibration Algorithm

```
┌────────────────────────────┐
│ -calculate θ3 to observe   │
│  lower target point        │
└────────────────────────────┘
             │
┌────────────────────────────┐
│ -rotate elbow down         │
│ -determine camera target   │
│  point coordinates         │
└────────────────────────────┘
┌────────────────────────────┐
│ -calculate θ3 to observe   │
│  upper target point        │
└────────────────────────────┘
             │
┌────────────────────────────┐
│ -rotate elbow up           │
│ -determine camera target   │
│  point coordinates         │
└────────────────────────────┘
             │
┌────────────────────────────┐
│ -calculate θ1, θ3 with     │
│  θ2 = 90 to observe central│
│  target points             │
└────────────────────────────┘
             │
┌────────────────────────────┐
│ -move robot                │
│ -take pictures             │
│ -determine camera target   │
│  point coordinates         │
└────────────────────────────┘
             │
┌────────────────────────────┐
│ -determine pitch yaw, PY,  │
│  transformation            │
└────────────────────────────┘
             │
┌────────────────────────────┐
│ -calculate θ3 to observe   │
│  lower target point        │
└────────────────────────────┘
             │
┌────────────────────────────┐
│ -rotate elbow down         │
│ -take pictures             │
│ -determine camera target   │
│  point coordinates         │
└────────────────────────────┘
             │
┌────────────────────────────┐
│ -calculate θ3 to observe   │
│  upper target point        │
└────────────────────────────┘
```

Continued on next page

Camera View

Camera View

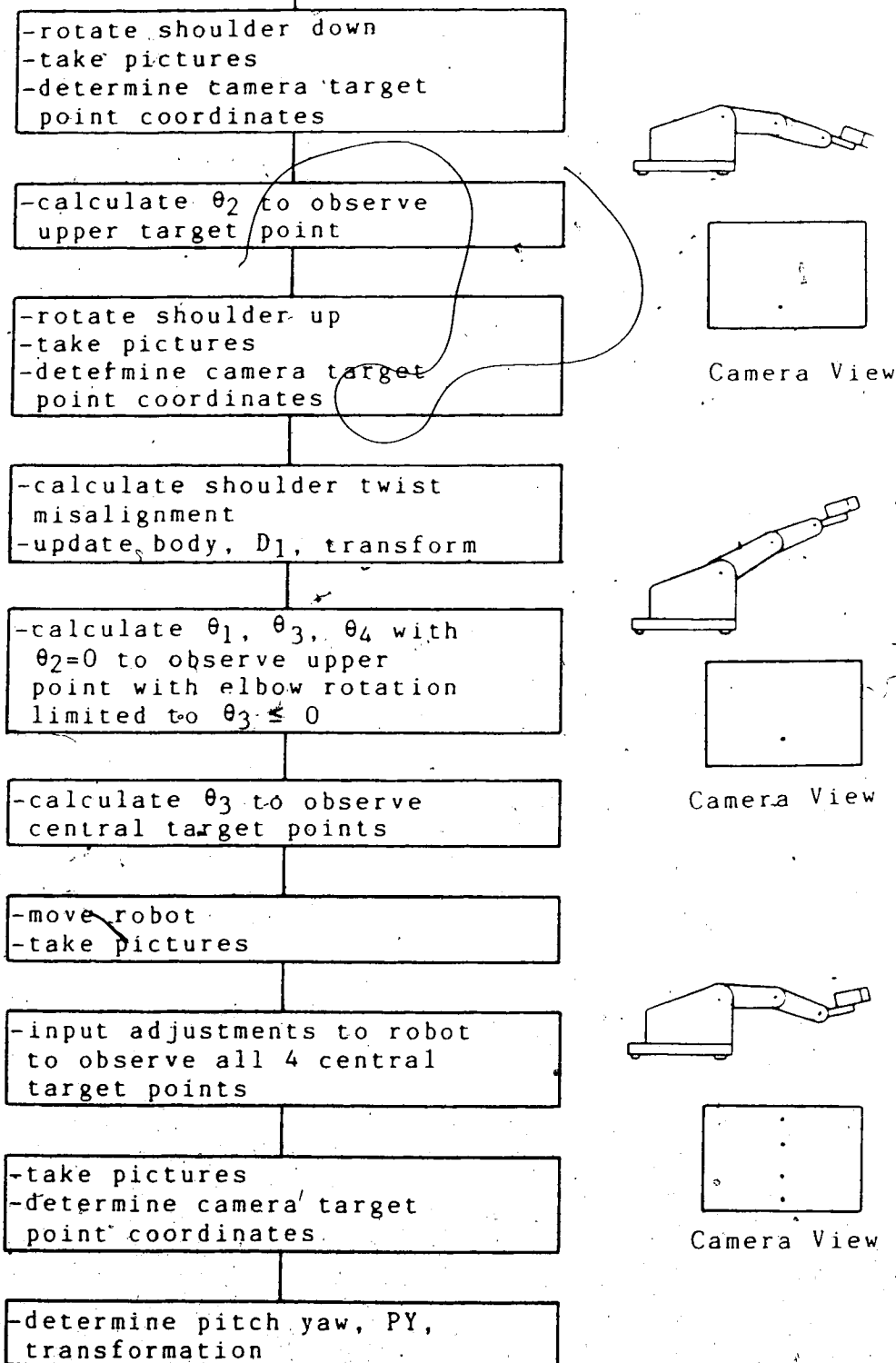
Camera View

Camera View

Figure 5-4 (continued) Calibration Algorithm

Camera View

Figure 5-4 (continued) Calibration Algorithm

Joint Axis
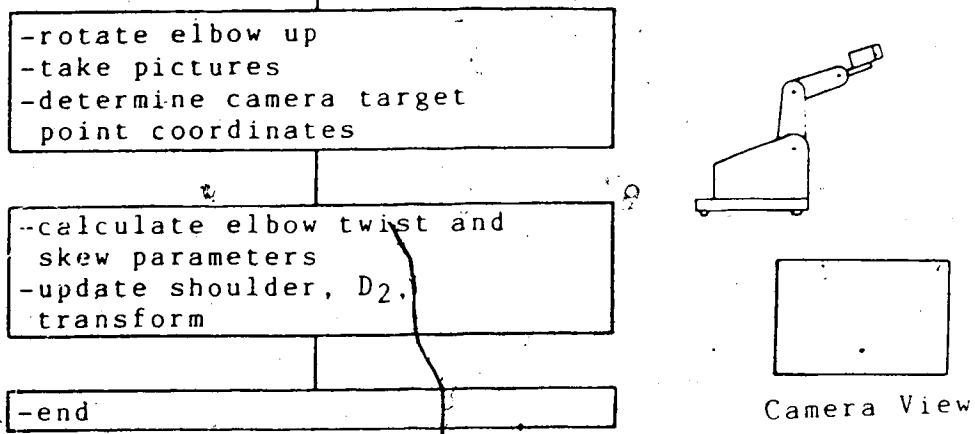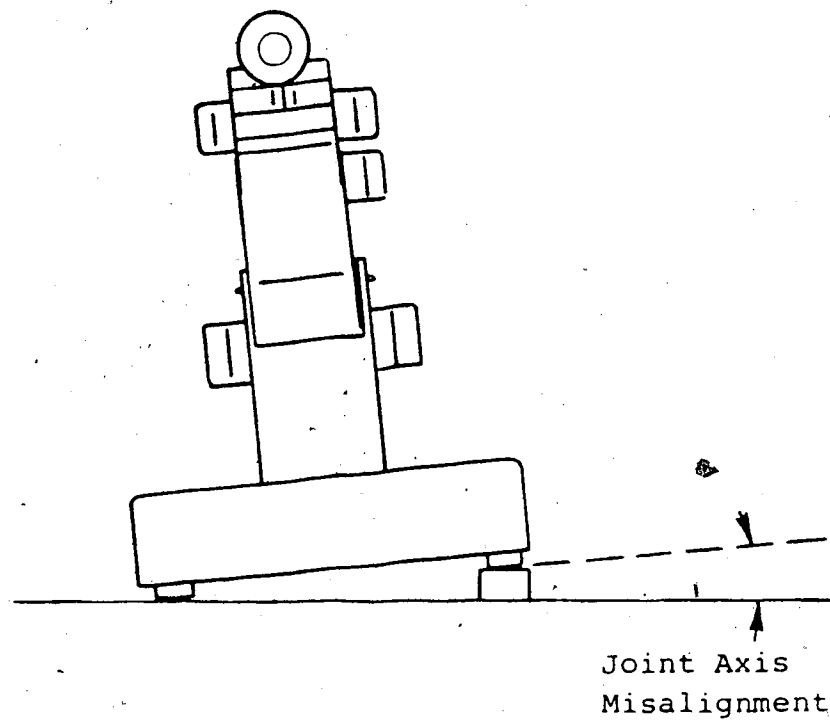Misalignment

Figure 5-5   Introduction of Misalignments into the RM-101
             Robot to Test the Calibration Method

calibration method correctly measures the misalignments placed in the robot and corrects for them in the base transformation. Therefore, when the calibration method proceeds and measures the misalignments in the shoulder and elbow the base transformation has already corrected the misalignment introduced in the body link.

To allow the shoulder and elbow procedures to measure the introduced misalignment, the measured base misalignments are returned to their former values prior to the body calibration. Thus, following the body calibration procedure the body misalignments are returned to zero. The base transformation will no longer correct for the misalignment introduced at the base of the robot. The shoulder calibration procedure will therefore measure the misalignment at the shoulder axis since the shoulder's wrong orientation has not been described by previous transformations.

Following the shoulder calibration, the shoulder twist misalignment is returned to its former value of 90 degrees and the elbow calibration procedure will measure the misalignment since neither the base or body transformations correctly describe the orientation of the elbow joint axis. In this manner, the single misalignment introduced at the base of the robot is measured three times, by the body, shoulder, and elbow procedures.

In the test of the calibration method, the calibration algorithm was first run on the robot without any

shims to determine the reference or normal misalignments present in the robot. Misalignments were then introduced by using pairs of shims 1.27 mm thick to produce misalignments in the range of -3 to +3 degrees. The introduced misalignments were then compared to the reference misalignments to determine the accuracy of the calibration method.

One of the major requirements for the new calibration method was that it could be conducted without requiring a precision calibration site. To comply with this requirement, the distances to the target points were measured using a tape measure to the nearest millimeter and the camera alignment was set by eye.

5.5   Results and Discussion

The results from the calibration test are shown in figure 5-6. The graph in figure 5-6 compares the measured misalignments with the true misalignments introduced in the robot for six calibration tests at each misalignment. This graph shows that the calibration method works well with the largest calibration error being -0.1 degrees at a misalignment of -3 degrees. A second more revealing graph in figure 5-7 compares the error in the calibration method with respect to the true misalignment introduced in the robot.

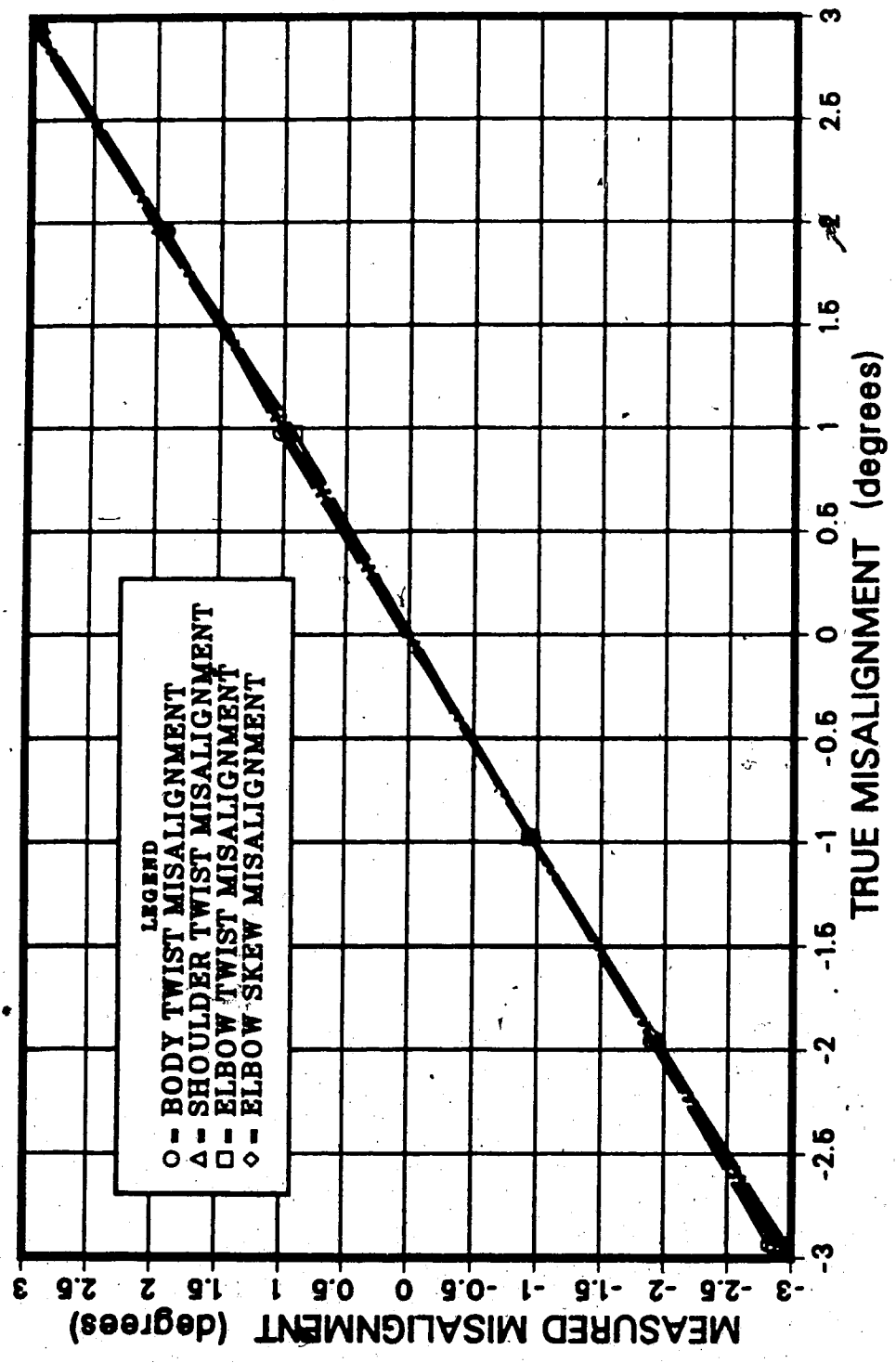The calibration procedure for measuring the vertical
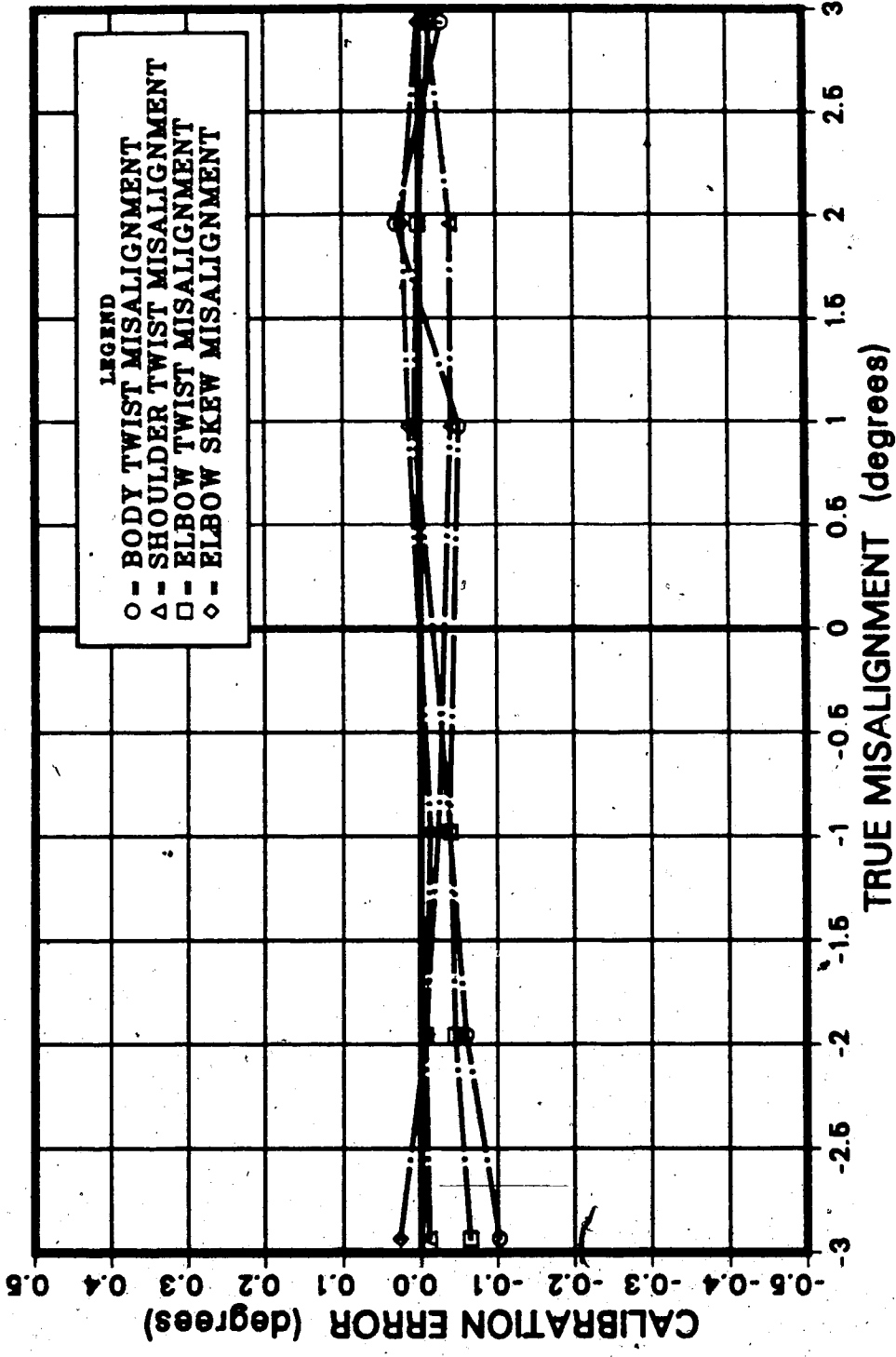
Figure 5-6   Test of the Calibration Method

Figure 5-7   Accuracy of the Calibration Method

body axis exhibited the greatest calibration errors ranging from -0.1 to +0.04 degrees. The calibration procedures for measuring misalignments in the horizontal shoulder and elbow joint axes proved to be more accurate. The calibration errors for the shoulder twist misalignment ranged from -0.04 to 0.0 degrees. The elbow twist misalignment procedure proved slightly less accurate with errors ranging from -0.06 to 0.01 degrees. The elbow skew misalignment procedure proved to be most accurate with errors ranging from -0.01 to 0.03 degrees.

To summarize the results, the average error of all the body twist calibrations was -0.041 degrees. The average error for the shoulder and elbow calibrations was -0.013 degrees. Analysis of all the data reveals that the repeatability of the calibration procedure for the body axis is 0.08 degrees (2 standard deviations) and 0.01 degrees for the elbow and shoulder axis calibrations.

There are several factors which affect the overall accuracy and repeatability of the calibration method. The inaccuracies of the calibration method are introduced from three sources: the robot, the vertical reference, and the digital camera. Each of these sources is analyzed separately to determine which factors cause the errors observed in the calibration tests.

The Mitsubishi RM-101 is an educational micro-robot. This robot is not an industrial robot manufactured to the tolerances required for precision work. The accuracy and

repeatability of the robot was hindered by large amounts of backlash in the gears. This significantly affected the tests of the calibration method.

As pointed out, the calibration method was tested by comparing the results of calibration tests with, and without introduced misalignments. During the process of tipping the robot to introduce the shims for the misalignment, the links would shift slightly because of the backlash in the gears and freeplay in the joints. This would introduce an error in the calibration test accuracy. This is not an accuracy problem with the calibration method itself, but with the test of the calibration method. For example, following extensive movement of the robot (tipping the robot on its side to access the circuitry in its base) the test accuracy changed by 0.15 degrees. As the tests were repeated the calibration results fluctuated until they settled on a new misalignment value. Therefore the accuracy measurements of the calibration method include the accuracy of the method itself and some error due to the backlash in the joints.

Another source of inaccuracy in the tests involves the joint angles and stepper motors. The positions of the joint angles controlled by the stepper motors introduced both accuracy and repeatability errors to the calibration method. Accuracy errors in the calibration tests are introduced by the inaccuracy of the robot home position, which is estimated by the robot operator. The home position refers to the starting robot configuration where the joint

variables should be in specific prefixed values. This would

introduce consistent offset errors in the joint angles, but

should not cause significant calibration errors because the

two pictures used to determine the misalignments would both

contain the effects of the error.

The ability of the stepper motors to consistently

reproduce the required number of steps also affects the

calibration repeatability. This was not expected to cause

significant repeatability problems for the method because

the variation of the link rotations would be small compared

to the total rotations of the links in the calibration

tests.

Another source of error in the calibration method is

the vertical reference. A calibration procedure is always

limited by the accuracy of its reference. There are two

possible errors in the vertical reference: how vertical it

is, and its location. The vertical orientation of the

reference was not a problem with the tests of the

calibration method since the accuracy of the method was

determined with respect to calibration tests of the robot

with no introduced misalignments using the same vertical

reference. Therefore, if there was an error in the vertical

orientation of the reference, it was accounted for by

comparing the calibration results with and without

introduced misalignments. For a real calibration however,

the accuracy of the vertical reference is of prime

importance.

An error in the location of the vertical reference
would also introduce an accuracy error in the calibration
method. The position error of the vertical reference would
however appear in both camera pictures of the calibration
procedure. Therefore it would not affect the joint
calibration significantly because the misalignments are
determined with respect to the relative motion of the target
points between the pictures.

The final source of error in the calibration method
is the digital camera. The digital camera can potentially
introduce errors in two ways, by the orientation of the
camera on the end effector, and the accuracy and
repeatability of the camera itself for observing the target
point locations. The error caused by the misalignment of
the camera on the end effector is accomodated in two parts
of the calibration procedure.

First, a pitch yaw transformation, PY, is placed
between the robot end effector and the digital camera. The
pitch yaw parameters were calculated upon observing the
locations of the target points for a known robot
configuration. The pitch yaw transformation would therefore
correct for the orientation of the camera on the end
effector as well as the combined effect of all the joint
misalignments which would affect the position and
orientation of the camera in the base coordinate frame.

The second way the camera orientation is
accommodated in the calibration method, is in the procedure

itself. The procedure of determining misalignments with respect to the relative motion of the target points between two pictures, prevents the camera orientation from significantly affecting the calibration accuracy. The mislocation of the target points in the camera pictures due to a misalignment of the camera would be present in both pictures and therefore not affect the calibration significantly.

The second source of error from the camera is the camera's repeatibility for observing the target point locations. This turned out to be a major source of repeatability error in the vertical body calibration procedure. The target point locations were determined by finding the centroids of the high pixels for each target point from ten pictures. The repeatability of the camera for determining the locations of the target points was 0.20 pixels for the camera x direction and 0.32 pixels for the camera y direction. This directly affects the repeatibility of the calibration method by differing degrees for the horizontal and vertical procedures.

In the vertical joint calibration the position error which determines the joint misalignment appears in the camera y direction. The vertical joint calibration also uses smaller link rotations compared with the horizontal joint calibration. The smaller link rotations and larger repeatability in the camera y direction partially explain the larger repeatability for the vertical joint calibration

compared with the horizontal joint calibration.

The vertical axis calibration also has another source of repeatability error from the camera which is not present in the horizontal axis calibration. For the vertical joint axis, the rotation of the single link and observation of the single target point determines the joint misalignment with respect to the camera coordinate frame. The orientation of the camera coordinate frame with respect to the global vertical direction is determined by observing four target points in the vertical reference and fitting a least squares fit line through the points. The repeatability for tests determining the camera orientation was 0.10 degrees.

This source of error associated with the repeatability of the camera observing the locations of the target points is only present for the vertical joint axis calibration. The repeatability error in determining the camera orientation and the larger repeatability in the camera y direction explains the significant difference between the repeatabilities of the vertical and horizontal calibration procedures.

The development of the calibration method focused attention on the potential sources of error and tried to reduce their effect on the calibration accuracy. The robot was the major source of uncertainty in the accuracy observed in the calibration tests. To effectively determine the true accuracy of the calibration method the calibration tests

procedure used for determining the misalignments of horizontal axes could be used for vertical axes. This would allow larger rotations of the link about its vertical axis which would increase the calibration accuracy. Using a horizontal reference would also eliminate the need to determine the orientation of the vertical reference in the camera coordinate frame, which had a large repeatability of 0.10 degrees.

The third improvement in the calibration method involves the number of target points observed to determine the misalignments. The accuracy of the calibration method could be improved by taking pictures of more target points. Instead of generating only one equation which determines the misalignment, pictures of several target points would generate several equations for each misalignment. The equations could be solved using the Gauss-Seidel method with a least squares error fit to the misalignment solution.

In summary, the results of the calibration tests revealed that the average error for the vertical body axis twist calibration was -0.041 degrees. The calibration tests for the horizontal shoulder and elbow axes had an average error of -0.013 degrees. These results confirm that the calibration method works with relative insensitivity to the imprecise calibration site.

The following chapter discusses the importance of the link joint variable on the accuracy of a robot.

CHAPTER 6

Joint Variable Calibration

The results of chapter 2 revealed that the joint variable, θ, and the joint axis orientation parameters, α and γ, cause the greatest manipulator errors. The calibration method developed in this investigation measured the fixed twist and skew parameter errors. Though the object of this investigation to develop a calibration procedure for the fixed link parameters without requiring a precision calibration site has been achieved, consideration of the joint variable can not be neglected.

Calibration of the dominant fixed joint orientation parameters will improve robot accuracy, but it should not be forgotten that the joint variable was also a dominant term for causing manipulator errors. Errors in the fixed robot parameters cause robot accuracy errors. Errors in the joint variables will cause both accuracy and repeatability errors in the robot. The repeatability of the joint variables is generally very good with many robots having a repeatability of 0.1 mm.

The remaining concern is therefore, the accuracy of the joint variable. The accuracy of the joint variable depends on the resolution of the joint encoders and resolvers, the number of bits of controller memory assigned

122

for storage, and the accuracy of the robot construction.

Following the calibration of the joint axes orientations, inaccuracies in the end effector will be dominated by joint variable errors. Unfortunately, the digital camera mounted on the end effector for the joint, axis calibrations cannot calibrate the joint variables without requiring precise mounting of the camera and very accurate locations for the target points. The joint variables can however be calibrated without requiring any changes to the work cell.

The calibration method developed by Wu, requiring precision calibration points in the robot work cell can be used to calibrate the joint variables. The drawback with Wu's method was that it required precision calibration points over a fairly large volume of the work space to estimate all the robot kinematic parameters. In general, the only convenient precision points in the work cell are the locations of working points where specific operations are to be conducted; for example, the location of a chuck or clamp where a work piece is held.

Using these existing work cell precision locations the joint variables can be calibrated. The method to calibrate the joint variables would position the robot at several of these work space precision locations. At each location the position errors of the end tool are measured. By using the position equations (2-61) through (2-63) in equation (2-84) the errors in the joint variables can be

estimated. After repeating the procedure at several points, the position errors should converge to zero.

This is one method to calibrate the joint variables. The purpose of this chapter is not to precisely define a calibration method for the joint variables but to impress upon the reader that the joint variable is another dominant parameter for causing manipulator errors and should not be neglected when considering robot accuracy.

The following chapter contains a summary of the development of the joint axis calibration method and the conclusions from this investigation.

CHAPTER 7

Summary and Conclusions

Major advancements in robot programming will soon be
on the factory floor because of the need for less tedious
programming of large numbers of robots. The advanced
methods of programming off-line (without a robot) are
performed at computer terminals using high level languages.
In high level languages the end effector is positioned by
calculating the joint variable positions (software defined
targeting) using the ideal robot geometry. However, errors
in the ideal geometry of the robot cause software defined
targeting to be inaccurate. In response to this problem,
calibration methods have been developed to measure these
errors in the robot geometry and use the correct geometric
parameters to increase robot accuracy.

The purpose of this investigation was to develop a
new calibration method which overcomes several of the
shortcomings of the previously developed methods. The major
drawback exhibited by other calibration methods was the need
for a precision measurement environment to conduct the
procedure. This required either moving the robot to a
precision environment to conduct the calibration or the
conversion of the robot work space into a precision
calibration site. For large numbers of robots, both of

these options are time consuming and therefore undesirable.

It was desired that the new calibration method of this investigation overcome this disadvantage and satisfy several other requirements. The major requirement for the new calibration method was that it could be conducted without the need for a precision calibration site. The calibration procedure could therefore be conducted in the robot work environment without requiring the relocation of the robot. It was further required that the calibration procedure not require extensive or time consuming changes to the work space. It was also desirable that the procedure be automated to aid in the speed and ease of conducting the calibration method.

The development of the new calibration method began with developing a linear error model to determine which errors in the kinematic parameters describing the robot link geometry caused the greatest manipulator errors. The largest manipulator errors were caused by errors in the joint axis orientation and joint variable of each link. Errors in the joint axis orientation are described as twist and skew misalignments. Joint axis twist and skew misalignments cause the greatest manipulator errors because they are magnified over the lengths of the successive links from the misaligned axis to cause position errors at the end effector. It is also these two parameters which are the most difficult to manufacture accurately in a robot. If these two parameters were measured and used in describing

the robot geometry, robot accuracy would be increased for

software defined targeting.

The decision to develop the new calibration method
was made because it was intuitively visualized that a camera
mounted on the end effector of a robot would be able to
observe joint axis misalignments relative to a vertical
reference. This new calibration method would not require a
precision calibration site. The calibration method
developed in this investigation consists of three
components: a digital camera, a vertical set of reference
target points, and the calibration procedure using the
robot, camera, and vertical reference.

The calibration method begins at the base of the
robot and proceeds calibrating each link in succession
towards the end effector. The general procedure for
determining the joint misalignments consists of taking two
pictures of the reference target points separated by the
rotation of a single link. By rotating only one link, the
relative motion of the target points in the camera pictures
with respect to the vertical reference will only describe
the misalignments of the rotated link.

Equations from the linear error model were used to
determine the robot configurations and rotations which would
reveal the misalignments in the camera pictures. Twist
misalignments are revealed by link variable rotations in the
vicinity of 0 degrees and skew misalignments in the vicinity
of +/- 90 degrees. Forward links, from the link being

rotated, should be positioned to produce the largest position vector for the robot.

Two procedures were developed: one for horizontal joint axes and one for vertical joint axes. The vertical reference used in the calibration procedure is ideally suited for measuring misalignments of horizontal joint axes. For horizontal joint axes the robot is positioned such that the misalignment axis (x for twist misalignments and y for skew misalignments) is perpendicular to, and intersects the vertical reference. The link being calibrated is then rotated about its horizontal axis to observe two target points from the same vertical reference.

The procedure for determining the misalignments of vertical joint axes is slightly more complicated. Vertical references are positioned near the x twist axis and y skew axis of the vertical joint axis being considered. The calibration procedure consists of observing a single target point in either side of the camera view. This determines the joint misalignment with respect to the camera coordinate frame. The orientation of the camera coordinate frame is determined with respect to the robot base coordinate frame by observing several target points from the vertical reference in one picture. The joint misalignment with respect to the base coordinate frame is obtained by comparing the results from the misalignment determined with respect to the camera coordinate frame, and the orientation of the camera coordinate frame in the base coordinate frame.

The equations which are used to determine the joint misalignments were developed from the transformation equations which describe the robot-camera system. The nine orientation equations from the transformation equation are trivial for the robot-camera system observing target points since a point in space does not have an orientation. The position equation which describes the dominant error observed in the camera, corresponds with the orientation of the joint axis being calibrated. Therefore, if the joint axis lies in the base z direction, the z position equation from the robot-camera transformation equation is used to generate the misalignment equation.

If the proper misalignment equations have been chosen, the coordinate positions of the target points which appear in the equations for both pictures will be the same. The misalignment equation which determines the joint axis orientation is generated by equating the positions of the target points. For vertical joint axes, only the camera terms are kept in the equation because only the motion of a single target point is observed to determine the misalignment. For horizontal joint axes, all of the terms are required to describe the joint misalignments.

The calibration method was tested using a Mitsubishi RM-101 robot and a Micromint, Micro D-cam digital camera. Misalignments were introduced into the base of the robot by tipping the robot to one side using shims of known thickness. By comparing the joint misalignments measured

with and without the shims, the accuracy of the calibration method was determined for the equipment used.

The results from the tests revealed that the vertical axis calibrations had accuracies ranging from -0.1 to 0.04 degrees with repeatabilities of 0.08 degrees (2 standard deviations). The calibration tests for the horizontal axes had accuracies ranging from -0.06 to 0.03 degrees with repeatabilities of 0.01 degrees.

The inaccuracy of the calibration method observed in the tests was partially due to the method of testing the calibration procedure. The backlash and freeplay in the robot joints allowed the robot's links to move when the robot was tipped to introduce the misalignments. To determine the true accuracy of the calibration method would require the tests to be repeated on a robot without backlash and freeplay in its joints.

The difference in accuracy between the vertical and horizontal axes was the result of the different procedures used. The vertical reference is better suited for measuring misalignments of horizontal axes since it allows larger rotations of the link being calibrated. Larger rotations will produce larger position errors in the camera pictures and therefore reduce the effects of the inaccuracies of the method and equipment.

The difference in repeatability between the vertical and horizontal axis calibrations was also the result of the different procedures used. For the vertical axis

calibration the camera exhibited a large repeatability error of 0.10 degrees for determining the global vertical orientation in the camera coordinate frame.

The objective of this investigation was to develop a calibration method which overcame several shortcomings of the previously developed methods. This was achieved with the new method. The calibration method developed can easily be conducted in the robot work environment without the need for a precision calibration site. The vertical references used in the calibration method are easily moved in and out of the robot work space with little inconvenience. The digital camera can also be easily mounted on the robot end effector and alignment of the camera by eye was sufficient to produce the accuracy of the results obtained in this investigation. The calibration algorithm requires very little human input to complete the procedure and it would be possible to develop an algorithm which would be entirely automated.

The calibration method fulfilled the requirements set out in this investigation which essentially required a method which is insensitive to errors in the robot and calibration equipment, yet measures the joint orientation errors. The accuracy obtained by the procedures was satisfactory but the repeatability error was larger than desired for the vertical axis calibration. Three improvements are suggested which would increase the accuracy and repeatability of the calibration method.

The first improvement would be to use a better digital camera with higher resolution and repeatability. The digital camera used in this investigation was a major source of the repeatability problem for the method. The repeatability for locations of the target points was 0.20 pixels for the camera x direction and 0.32 pixels for the camera y direction. This large repeatability for the camera resulted in a repeatability of 0.10 degrees for determining the orientation of the vertical reference in the vertical axis calibration.

A second improvement which would both improve the accuracy and repeatability of the vertical axis calibration would be to use a horizontal reference. The new reference for the calibration would be in a cross configuration with both a vertical and horizontal reference. Care would have to be taken to properly balance the reference to ensure the integrity of the reference. With a horizontal reference with two target points, larger rotations of the vertical axis links would increase the accuracy and repeatability of the vertical calibration. Two target points from a horizontal reference would also eliminate the need to determine the orientation of the vertical reference in the camera coordinate frame.

The third improvement suggested is to use more than two target points to determine the misalignments. If each link was rotated to observe several separate target points, more than one equation describing each misalignment would be

obtained. These equations could be solved using an iterative method, like the Gauss-Seidel method, with a least squares method to obtain the best misalignment solution.

Though the calibration of this investigation will improve robot accuracy, further calibration of the joint variables may also be required. The joint variable was the third parameter describing each link which dominated end effector errors and should not be neglected when considering robot accuracy.

Robot accuracy has only become an issue with the advent of off-line programming of robots. Once a more accurate model of a robot is obtained for the computer software, the robot accuracy will be improved throughout its work space. This will eliminate a serious impediment to off-line programming methods.

REFERENCES

Albertson, P., Verifying Robot Performance. Robotics Today,
     Vol. 5 No. 5, 1983, p.33-36

Berlenbach, K., How to Verify Robotic Performance. CAD/CAM
     and Robotics, Vol. 2 No. 5, 1984, p.15

Denavit, J., Hartenburg, R.S., A Kinematic Notation for
     Lower-Pair Mechanisms Based on Matrices. ASME
     Journal of Applied Mechanics, June 1955, p.215-221

Dubowsky, S., A Parameter Identification Study of Kinematic
     Errors in Planar Mechanisms. ASME Journal of
     Engineering for Industry, May 1975, p.635-642

Foulloy, L.P., Kelley, R.B., Improving the Precision of a
     Robot. IEEE Internation Conference on Robotics,
     1984, p.62-67

Kermack, I. Effects of Joint Misalignments on Manipulator
     Performance, M. Sc. Thesis, University of Alberta,
     expected spring 1986

Kreamer, W.C., Measuring Robot and Sensor Accuracy. Robots
     West Conference, SME Technical Paper MS84-1038,
     1984

Lammineur, P., Cornillie, O., Industrial Robots. EPO
     Applied Technology Series - Volume 2, Pergamon
     Press, 1984, p.2

Mooring, B.W., The Effect of Joint Axis Misalignment on
     Robot Positioning Accuracy. ASME Computers in
     Engineering, Vol. 2, 1983, p.151-155

Patrick, M., The ABC's of Robot Programming. CAD/CAM and
     Robotics, Vol. 2 No. 5, 1984, p.10-13

Paul, R.P., Robot Manipulators: Mathematics, Programming,
     and Control. The MIT Press, 1981

Scheffer, B., Geometric Control and Calibration Method of an
     Industrial Robot. 12th International Symposium on
     Industrial Robots and Robots 6, 1982, p.331-339

Snyder, W.E., Industrial Robots: Computer Interfacing and
     Control. Prentice-Hall Inc., 1985

Stauffer, R.N., Robot Accuracy.   Robotics Today, Vol. 7 No.
        2, 1985, p.43-49

Suh, C., Radcliffe, C.W., Kinematics and Mechanism Design,
        John Wiley and Sons, 1978

Toepperwein, L.L., Blackmon, M.T., Park, W.T., Tanner, W.R.,
        Adolfson, W.F., Robotics Applications for Industry,
        A Practical Guide.   Noyes Data Corporation, 1983,
        p.22

Wu, C., A Kinematic CAD Tool for the Design and Control of a
        Robot Manipulator.   The International Journal of
        Robotics Research, Vol. 3 No. 1, Spring 1984,
        p.58-67

Yu., L., Zhang, X., The Positioning Accuracy of Industrial
        Robots.   13th International Symposium on Industrial
        Robots and Robots 7, 1983, p.176-183

Zeldman, M.I., What Every Engineer Should Know About Robots.
        Marcel Dekker, Inc., 1984

Appendix A

Homogeneous Transformations

This appendix has been included for the reader who

is unfamiliar with homogeneous transformations. Unfamiliar

readers are also referred to references by Paul (1981) and

Snyder (1985). The elements of a homogeneous transformation

may be viewed as four vectors describing a second coordinate

frame. The elements of a general transformation are given

in the form

$$T = \begin{bmatrix} n_x & o_x & a_x & p_x \\ n_y & o_y & a_y & p_y \\ n_z & o_z & a_z & p_z \\ 0 & 0 & 0 & 1 \end{bmatrix} \qquad (A-1)$$

Figure A-1 illustrates an example where the orientation and

position of an end effector is described by a homogeneous

transformation. The elements of the transformation T,

comprise one position and three orientation vectors. The

position vector $p = [p_x , p_y , p_z]^T$ describes a

translation from coordinate frame 1 to the origin of the

coordinate frame 2 on the end effector. The orientation of

the end effector coordinate frame is described by the three

remaining unit vectors n, o, and a whose components are

given with respect to coordinate frame 1. The approach
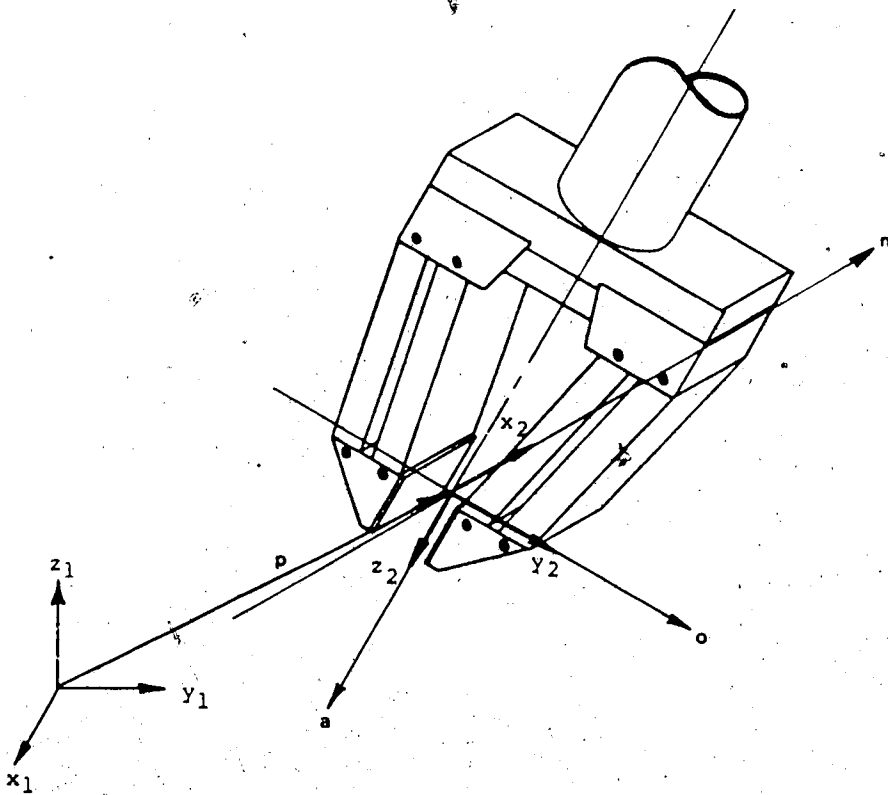
Figure A-1 Homogeneous Transformation Vectors

vector, **a**, is directed along the z_2 axis and corresponds with the direction the gripper would approach a position. The orientation vector, **o**, is directed along the gripper y_2 axis and the normal vector **n**, is defined by the x_2 axis determined by the cross-product of the orientation and approach vectors. Complex transformations are generated by the product of several simple translation and rotation transformations. The general translation transformation is given by

$$\text{Trans}(a,b,c) = \begin{bmatrix} 1 & 0 & 0 & a \\ 0 & 1 & 0 & b \\ 0 & 0 & 1 & c \\ 0 & 0 & 0 & 1 \end{bmatrix} \qquad (A-2)$$

which corresponds to the position vector $[a, b, c]^T$.

Rotation transformations about the x, y, and z axis by an angle theta (θ) are given by

$$\text{Rot}(x,\theta) = \begin{bmatrix} 1 & 0 & 0 & 0 \\ 0 & \cos\theta & -\sin\theta & 0 \\ 0 & \sin\theta & \cos\theta & 0 \\ 0 & 0 & 0 & 1 \end{bmatrix} \qquad (A-3)$$

$$\text{Rot}(y,\theta) = \begin{bmatrix} \cos\theta & 0 & \sin\theta & 0 \\ 0 & 1 & 0 & 0 \\ -\sin\theta & 0 & \cos\theta & 0 \\ 0 & 0 & 0 & 1 \end{bmatrix} \qquad (A-4)$$

$$Rot(z, \theta) = \begin{bmatrix} \cos \theta & -\sin \theta & 0 & 0 \\ \sin \theta & \cos \theta & 0 & 0 \\ 0 & 0 & 1 & 0 \\ 0 & 0 & 0 & 1 \end{bmatrix} \qquad \text{(A-5)}$$

As an example, the transformation describing a rotation about the z axis of 90 degrees followed by a translation of 2 units in the new x direction is given by

$$T = Rot(z, 90) \quad Trans(2, 0, 0)$$

$$= \begin{bmatrix} 0 & -1 & 0 & 0 \\ 1 & 0 & 0 & 2 \\ 0 & 0 & 1 & 0 \\ 0 & 0 & 0 & 1 \end{bmatrix} \qquad \text{(A-6)}$$

A second frame, B, is given by the transformation

$$B = \begin{bmatrix} 1 & 0 & 0 & 2 \\ 0 & 1 & 0 & 0 \\ 0 & 0 & 1 & 0 \\ 0 & 0 & 0 & 1 \end{bmatrix} \qquad \text{(A-7)}$$

Two transformations of coordinate frame B may be accomplished using T. The coordinate frame B may either be premultiplied or postmultiplied by T. If frame B is postmultiplied by T the transformation is made with respect to the coordinate frame B.

$$X \triangleq B \quad T$$

$$= \begin{bmatrix} 0 & -1 & 0 & 2 \\ 1 & 0 & 0 & 2 \\ 0 & 0 & 1 & 0 \\ 0 & 0 & 0 & 1 \end{bmatrix} \qquad \text{(A-8)}$$

If the coordinate frame B is premultiplied by T then the transformation is made with respect to the base coordinate frame.

$$X = T \quad B$$

$$= \begin{bmatrix} 0 & -1 & 0 & 0 \\ 1 & 0 & 0 & 4 \\ 0 & 0 & 1 & 0 \\ 0 & 0 & 0 & 1 \end{bmatrix} \qquad \text{(A-9)}$$

The results of these two transformations are shown in figure A-2. Homogeneous transformations may be used to describe the coordinate frames of each link in a robot manipulator and generate the manipulator kinematic equations. Two conventions for representing revolute links are discussed in Appendix B.
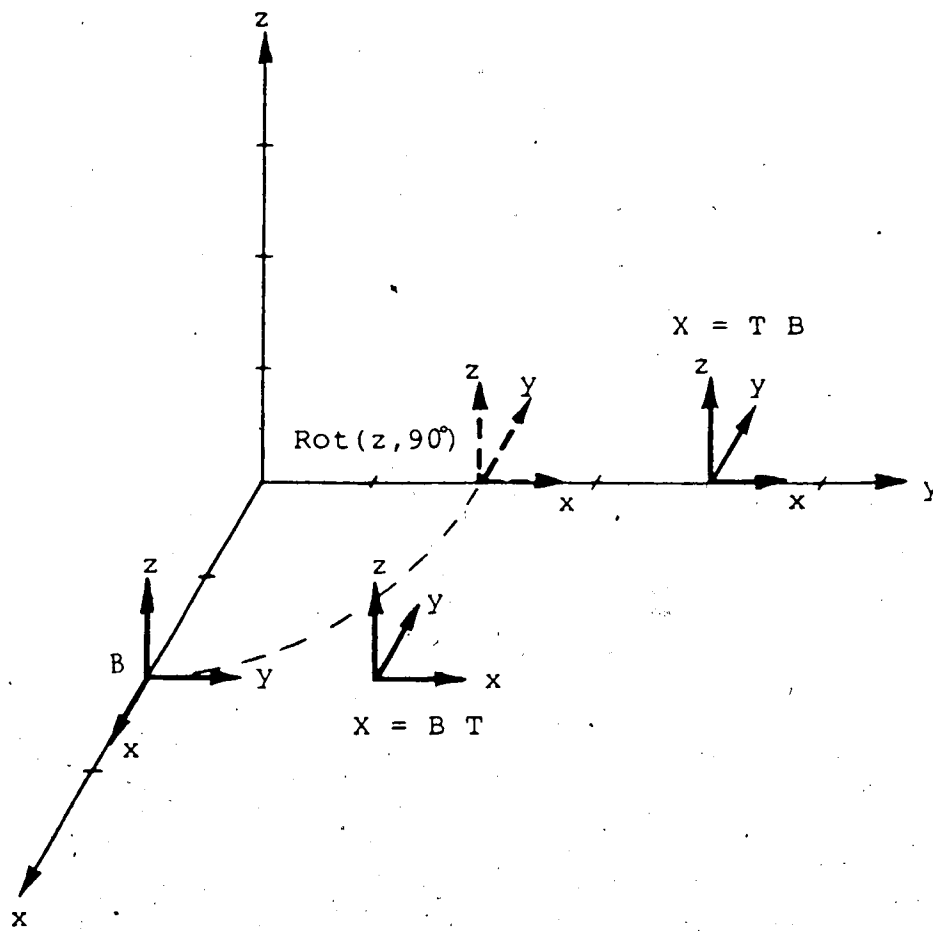

Figure A-2   Relative Transformations

Appendix B

Denavit-Hartenburg and Modified Conventions

The relationship between connected links of a serial link robot manipulator can be described using homogenous transformation matrices. By placing constraints on the orientation of the coordinate frame in each link, Denavit and Hartenburg were able to describe a link using only 4 kinematic parameters.

Figure 2-1 illustrates a revolute link in a sequence of links. For a revolute joint, θ_i is the joint or dependent variable. Three other fixed kinematic parameters describe the relationship between link i-1 and link i. The link length is denoted by the variable l_i. The link length is the common normal distance between the joint axis z_{i-1} and z_i. The link distance, r_i is the measure of the distance between the two normals describing the link lengths. If the joint axes are parallel the joint distance is taken to be zero. The twist angle of a link α_i, is the angle between the z_i and z_{i-1} joint axis in a plane perpendicular to l_i.

This investigation deviates slightly from the usual nomenclature used to describe the link parameters. The usual nomenclature uses a_i for the link length and d_i for the link distance. These were changed to avoid confusion

with the approach vector, **a**, and the differential

translation vector, **d**.

The Denavit-Hartenburg transformation for the

assigned coordinate frame is given the following rotations

and translations.

     a) rotate about z_{i-1} axis the joint angle θ_i

     b) translate along z_{i-1} axis the distance r_i

     c) translate along rotated x_{i-1} axis the length l_i

     d) rotate about x_i axis the twist angle α_i

These rotations and translations may be expressed by four

homogenous transformations called an A matrix

$$A_i = Rot(z,\theta) \quad Trans(0,0,r) \quad Trans(1,0,0) \quad Rot(x,\alpha)$$

$$= \begin{bmatrix} C\theta_i & -S\theta_i C\alpha_i & S\theta_i S\alpha_i & l_i C\theta_i \\ S\theta_i & C\theta_i C\alpha_i & -C\theta_i S\alpha_i & l_i S\theta_i \\ 0 & S\alpha_i & C\alpha_i & r_i \\ 0 & 0 & 0 & 1 \end{bmatrix} \qquad \text{(B-1)}$$

Abbreviations for the cosine and sine functions are given by

C and S respectively.

The four kinematic parameters accurately describe

the geometry between connected links and can be used to

describe an entire robot manipulator. The difficulty with

the Denavit-Hartenburg convention arises when it is desired

to describe small skew misalignments in parallel joint axis

(see figured 1-6 and 2-2).

The kinematic parameters for the Denavit-Hartenburg

convention which describe two links with parallel joint axes are shown below.

θ (joint variable) = dependent variable

α (twist angle) = 0 degrees

1 (link length) = 1_i

r (link distance) = 0

For a slight skew misalignment the connected joint axes are no longer parallel. The joint variable θ and twist angle α are unaffected in the description of the misaligned link. The two joint axes, no longer parallel, will intersect at some large distance from the link itself unless a twist misalignment also exists. The link length 1_i, the common perpendicular distance between the two joint axis, will become 0 instead of 1_i. The distance between the common normals (r_i) will approach infinity instead of being equal to zero. The A matrix for this misaligned link is ill conditioned and therefore numerically difficult to work with. To accomodate the skew error, Kermack (1986) introduced a fifth transformation at the end of the Denavit-Hartenburg convention. The rotations and translations which describe the modified convention called a D matrix are

D_i = Rot(z,θ) Trans(0,0,r) Trans(1,0,0)

Rot(x,α) Rot(y,γ)   (B-2).

The skew misalignment is described by a final rotation

transformation about the y_i axis. With this modified

convention the link length (l_i) and distance (r_i) remain

unchanged and the skew rotation transformation describes the

misalignment.

The modified Denavit-Hartenburg transformation is

given by

$$
D_i = \begin{bmatrix}
C\theta_i C\gamma_i - S\theta_i S\alpha_i S\gamma_i & -S\theta_i C\alpha_i & C\theta_i S\gamma_i + S\theta_i S\alpha_i C\gamma_i & l_i C\theta_i \\
S\theta_i C\gamma_i + C\theta_i S\alpha_i S\gamma_i & C\theta_i C\alpha_i & S\theta_i S\gamma_i - C\theta_i S\alpha_i C\gamma_i & l_i S\theta_i \\
-C\alpha_i S\gamma_i & S\alpha_i & C\alpha_i C\gamma_i & r_i \\
0 & 0 & 0 & 1
\end{bmatrix}
$$

$$(B-3)$$

Readers who would like further information on the

Denavit-Hartenburg transformation convention are referred to

references by Paul (1981) and Snyder (1985).